2024-05-01

Dispersal And Population Structure Of Euchlanis Chihuahuaensis Via Anemochory In The Chihuahuan Desert

Tristan Chavez-Poeschel
University of Texas at El Paso

DISPERSAL AND POPULATION STRUCTURE OF *EUCHLANIS CHIHUAHUAENSIS* VIA ANEMOCHORY IN THE CHIHUAHUAN DESERT

TRISTAN A. CHAVEZ-POESCHEL

Master's Program in Environmental Science

APPROVED:

Elizabeth J. Walsh, Ph.D., Chair

Thomas E. Gill, Ph.D.

Michael G. Harvey, Ph.D.

Stephen L. Crites, Jr., Ph.D.
Dean of the Graduate School

DISPERSAL AND POPULATION STRUCTURE OF *EUCHLANIS CHIHUAHUAENSIS* VIA ANEMOCHORY IN THE CHIHUAHUAN DESERT

by

TRISTAN A. CHAVEZ-POESCHEL, B.S.

Thesis

Presented to the Faculty of the Graduate School of

The University of Texas at El Paso

in Partial Fulfillment

of the Requirements

for the Degree of

MASTER OF SCIENCE

Department of Earth, Environmental and Resource Sciences

THE UNIVERSITY OF TEXAS AT EL PASO

May 2024

ACKNOWLEDGEMENTS

I would like to thank my committee members, Dr. Elizabeth J. Walsh, Dr. Thomas E. Gill, & Dr. Michael Harvey, for their support and mentorship throughout this process. I would especially like to thank Dr. Walsh for her confidence in me and continued support. This project would not have been possible without our community partners which include The City of El Paso, Hueco Tanks State Park and Historic Site (Permit #TPWD 07-21 (E. J. Walsh)), White Sands National Park (Permit #WHSA-2006-SCI-004 (E.J. Walsh)), and The Bureau of Land Management - Las Cruces Offices. Funding for this project was from the National Science Foundation: NSF DEB-1257068, 2051704 (E.J. Walsh). I would also like to thank the Indio Mountain Research Station group, the Johnson Lab, the Mata Lab, Dr. Josh Banta, my colleagues Santiago Hoyos, Perry Houser, and many others who have helped throughout my studies. Lastly, I would like to thank my colleague Joseph McDaniel, that without his passion for outdoor and aquatic research, I would not have been introduced to this field of research and led to this current path.

ABSTRACT

Desert ecosystems present challenges for aquatic organisms as habitats are fragmented, both in space and time; however, diapausing stages of rotifers can travel hundreds of kilometers during wind events. I used the rotifer *Euchlanis chihuahuaensis* as a model species to investigate the influence of wind dispersal on gene flow and population genetics in Chihuahuan Desert populations. I hypothesized that anemochory facilitates gene flow from source populations in the Northern Chihuahuan Desert in Mexico and the western United States to habitats in the Trans-Pecos region via delineated wind corridors. To test this hypothesis, the genetic diversity of populations from both inside and outside of the wind corridors were compared. The corridors were constructed using data from modeled HYSPLIT trajectories of dust events over 40 years. Genetic variation in the COI gene among populations from inside and outside of the dust corridor were analyzed to determine possible isolation by distance, fixation (F_{ST}), and haplotype distributions. My results provided limited evidence for gene flow from populations from Southern New Mexico with individuals with shared haplotypes occurring in non-hydrologically connected habitats between 100 – 200 km apart; however, many discrete haplotypes were identified which belonged to single sites or local areas. My results elucidated the population structure of *E. chihuahuaensis*, with three haplogroups identified with discrete geographic boundaries in Southern New Mexico, Trans Pecos, and the Mexican border area in northern Chihuahua state, along with the identification of a putative cryptic species. Regionally partitioned populations indicated that "West" (Mimbres River Delta Region -PLP) and "East" (IMRS) regions had higher levels of haplotype diversity ranging from 0.85 to 0.93. Limited evidence points to genetic differences in diversity from populations located both inside and outside the dust corridor (58% among and 42% within populations). Investigating anemochory's

role in gene flow in desert environments can help us further understand evolutionary and ecological processes in aquatic microinvertebrates inhabiting ephemeral systems.

TABLE OF CONTENTS

LIST OF TABLES

LIST OF FIGURES

INTRODUCTION

Of the several forms of biological dispersal, passive dispersal can be a complex process and often relies on stochastic events. Aquatic organisms in arid environments, such as in the Chihuahuan Desert, inhabit many fragmented and isolated habitats that are sometimes hundreds of kilometers apart (Dinerstein et al., 2000). Many of these taxa, such as the littoral rotifer *Euchlanis chihuahuaensis*, are obligate aquatic organisms that need to adapt to local conditions or traverse large dry areas to colonize new habitats via anemochory, zoochory, or hydrochory. Thus, many taxa have developed adaptations to harsh conditions. One of these adaptations was the development of dormant or diapausing stages, which can be dispersed passively via dust wind events in the Chihuahuan Desert (Rivas et al., 2018, 2019); however, the degree and frequency with which these events contribute to population connectivity via gene flow remains unclear. Gene flow in arid aquatic habitats may be limited by allopatric (e.g., geographical) or temporal barriers, with other factors such as genetic drift, selection, or pre- and post-zygotic barriers also playing a role in population structure and gene flow.

The Chihuahuan Desert, with an approximate area of 629,000 km^2 (Dinerstein et al., 2000), comprises parts of northern Mexico and several US states including Texas, New Mexico, and Arizona and is a cooler desert ecosystem due to its altitude with an average annual rainfall of approximately 235 mm (Dinerstein et al., 2000). Given its large area, the desert also has various gradients of habitats, ranging from desert grasslands to woody scrubland and many isolated aquatic communities (Dinerstein et al., 2000). However, large swings in temporal heterogeneity in climatic conditions have been documented (Fawcett et al., 2011; Wells, 1966; Turner et al., 2022). Wells (1966) noted that wetter periods, specifically during the Pleistocene, resulted in higher rainfall, cooler temperatures, and large pluvial lakes and interconnected waterways in the

region. According to Fawcett et al. (2011) droughts and megadroughts, lasting hundreds and thousands of years, occurred regularly in the desert southwest of North America and were associated with the interglacial expansion and contractions. These cyclical dry and wet periods during the Pleistocene may have resulted in populations of aquatic organisms becoming fragmented during drier periods, forming refugia for some species and then expanding permitting sympatry, secondary contact, and introgression during wetter periods (Turner et al., 2022). The "wetter" periods provided potentially interconnected habitats for aquatic-bound invertebrates. Previous studies have shown the existence of numerous large lakes in contemporary Chihuahuan Desert basins that were present during the Pleistocene and would have inundated present day basins (Reeves, 1965). Current climatic conditions however only provide a glimpse as to what the area was like, in that several contemporary basins can fill partially during very wet periods (Castiglia & Fawcett, 2006; Scuderi, Laudadio, & Fawcett, 2010). These paleolakes were substantially larger than the lakes present today; for example, Pluvial Lake Palomas, is estimated to have covered ~60,000 km^2 in Northern Mexico and southern New Mexico (Castiglia & Fawcett, 2006). These large lakes and wetter periods lasted for extended periods (Castiglia & Fawcett, 2006; Scuderi, Laudadio, & Fawcett, 2010) and basins were more interconnected hydrologically than they are today. This interconnectivity is rare in the modern era in the Chihuahuan Desert.

Current desert conditions are much different, with regional variance in precipitation. For instance, higher elevations in the sky islands of northern Mexico and Arizona can receive 2-3 times as much rainfall as the plains (Castiglia & Fawcett, 2006). The large pluvial lakes are either no longer present, are substantially reduced, or only have standing water during exceptionally wet seasons. Little irregular moisture, low quantities of ground cover, and high

wind events have made these areas some of the most regular sources of dust in North America (Prospero et al., 2002). This area produces regular dust storms, which can vary in size and intensity (Baddock et al., 2011; Dominguez Acosta, 2009; Lee et al., 2009; Rivera Rivera et al., 2009). The dust storms in this area are not only seasonal, but also appear to originate from numerous, widely dispersed sites and where land area "edges" or margins abut other land features (Rivera Rivera et al., 2010). The dust sources can include fallow farm fields, playas, shrublands, and areas with sparse groundcover. Some of these areas are associated with either current or past agricultural practices that led to soil degradation (Sandor & Homburg, 2017), and thus unstable soil crusts.

Dominguez Acosta (2009) and Prospero et al. (2002) identified the Mimbres Basin, the Pluvial Lake Palomas Basin areas, and areas along the Casas Grandes River as areas that contain a multitude of ephemeral aquatic habitats which function as primary dust sources that make this region one of the dust hotspots of North America (Prospero et al., 2002), and which also encompasses an aeolian corridor – a preferred wind transport pathway for airborne dust/sand (Dominguez Acosta, 2009). The geographic heterogeneity provides for varied aquatic habitats within the aeolian corridor. This heterogeneity in contemporary desert aquatic habitats provides for varying levels of resource availability, hydroperiods, water quality and quantity, and variable temperature and chemical parameters depending on the substratum. The high variability in conditions can be challenging for many organisms, and specifically for aquatic-bound invertebrates. One of the important adaptations that some desert aquatic zooplankton have evolved is the ability to withstand harsh conditions by the production of diapausing eggs (resting eggs) and xeroxomes (Gomez et al., 2002a, Wallace et al., 2006, Walsh et al., 2016). One class of zooplankton, monogonont rotifers, not only use diapausing eggs as a means to avoid adverse

conditions, but they also have adaptations such as rapid explosive growth in their populations via cyclical parthenogenesis, which allow them to maximize life cycle processes during the short-wet periods now present in the Chihuahuan Desert (Schroder et al., 2007). Rotifers can complete their life cycles in days, usually from hatching amictic females, which produce amictic daughters to generate large populations quickly. Monogonont rotifers produce smaller, reduced males under certain conditions, such as high population density or low water quality. Being water bound, however, presents difficulties in colonizing new habitats. Thus, populations could experience reduced gene flow from source populations and these potentially isolated habitats, in some respects, mimic islands and some of the biogeographic theories developed by MacArthur and Wilson (1967) could be applied. One of the theories notes that an island's population would reflect a subset of the populations from the continent, and this would be noted in desert habitats in what alleles would be present in the "islands" from the source populations. The theory also notes that islands that are further away, more isolated, would also have lower rates of colonization which again could potentially be shown in what alleles are present in those populations; however, for aquatic invertebrates reaching those "isolated" habitats would require mechanisms to be able to reach those sites.

For desert aquatic invertebrates that can fly or are more mobile, reaching new habitat might be easy; however, for others such as the giant water bug *Abedus herberti*, which are considered to generally be water bound, have legs that allow for overland movement over short distances but generally not much further, and in some instances when habitat conditions deteriorate, it can lead to local extirpation (Phillipsen & Lytle, 2012). Rotifera do not have the option of physical, directed, overland movement, and instead appear to rely on passive dispersal via anemochory or zoochory, and hydrochory. Several studies investigated dispersal via

anemochory at local and regional distances (e.g., Cáceres & Soluk, 2002; Rivas et al., 2018; 2019). Cáceres and Soluk (2002) found that rotifer community assemblage similarities were correlated with distance from the source of the population, thus implying dispersal via anemochory or hydrochory rather than via zoochory. Rivera Rivera et al. (2009), Baddock et al. (2011) and Gill et al. (2016) identified wind transport corridors leading into the Paso del Norte region which had regular dust events and wind directions crossing ideal rotifer habitats. In prior research on passive dispersal, Rivas et al. (2018, 2019) found that multiple taxa of aquatic invertebrate diapausing stages, including monogonont rotifer diapausing eggs, were transported during Chihuahuan Desert dust storms and can disperse far, likely up to hundreds of kilometers overland, which could provide routes to new habitats. Thus, while dispersal via anemochory does occur in monogonont rotifers, the genetic effect on population structure and gene flow has not been fully investigated. Since diapausing eggs in sediment egg banks can be viable for decades (Gomez & Carvalho, 2000), they can persist until optimal conditions for hatching occur. The combination of a delineated dust source area and *Euchlanis chihuahuaensis* populations within this corridor could provide frequent opportunities for dispersal and potentially gene flow among populations in highly fragmented and isolated sites in the Chihuahuan Desert.

Previous research on spatial distribution and its genetic effect on bdelloid (e.g., (*Adineta*, *Habrotrocha*, *Macrotrachela*, and *Philodina* species) : Fontaneto et al., 2009, Iakovenko et al., 2015) and monogonont species (e.g., *Brachionus plicatilis* complex: Gómez et al., 2002a, Mills et al. 2016; *Epiphanes senta* complex: Schröder & Walsh, 2007; *Brachionus calyciflorus* complex: Gilbert & Walsh,Xiang et al., 2011; *Polyarthra* spp. complex: Obertegger, Flaim, & Fontaneto, 2014) found that many of these species that had been considered “cosmopolitan” in distribution were in fact species complexes and had varying levels of genetic structure and low

levels of gene flow. Research on *Euchlanis dilatata* also showed that this species was a cryptic species complex (Kordbacheh et al., 2017, 2018), with substantial genetic differentiation in the COI gene sequences (uncorrected p distance varied from 0-21.9%) between populations with little within population variation (0 to 2.5%). Upon delimitation, within genetic distances of the cryptic species in the *Euchlanis dilatata* complex were between 0.0-18.7% and among the species, distances ranged from 0.2 -21.9% (Kordbacheh et al., 2017). This level of genetic diversity could indicate that the populations are less connected and gene flow could be limited. The focal species of this study, *Euchlanis chihuahuaensis*, was delimited from the *Euchlanis dilatata* species complex and was found to have a broad distribution in the Trans Pecos region (Kordbacheh et al., 2018). Most of the populations identified are located hundreds of kilometers apart from one another, in habitats that are separated by harsh desert conditions with few to no hydrological connections. Any aquatic-bound species would not only have to contend with the geographic separation but would have to pass several biotic and abiotic filters to achieve successful population establishment (De Meester et al., 2002). This separation could have profound effects on populations, and depending on the length of time and other conditions and could lead to radiation , speciation, extirpation, extinction, or various other evolutionary processes. Assuming that a resting egg manages to make it to a habitable area, many factors can come into play for any new colonist in a new habitat that can affect successful colonization and gene flow. De Meester et al. (2002a) noted that factors such as local adaptation, large propagule egg banks, and priority effect create conditions to constrict gene flow. This was also supported by Gomez et al. (2002b), where local adaptation appeared to play a large role in determining rotifer genetic structure; however, they noted that gene flow appeared to occur, but in a more restricted manner.

Several genetic analysis methods to determine population differentiation have been developed including fixation measures such as F_{ST} (Wright, 1950) and G_{ST} (Nei, 1973). The fixation values can provide an indication as to the level of differences between the populations. Previous studies (e.g., Kimpel et al., 2015; Kordbacheh et al., 2017, 2018) investigated gene flow, using the cytochrome oxidase 1 gene (COI) in regional and continental level populations of monogonont rotifers via haplotypic diversity comparisons. The use of haplotype networks in that study showed that the smaller, regional, populations had several clustered haplotypes and some sites had unique haplotypes that could indicate populations are genetically isolated from one another. The authors also noted that the meta-populations had some shared haplotypes, which could indicate dispersal between the larger geographical populations. Haplotype networks provide a visual mapping of the haplotypes and can be analyzed to determine haplotype diversity, haplotype distribution, and possible source populations (Kimpel et al., 2015; Sun et al., 2019). The visual patterns can be interpreted to determine the type of dispersal (island model, steppingstone, refugia) and the relationships among the populations (Mardulyn, 2001). These processes may provide clues into the present-day genetic structure of *E. chihuahuaensis* as well as to patterns of dispersal.

The overarching hypothesis for this project is that the wind/dust storms, with a regular pattern of occurrence and transport pathways, provide a mechanism and opportunities for dispersal and potential gene flow between populations of aquatic invertebrates inhabiting ephemeral aquatic sites via their diapausing stages. For this research, the following two main objectives were pursued.

1. Describe the aeolian corridor in the Trans Pecos, southern New Mexico, and northern Mexico Region
2. Examine the genetic population structure of *Euchlanis chihuahuaensis* of the northern Chihuahuan Desert
3. Compare the populations of *Euchlanis chihuahuaensis* outside and inside the aeolian corridor, to ascertain potential genetic influence from anemochory.

My initial prediction was that populations within the dust corridor would be genetically more similar to one another, even at large distances, compared to populations of the same species outside the corridor, given that the populations outside the dust corridor have fewer opportunities for dispersal among habitats. Because some of these populations are also located in marginal areas of the dust corridor, they could also experience some level of increased dispersal which could show a potential "stair step" pattern of increasing genetic distance, depending on the proximity to the dust corridor.

METHODS

Study System

The monsoon season in the Paso Del Norte region generally runs from July – October, which is when opportunities to sample ephemeral areas are at their greatest. Wet samples were chosen after rain events primarily over sediment rehydration due to the ready ease of noting the presence or absence of the target species. This study species was chosen in part to past collection data where it appeared to have a large distribution ranging from near White Sands New Mexico, Hueco Tanks State Park and Historic Site, Indio Mountains Research Station, and Big Bend National Park (Texas); and northern Chihuahua state in Mexico. Sample sites for this species were composed of ephemeral sites with varying habitat types and lengths of hydroperiod. Consequently, due to the ephemeral nature of the sites, live specimens of *E. chihuahuaensis* were collected after rain events during different seasons, January through October, and over the course of several years from 2006 to 2023. Additional samples were obtained from dry sediment from the sample sites when rain events were limited.

Table 1. Known populations of *Euchlanis chihuahuaensis*, with GenBank accession numbers for COI gene sequences from Kordbacheh et al. (2019). Location abbreviations include Cattle Tank (CT), Peccary Tank (PEC), Paint Gap Tank, Big Bend (PGTBB), Laguna Santa Maria (OSM), Hueco Tanks State Park and Historic Site (HTSPHS), and Indio Mountains Research Station (IMRS).

Collection Site	Collection Type	Date	CODE	GPS coordinates	GenBank Accession#
Cattle Tank, White Sands National Park, NM	Live	09.20.2006	Ed.CT.NM	32.675, -106.443	KU665883
Mescalero Canyon, HTSPHS, TX Pond Sediments	Sediment	NA	Ed.MCHT.TX	31.919, -106.040	KU665846
Peccary Tank,IMRS, TX)	Live	06.03.2013	Ed.PEC.TX	30.756, -105.004	KY564362
Laguna Prieta, HTSPHS, TX	Sediment	09.02.2013	Ed.LPSHT.TX	31.925, -106.047	KU665849
Paint Gap Tank, Big Bend National Park, TX	Live	05.14.2006	Ed.PGTBB.TX	29.388, -103.303	KU665841
Laguna Santa Maria,Chihuahua, MX	Live	07.31.2009	Ed.OSM.M	31.155, -107.317	KU665871

Sanger sequencing (Sanger et al., 1977) modified from Kordbachech et at., 2017 was used to sequence each clonal lineage. Each sequenced isolate COI gene was compared to the individuals identified by Kordbacheh et al., 2019 (**Table 1**) via a Bayesian phylogenetic reconstruction (**Appendix 13**) for confirmation of species identity. Sample locations are referenced in **Table 2** which include 52 new clonal populations and four previously obtained sequences from GenBank (Kordbachech et al, 2019)**.** Cryptic species delimitation analyses were also conducted using several programs including Automatic Barcoding Gap Discover (ABGD; Puillandre et al., G. 2011), K/Θ (Birky et al., 2010; Spöri et al., 2021), and Bayesian GMYC (Fujisawa & Barraclough, 2013).

Table 2. Sample locations of *Euchlanis chihuahuaensis* in the Trans Pecos, Mexico, and Southern New Mexico region with abbreviation code.

Sampling Site	Location	Abbreviation (Code)
Pluvial Lake Playa #1	Southern New Mexico	P1
Pluvial Lake Playa #2,	Southern New Mexico	P2
Columbus Playa	Southern New Mexico	CNM
Laguna Santa Maria	Chihuahua, Mexico	OSM
404 A	Southern New Mexico	404
Cattle Tank	White Sands, New Mexico	CAT
Behind Ranch House	HTSPHS, Texas	BRH
Album Park, TX	El Paso, Texas	ALB
Dowling, Moon, Gray Oak	HTSPHS, Texas	DOW, MOO, GOK
Luna 26, NM	Southern, New Mexico	LNA
Draw 2, NM	Southern, New Mexico	DRW
Bailey Evans B, Lonely Tank, Peccary Tank, Red Tank, Rattle Snake Tank	Indio Mountains Research Station, Texas	BEB, LNY, PET, RET, RAT
Paint Gap Tank	Big Bend National Park, TX	PGTBB
Kent Bridge	Kent, Texas	KNT

Aeolian Corridor

This study aimed to examine genetic population structure within a dust (aeolian) (wind) corridor (a path of regular and frequent atmospheric transport of dust or dust and sand) originally inferred by the research of Rivera Rivera et al. (2009), Dominguez Acosta (2009) and Baddock et al. (2011). The existence of such a dust corridor in the northern Chihuahuan Desert was further suggested the NOAA HYSPLIT modeling (Hybrid Single-Particle Lagrangian Integrated Trajectory; Stein et. al., 2015) using dust events included in studies by Rivera Rivera et al. (2009), Baddock et al. (2011), Gill et al. (2016), and Rivas et al. (2018, 2019). Their studies identified a distinct geographic region where they were able to back trace a preferred transport pathway of strong winds and dust from the Janos/Ascension region (Casas Grandes River drainage, Chihuahua) to the El Paso/Ciudad Juarez metropolitan area of Texas, Chihuahua, and New Mexico, extending to the Van Horn, TX, area, crossing many ephemeral wetlands. Another aeolian corridor, starting at the southern part of the Paleolake Palomas complex and affecting sites northeast (Dominguez, 2009; Baddock et al., 2011) was included in the combined aeolian

corridor for this site as there is overlap between the two corridors, which also affect the same regions downwind. For this study, the dual overlapping corridors were treated as a single regional corridor (**Figure 1**). Sites outside the corridor were identified as areas with sparse to no known dust events during the 1980–2016 timeframe from HYSPLIT modeling and satellite remote sensing (Baddock et al. 2011; Gill et al. 2016; Rivera Rivera et al. 2010). The back traced storm paths from the 1980-2016 HYSPLIT data were merged into a polygon and the shape files were then processed with ESRI ArcGIS Pro version 3.0.1. The Paso del Norte region receives dust storms from several directions, with the trajectories from the Southwest being the predominant sources of dust for the region (Rivera Rivera et al., 2009; Baddock et al., 2011; Gill et al., 2016; Rivas et al., 2018, 2019; Novlan et al., 2007).

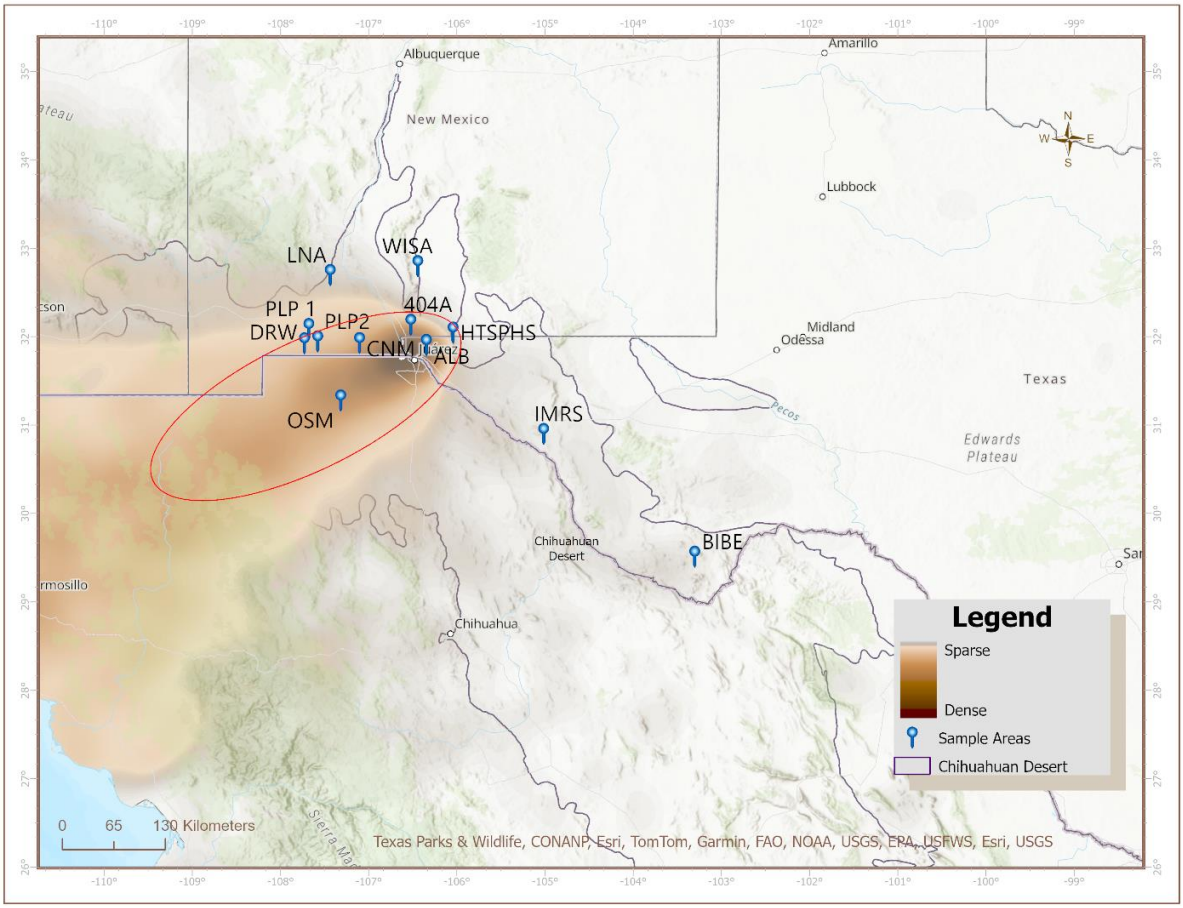

Figure 1. Heat map of dust storm event paths in the Paso Del Norte Region from 1980 to 2016, using the HYSPLIT modeling program (Stein et al., 2015) from NOAA adapted from Gill et al. (2016). Lighter areas indicate lower density of dust events crossing a site and darker areas indicate more dust events going through that area. The map also shows *Euchlanis chihuahuaensis* sampling sites. abbreviations (OSM – Laguna Santa Maria, PLP1 &2 – Pluvial Lake Palomas (Mimbres River Valley), DRW – Draw 2, LNA – Luna 26, WISA- White Sands National Park, HTSPHS – Hueco Tanks State Park & Historic Site, ALB- Album Park, IMRS – Indio Mountains Research Station, BIBE – Big Bend National Park, and CNM – Columbus, NM Playa.

Data for wind direction and wind speed were also obtained from the NASA Prediction of Worldwide Energy Resource (POWER) database, to determine potential sample areas, wind mixing areas, and average annual wind speed and direction values from 1980 – 2020. Average wind direction and speed data from 1981 – 2020 from the NASA Prediction of Worldwide Energy Resources (POWER) site was used to determine wind patterns over the 40-year span.

Python version 3.9.12 was used for creating the windroses. The following libraries were used: Windrose version 1.9.0, matplotlib version 3.5.1, numpy version 1.26.1, and pandas version 1.4.2.

Table 3. Sampled populations of *Euchlanis chihuahuaensis* inside the dust corridor within the Trans-Pecos region, Mexico, and Southern New Mexico. N = number of isolates

Collection Site	Type	Date	Code	GPS coordinates	N
Pluvial Lake Playa #1, NM	Live	07.06.2022	PLP1	31.964, -107.679	10
Pluvial Lake Playa #2, NM	Live	07.06.2022	PLP2	31.824, -107.578	7
Columbus Playa (HW9), NM	Live	08.19.2021	CNM	31.805, -107.104	1
Laguna Santa Maria, CI, MX		07.31.2009	OSM	31.155, -107.317	1
404 A, NM	Live	07.03.2021	404A	32.012, -106.523	1
Behind Ranch House (HTSPHS), TX	Live	09.21.2021	BRH	31.923, -106.041	6
Album Park, TX	Live	10.24.2022	ALB	31.783, -106.346	2
Moon (HTSPHS), TX	Live	10.03.2021	MOO	31.917, -106.041	1
Gray Oak (HTSPHS), TX	Live	10.03.2021	GOK	31.922, -106.046	1
Draw 2, NM	Live	05.28.2023	DRW	31.802, -107.729	1

Collection Sites

Populations were obtained from ephemeral habitats that are found in the Paso del Norte, Southern New Mexico, Trans Pecos, and Northern Mexico and include playas, tanks, rock pools, floodplains, and ephemeral stream channels in the western portion of the aeolian corridor (**Figure 2**). These sites are in three geographic areas within the Northern region in the Chihuahuan Desert (Dinerstein et al., 2000). The central geographic sampling area (**Table 3**) within the boundaries of the wind corridor extends from Ascension, Chihuahua, Mexico (GPS coordinate 1.324, -108.026 WGS84) to Hueco Tanks State Park and Historic Site, Texas, USA (31.911, -106.044 WGS84).

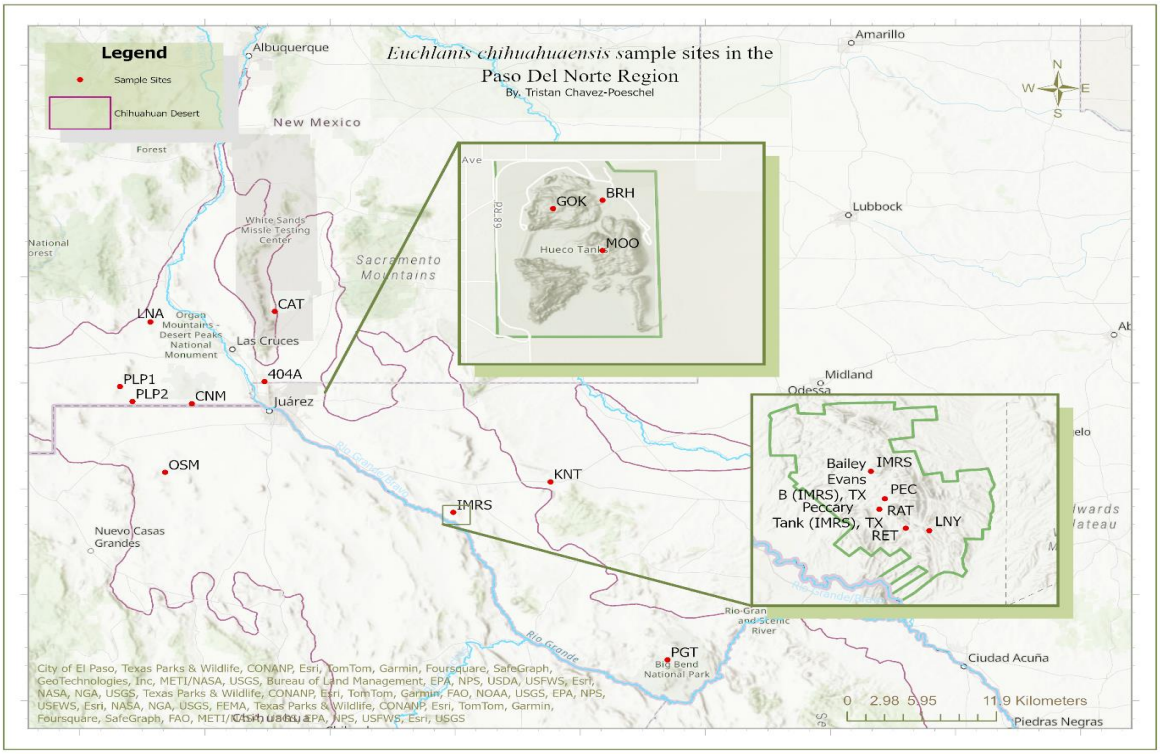

Figure 2. Sample locations in the Trans Pecos, Mexico, and Southern New Mexico regions of *Euchlanis chihuahuaensis* used for this study. Abbreviations are defined in **Table 2**.

The Eastern portion sample sites (**Table 4**) included UTEP's Indio Mountains Research Station, Big Bend National Park, and Kent, Texas. The sites were selected in areas that were not hydrologically connected and isolated from populations that were expected to have colonized via anemochory (**Figure 3**).

Table 4. Sampled populations of *Euchlanis chihuahuaensis* outside the dust corridor within the Trans-Pecos region from West to East.

Collection Site	Type	Date	Code	GPS coordinates	N
Bailey Evans B (IMRS), TX	Live	08.10.2021	BEB	30.778, -105.014	1
Horizon Tank (IMRS), TX	Live	08.21.2021	HRZ	30.766, -105.065	1
Peccary Tank (IMRS), TX	Live Sed	06.03.2013 09.25.2023	PEC	30.755, -105.004	11
Red Tank (IMRS), TX	Live	06.04.2014	RET	30.730, -104.989	1
Rattle Snake Tank (IMRS), TX	Sed	10.01.2022	RAT	30.746, -105.008	2
Paint Gap Tank, BIBE, TX	Live	05.14.2006	PGTBB	29.387, -103.302	1
Lonely Tank, (IMRS), TX	Sed	04.06.2022	LNY	30.727, -104.972	3
Kent Playa, Kent, TX	Live	06.18.2023			
Cattle Tank (White Sands), NM	Live Live	01.12.2006 08.08.2022	CAT	32.674, -106.443	5
Luna 26, NM	Live	07.07.2022	LNA	32.574, -107.436	2

The sites are ephemeral and unpredictable, which could also limit zoochory by migrating birds such as ducks, which have been shown to be mediators in aquatic invertebrate dispersal via both endo- and ecto-zoochory (Brochet et al., 2009; Coughlan et al., 2017). Other studies have shown that even invertebrates that are able to travel via land have very limited dispersion (Phillipsen & Lytle, 2012) and limiting these other factors could highlight possible anemochory dispersal in *Euchlanis chihuahuaensis*.

Figure 3. Sampling sites where *Euchlanis chihuahuaensis* occurs, including playas, rock pools, tanks, and draws: (1) Moon, (2) Horizon Tank, (3) Behind Ranch House Playa, (4) Draw 2, (5) Bailey Evans B, (6) Album Park, (7) Lonely Tank, (8) 404A, (9) Kent Bridge, (10) Gray Oak, (11) Pluvial Lake Palomas 1, (12) Luna 26, (13) Columbus Playa, (14) Peccary Tank, and (15) Pluvial Lake Palomas 2.

Sampling and Culture Methods

Water samples were obtained from sites within the dust corridor and outside the dust corridor to establish clonal lineages from each site. For areas where we were unable to obtain live samples, soil samples, from the top 5 cm of the site, were collected and rehydrated with 100– 200 ml of modified MBL media (Stemberger, 1981) and with 1 – 4 g of sediment. Larger rehydrations were conducted with 6 – 50 g of sediment and 500 ml of water due to low hatching success for Peccary tank (PET), Horizon Tank (HRZ), and the Mimbres River Valley -Pluvial Lake Palomas (PLP1) samples. Each isolate that was collected or hatched represented a clonal lineage of *E. chihuahuaensis*, established from a single amictic female. The clonal lineages were cultured in modified MBL media (Stemberger, 1981). Maintenance of the clonal colonies were maintained at ambient room temperatures and fed two to three times a week an MBL mixture of

both *Chlorella vulgaris* and *Chlamydomonas reinhardtii*. Both cultures were obtained from The University of Texas at Austin UTEX algae culture collection strain 30 and strain 90 respectively.

DNA Extraction, Amplification & Sequencing

DNA was extracted from 10-60 clonal individuals, which were cleaned with MBL media prior to extraction. The Insta-gene Matrix Chelex based DNA purification was used for DNA extraction for PCR template creation. The DNA templates were processed with 13 µL of InstaGene matrix (Bio-Rad) and 1 µL of Proteinase K (20mg/ml). Qiagen Hotstar MasterMix was used for PCR amplification and the PCR cycles included an initial cycle of 94°C for 15 minutes and 37 cycles of 94 °C for 1 min, 47 °C for 1 min and 72 °C for 1 minute. PCR on the extracted DNA was done using DNA conserved COI primers: HCO (TAAACTTCAGGGTGACCAAAAAATCA) and LCO (GGTCAACAAATCATAAAGATATTGG) (Folmer et al., 1994). After amplification, DNA was visualized via gel electrophoresis. The agarose gel containing the amplified product was purified using the MPBIO GENECLEAN® Kit. The gel was dissolved in 500-600 µl of 750 ml of sodium iodide (NaI) solution and warmed at 60°C until the agarose melted. Ten µl of GLASSMILK was added to each sample and mixed on ice for 45 min, with five min of resting between each mixing event. The samples were then centrifuged and the NaI removed. New Wash Concentrate, with a total of 1500 µL, was then added to each sample, with a starting volume of 500 µL, and repeated a total of three times, to continue the purification process. The remaining purified DNA was adhered to on the GLASSMILK beads and suspended in ultrapure autoclaved water, for a total of 12 µl of purified DNA solution.

The purified product was then sequenced at UTEP's Border Biomedical Research Center (BBRC) Genomic Analysis Core Facility. The sequencer used for this project is a 3500 Genetic Analyzer from Applied Biosystems, using the reagent BigDye Terminator v3.1 cycle sequencing kit (part 4337458) and polymer POP7 (part 4393708), and using the diluted reaction (0.5x) protocol. Successful sequencing yielded chromatograms which were then analyzed with DNA Sequence Assembler v4 (2013) and contig creation, subsequently then compared to sequences from previously described populations (**Table 1**).

Genetic Analysis

The cleaned sequences were aligned using MAFFT on the CIPRES Science gateway (Miller et al., 2010) and populations were then determined using STRUCTURE (Pritchard et al.2000). The number of populations were confirmed using STRUCTURE HARVESTER (Earl & vonHoldt, 2012). STRUCTURE (v2.3.4 July 2012) was run with K varying from 1–9, duplicate runs, with a burn-in period of 100,000 generations and the number of MCMC replicates after burning set at 500,000. The lowest log probability of the data was used to determine the number of K populations. Using the CIPRES portal (Miller et al. 2010), jModelTest2 on XSEDE (Guindon & Gascuel, 2003; Darriba et al., 2012) was used to obtain the model of evolution of TPM2uf+G. A Bayesian phylogenetic analysis was conducted using MrBayes v 3.2.7 on the CIPRES Science gateway (Miller et al.2010) using 10^7 generations, 25% burn-in, and two parallel runs and nst =6 (GTR) which is similar to the TPM2uf+G. A Maximum Likelihood analysis was also conducted with MEGA 11 (Tamura et al., 2021) with a bootstrap of 1000 replicates.

Distance matrices were constructed with MEGA11 (Tamura et al., 2021) and genetic distances were calculated for populations within the corridor and populations outside the

corridor, using an uncorrected p-distance model, with substitutions for transitions and transversions equally weighted, and with uniform rates among sites. Genetic diversity and structure were determined via a test for fixation (F_{ST}) and an AMOVA using Arlequin v3.5.2.2 (Excoffier & Lischer, 2010). To determine any possible correlation between geographic distances and genetic variability, R packages VEGAN (Oksanen, et al., 2022), GEOSPHERE (Hijmans et al., 2022), and APE (Paradis & Schliep, 2019) were used. A Mantel test analysis was conducted between the pair-wise genetic distances (K80) and geographic distances of the studied populations (Diniz-Filho et al., 2013), using the aligned FASTA sequences and the R packages VEGAN (Oksanen, et al., 2022), GEOSPHERE (Hijmans et al., 2022), and APE (Paradis & Schliep, 2019). To determine potential gene flow, a haplotype diversity (Hd) and nucleotide diversity π were conducted using DnaSP V6 (Rozas et al., 2017; 2009). Nucleotide and haplotype diversity can be used to infer genetic diversity in the populations, with higher values closer to 1 indicating more genetic diversity and with lower values closer to 0 indicating possible recent founder events or bottlenecks and low genetic diversity.

To visualize gene flow, an additional haplotype diversity test was conducted via Network v10.2.0.0 (Fluxus Technology Ltd., Clare, Suffolk, England Bandelt et al., 1999) using the population sets established on DnaSP V6 (Rozas et al., 2017; 2009) and STRUCTURE (Pritchard, Stephens, & Donnelly, 2000) from the aligned sequences. A population expansion analysis was conducted via a Tajimas D analysis on the data (Tajima, 1989) with SambaR (De Jong et al., 2020) using the R package APE (Paradis & Schliep, 2019).

RESULTS

Dust Corridor

Wind direction and wind speed data, from 1981 to 2020 and 126 sites in Southern New Mexico, Northern Mexico, and West Texas, from the NASA Prediction of Worldwide Energy Resources (POWER) site was used to visualize wind trends in the study area. Mean wind direction for the region appeared to follow the following patterns: from the West/Southwest area from January to June, and then from the Southeast from June to September. Some South/Southeast winds were observed in October; however, the direction appeared to change strongly back to originating from the West/ Southwest direction from October – December (**Figure 4**).

Wind speed was noted as mostly ranging from 4 m/s to over 7 m/s throughout the year and certain areas, such as in Southern New Mexico, past the Delaware Mountain, and into Reeves and Pecos Counties in Texas, appeared to show higher general wind speeds throughout the year (**Figures 4** & **5**). Average wind speeds in the area were noted to be lower as well during the monsoon season (4 m/s) before increasing again in September and changing back towards the West - East direction in October.

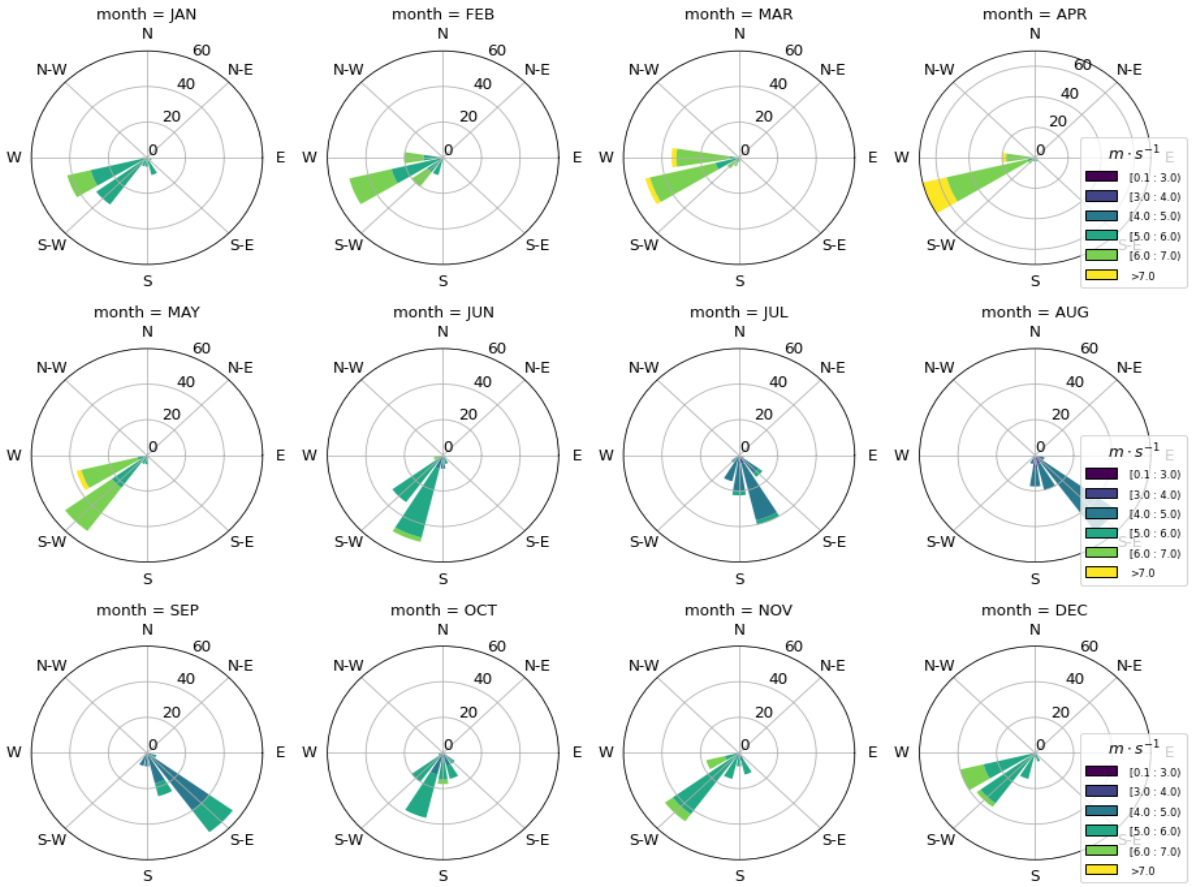

Figure 4. Average monthly wind direction and speeds, in the Trans Pecos, Mexico, and Southern New Mexico region, for the period from 1981 – 2020 from the NASA Prediction of Worldwide Energy Resources (POWER) site for the El Paso del Norte region. The concentric circles note the frequency of the observed with the triangular wedges denoting the general wind directions. The larger the wedge, the more dominant the direction of wind. The triangular wedges also are split into the proportion of wind speeds observed.

Wind speeds and directions from 1980 -2020 (**Figure 5**) were also noted and appeared to show consistent predominant patterns, of West to East from October to June, and then East to West from July to September during this period. Deposition areas include near White Sands, Big Bend National Park, and near Indio Mountain Research Station (shown in lighter colors (yellow and blues)).

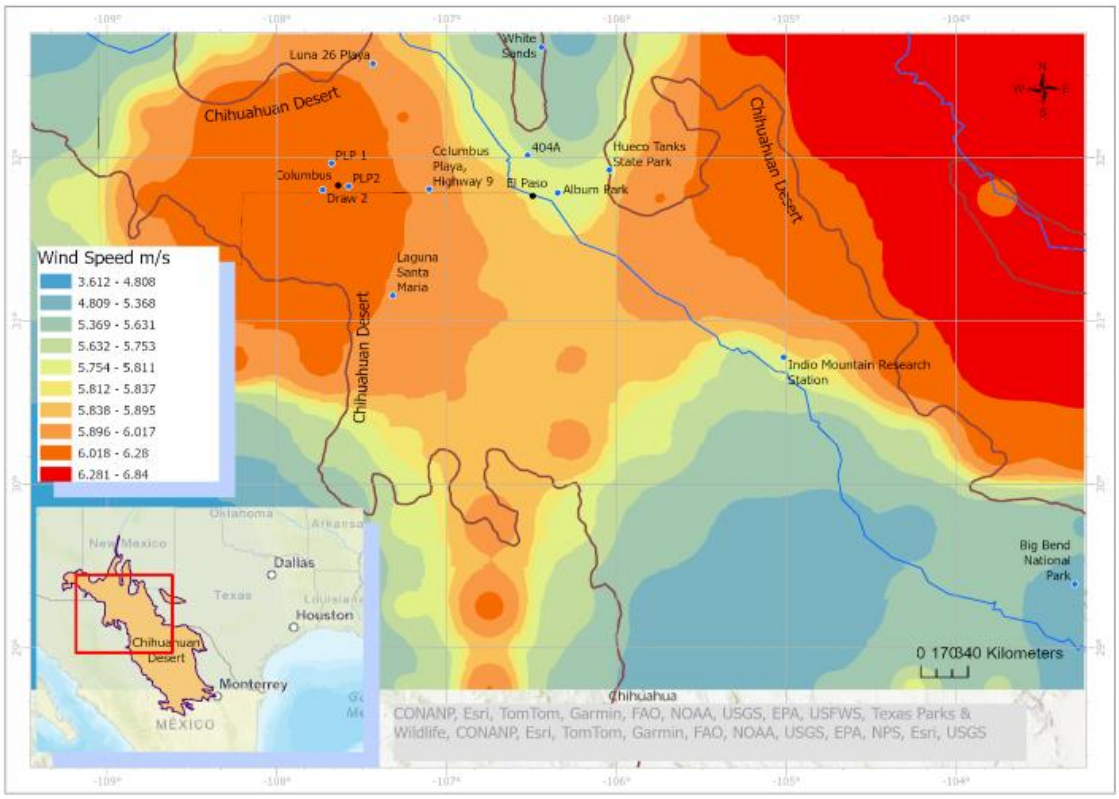

Figure 5. Average annual wind speeds for 2020 in the sample sites of this study. Areas in darker red have higher average wind speeds as compared to the lighter / bluer colored areas.

Cryptic Species Delimitation

A cryptic species analysis of individuals, of all *Euchlanis* lineages in Kordbacheh et al. (2017) with a total of N = 130 sequences, including two outgroups as well as the *E. chihuahuaensis* isolates used in this study. The cryptic species analysis identified 59 isolates as belonging to *E. chihuahuaensis* via Automatic Barcode Gap Discovery (ABGD; **Appendix 7b)**. Additional partitioning of *E. chihuahuaensis* isolates and the *E. dilatata* cryptic species complex (**Table 5**) was conducted to determine whether the isolates used for this study were *Euchlanis chihuahuaensis* as defined by Kordbacheh et al. (2017; 2019). The most conservative number of putative cryptic species within the studied isolated was four as identified by ABGD.

Table 5. Putative cryptic species determined by GMYC (Generalized Mixed Yule Coalescent models) using single and multi-threshold processes, K/Θ (K over Theta), ABGD (Automatic Barcoding Gap Discovery), and PTP (Poisson Tree Process) based on partial COI gene sequences to verify identity of *Euchlanis chihuahuaensis* isolates and *Euchlanis dilatata* cryptic species complex, used in this study. The analysis of N = 61 includes *E. chihuahuaensis*, the three individuals belonging to the putative cryptic species, and two outgroups.

Table 5. Putative cryptic species determined by GMYC (Generalized Mixed Yule Coalescent models) using single and multi-threshold processes, K/Θ (K over Theta), ABGD (Automatic Barcoding Gap Discovery), and PTP (Poisson Tree Process) based on partial COI gene sequences to verify identity of *Euchlanis chihuahuaensis* isolates and *Euchlanis dilatata* cryptic species complex, used in this study. The analysis of N = 61 includes *E. chihuahuaensis*, the three individuals belonging to the putative cryptic species, and two outgroups.

Method	**COI Gene Groups N = 61**	**COI Gene Groups (*E. dilatata* complex) N = 130**
GMYC (Single Threshold)	5 (1-14)	4 (1-129)
GMYC (Multi Threshold)	9 (1-13)	43 (36-67)
K/Θ	18	48
ABGD	4	23
PTP (Poisson tree processes)	19-44	44 – 79 (mean 61.71)

The highest partitioning of individuals based on the COI gene sequences was obtained from the PTP (Poisson Tree Processes) analysis which identified 19 – 44 putative species and K/Θ which estimated 18 independently evolving lineages. The lowest number of putative species was delimited by ABGD (Automatic Barcode Gap Discovery) which showed four putative species which grouped each outgroup as its own clade, the three individuals from the putative cryptic species (PLP1_06, PLP_14, PLP_18) as another group, and the remaining COI sequences as *E. chihuahuaensis* (**Appendix 7a**). GMCY single threshold showed five putative species with

the potential of there being 1 –14 separate groups and nine putative species, with the potential of there being 1 – 14 separate groups with the multi threshold method in GMYC. Isolates from Pluvial Lake Palomas site #1 (PLP1_06, PLP_14, PLP_18) clustered together and were similar to the outgroups *Euchlanis dilatata* and *Euchlanis kingi*, in the number of mutations; however, they were sister to the other two *Euchlanis chihuahuaensis* clades and thus were identified as a new putative species within the *Euchlanis dilatata* species complex. **Appendices** 1 to 8 includes the full results from the delimitation.

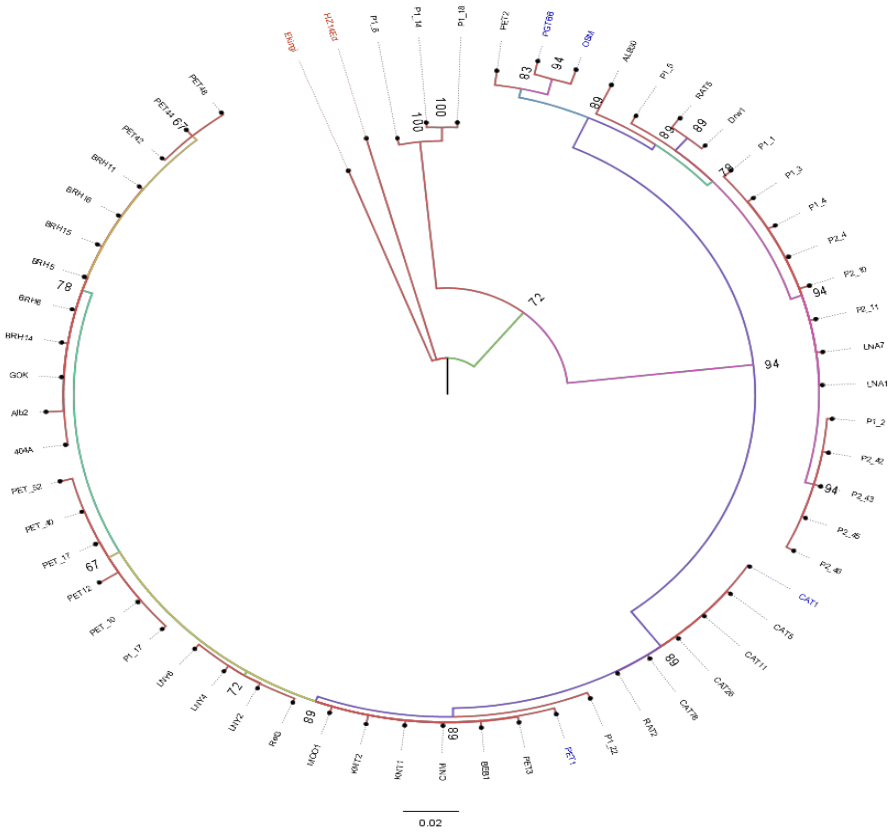

Figure 6. Bayesian phylogenetic reconstruction (Mr. Bayes v 3.2.7), of *Euchlanis chihuahuaensis* isolates used in this study based on a partial COI gene. The outgroups consisted of *Euchlanis kingi* (GenBank Accession number KX714920) and *Euchlanis dilatata* (isolate from Horizon Tank at Indio Mountains Research Station), and the 59 individuals genotyped in this study. Posterior probabilities for the respective nodes are based on Mr. Bayes.

A Bayesian analysis was conducted to construct a phylogenetic tree using partial COI sequences from *E. chihuahuaensis* isolates obtained in this study. The basal node for the putative cryptic (PLP1_06, PLP_14, PLP_18) species was highly supported (100%). The remaining isolates were clustered with individuals identified from Kordbacheh et al. (2017; 2019) and comprised two distinct clades. The Maximum Likelihood reconstruction (**Appendix 11**) also showed similar groupings; however, node support was generally less than that in the Bayesian reconstruction.

Population Structure

Three separate populations, Groups A, B, and C were identified by STRUCTURE with the best supported model being K = 3 with the estimated Ln Prob of – 446.8 (**Figure 7, Bar 1;** (**Appendix 9**)). Group A, which included three individuals (PLP1_06, PLP_14, PLP_18), was identified as a putative cryptic species (see **Appendices 1-8**) and was thus removed from the analysis.

Table 6. Haplogroup partitioning of populations by STRUCTURE v2.3.4 July 2012 and Structure Harvester of *E. chihuahuaensis* isolates, which does not include the putative cryptic species. Three Haplogroups were identified using partial COI sequences from 56 individuals.

Structure Grouping	**Sample Sites**
Haplogroup 1	OSM, PGTBB, PET2, ALB30
Haplogroup 2	BRH5, BRH6, BRH11, BRH14, BRH15, BRH16, GOK, 404A, CNM, LNY2, LNY6, MOO1, P1_17, PET_10, PET_17, PET_40, PET1, PET3, PET42_PET44, PET48, CAT26, CAT5, P1_22, PET_52, RAT2, RET3, CAT1, CAT11, CAT78, LNY4, KNT1, KNT2, BEB1, ALB2, PET12
Haplogroup 3	LNA1, LNA7, P1_2, P1_3, P2_11, P2_4, P2_42, P2_43, P2_45, P2_46, P2_10, P1_1, P1_4, P1_5, DRW1, RAT5

An additional STRUCTURE analysis, on the initial Groups B and C which were identified as *E. chihuahuaensis* and did not include the cryptic species, was conducted again. This analysis produced three separate populations (K=3; a mean Ln Prob of -386.3; **Appendix 10**).

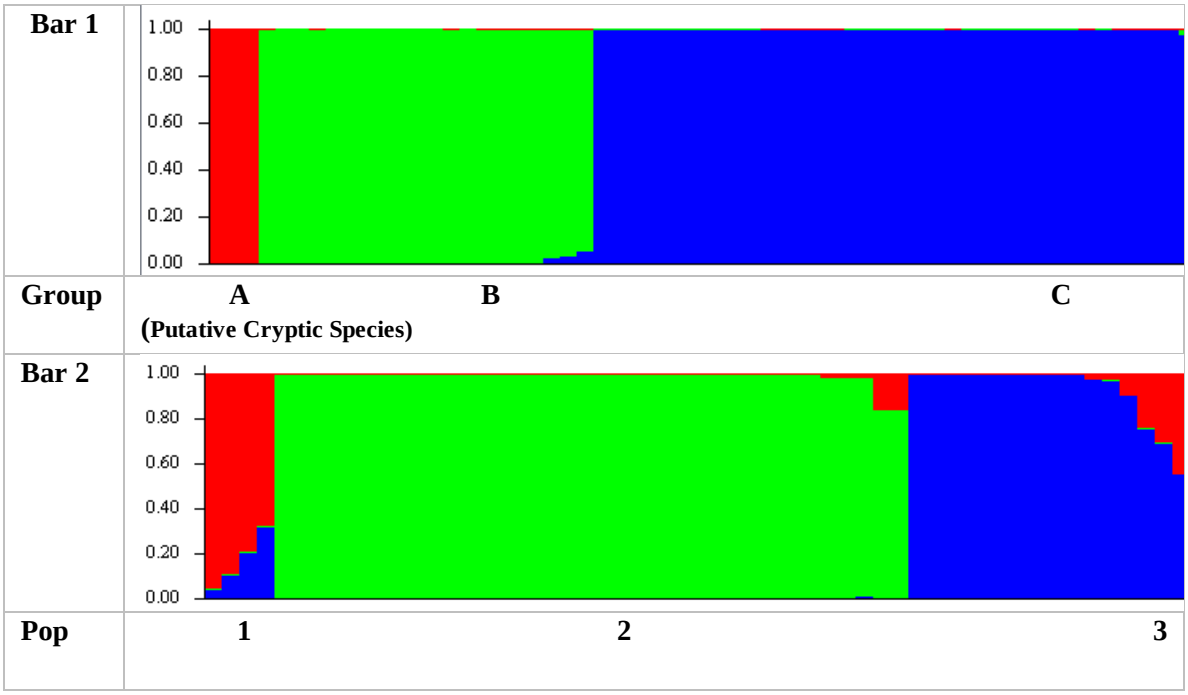

Figure 7. Bar plots of the estimated *Euchlanis chihuahuaensis* populations as identified by STRUCTURE analysis. Bar 1 denotes the partitioning including the putative cryptic species while Bar 2 does not.

Statistical Analysis

An AMOVA analysis was conducted with all individuals (see **Appendix 9)**, which included the three representatives of the putative cryptic species. The analysis (**Table 7**) noted most genetic variation of 90.34% among populations and 9.66 % variation within populations. This analysis showed significant genetic differentiation with an average F_{ST} of 0.90 over all loci and P value <0.05. An AMOVA analysis of the populations (**Table 8**) was conducted without the putative cryptic species isolates and showed genetic variation among populations to be 88.3 % and 11.7 % within populations, respectively, and an F_{ST} = 0.88 and P value <0.05.

Table 7. Genetic variation differences within and among sites assessed with the Analysis of Molecular Variance (AMOVA) to understand the partitioning of genetic variation across three populations of *Euchlanis chihuahuaensis* identified by STRUCTURE and found within the Trans Pecos, Mexico, and Southern New Mexico regions. This includes Group 1, which is a putative cryptic species (**Appendix 9**).

Source of variation	Sum of squares	Variance components	Percentage of variation
Among populations	508.51	16.77	90.34
Within populations	100.49	1.79	9.66
Total	609.00	18.57	100.00

F_{ST} 0.90335, P value <0.05

Populations were then partitioned into regions (**Table 9**) that included groups both within the dust corridor and outside the dust corridor, and an AMOVA analysis showed that variation among the populations was 58.00 % and 42.00 % within populations in the regions, respectively. The variation was statistically significant with a p value of < 0.05.

Table 8. Analysis of Molecular Variance (AMOVA) of the Haplogroups identified by STRUCTURE (**Table 6**) and Bayesian phylogenetic reconstruction. The analysis did not include the putative cryptic species and compares the molecular variance both within and between the partitioned sites.

Source of variation	d.f.	Sum of squares	Variance components	Percentage of variation
Among populations	2	186063.055	10.77679 Va	88.32
Within populations	35109	50036.034	1.42516 Vb	11.68
Total	35111	236099.089	12.20196	100.00

F_{ST} = 0.88320, P value <0.05

Table 9. An AMOVA of *Euchlanis chihuahuaensis* populations split by regions, conducted in Arlequin v. 3.5.2.2. Populations were divided by regions: 1 = sites in South Central New Mexico labeled (West) within the dust corridor; 2 (Central) = sites within dust corridor' 3 = (East) outside the dust corridor; 4 = (North) outside the dust corridor, and 5 = outside the dust corridor. Isolate abbreviations are given in **Table 2**.

Source of variation	d.f.	Sum of squares	Variance components	Percentage of variation
Among populations	4	119330.821	4.59343 Va	58.00
Within populations	35107	116768.268	3.32607 V b	42.00
Total	35111	236099.089	7.91949	100.00

F_{ST}:0.58002, P value <0.05

Region	Sites
1 (West)	LNA1, LNA7, P1_2, P1_3, P2_11, P2_4, P2_42, P2_43, P2_45, P2_46, Drw1, P1_1, P1_4, P1_5, P2_10, P1_17, P1_22
2 (Central	ALB30, OSM, 404A, BRH11, BRH14, BRH15, BRH16, BRH5, BRH6, CNM, GOK, MOO1, Alb2
3 (East)	RAT5, PET2, LNY2, LNY4, LNY6, PET_10, PET_17, PET_40, PET_52, PET1, PET3, PET42, PET44, PET48, RAT2, Ret3, PET12, BEB1
4 (North)	CAT11, CAT1, CAT26, CAT5, CAT78
5 (Far East)	PGTBB, KNT1, KNT2

To determine the genetic diversity of the populations inside the aeolian corridor, an AMOVA was also conducted solely with the populations located inside the corridor. The populations were

partitioned geographically to include West (PLP), Central (El Paso, Mexico, Anthony NM, Highway 9 playa) and Luna. The AMOVA (**Appendix 13**) noted higher genetic diversity among the populations inside the aeolian corridor (67.3%) compared to within population genetic diversity (32.7%). These values were also statistically significant at $p < 0.05$. Lastly, one additional AMOVA was conducted on populations located solely outside the aeolian corridor (**Appendix 14**). This analysis produced lower among population diversity values (25.28%) and higher within populations diversity (74.72 %) and statistically significant ($p< 0.05$).

Fixation indices were also obtained for both populations inside the aeolian corridor and populations outside the corridor. Pairwise F_{ST} values (**Table 10**) from the partitioned regional populations located both within the wind corridor and outside the dust corridor, were significant ($p < 0.05$) with values ranging from the lowest $F_{ST} = 0.08$ (regions 2&3) and the highest $F_{ST} = 0.77$ (regions 1 &4). The "Central" and "East" pairwise regions displayed the lowest F_{ST} value of 0.08 indicating less genetic differentiation between the two populations.

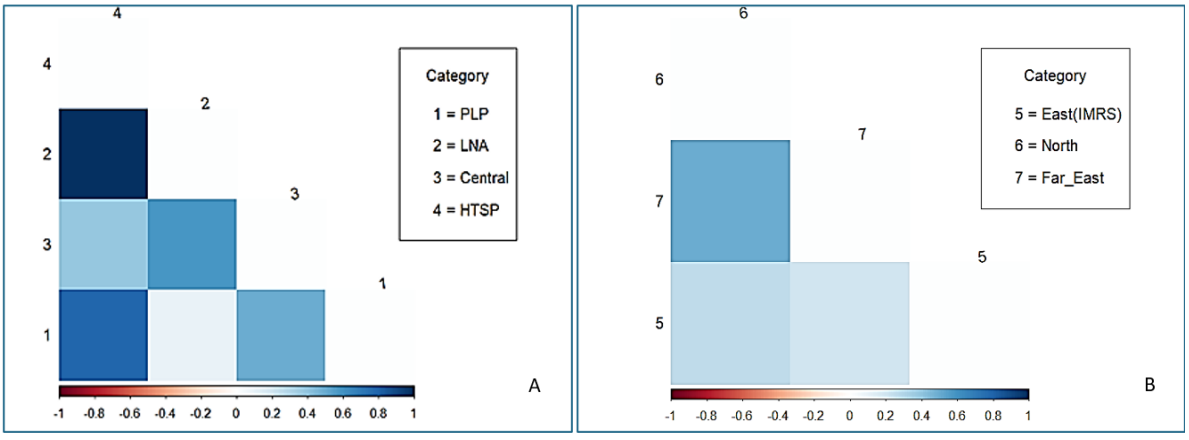

Figure 8. Pairwise F_{ST} values from populations of *Euchlanis chihuahuaensis* within the aeolian corridor (A) and outside the aeolian corridor (B). The populations are subdivided geographically in the different zones. Darker blue colors indicate higher F_{ST} values closer to 1, whereas lighter blue to white indicate F_{ST} values closer to 0.

However, a closer analysis of F_{ST} values overall showed higher values inside the aeolian corridor and that were statistically significant (**Figure 8, A**). Inversely, populations outside the aeolian corridor showed lower levels of F_{ST} values, which was also statistically significant (**Figure 8, B**).

Table 10. Pairwise F_{ST} values from the AMOVA analysis of *Euchalnis chihuahuaensis* populations in the Trans Pecos region of Texas and Southern New Mexico (**Table 9**). Populations are compared to one another depending on their location "In" inside the wind corridor and "Out" outside the wind corridor.

	1(West)	2(Central)	3(East)	4(North)	5(Far East)
1 (West) "In"	0.00000				
2 (Central "In")	0.68479	0.00000			
3 (East) "Out"	0.67702	0.07706	0.00000		
4 (North) "Out"	0.76803	0.34751	0.25753	0.00000	
5 (Far East) "Out"	0.59513	0.19538	0.19227	0.49644	0.00000

Genetic Diversity

The populations identified in **Table 9** were assessed for genetic diversity and the following values were found: Populations from the "North" regional group showed 0.00 for nucleotide diversity, indicating no diversity and a potential recent founder event or genetic drift. The Far East group shows the highest level of nucleotide diversity ($\pi = 0.0265$) compared to the other regions (**Table 11**). These values, however, are potentially influenced by the low number of individuals in both groups (N = 3 for Far East and N = 5 for North groups). When compared to which individuals are either located within the dust corridor or outside, the values show a larger π (0.02367) for populations within the dust corridor compared to populations outside the dust corridor (0.01215). This difference indicates that there is potentially more genetic diversity of the populations within the dust corridor, possibly providing support for more genetic exchange

within the dust corridor as compared to more isolated populations outside of the dust corridor influence.

Table 11. Nucleotide diversity of *Euchlanis chihuahuaensis* from the sampled sites, grouped by geographic region. Both the Far East and North have low sample numbers (3, 5 respectively). Three populations identified by STRUCTURE (**Table 6**). Population 1 includes individuals from OSM, PGTBB, PET2; Population 2 (Trans Pecos) includes those outside El Paso Texas, White Sands, IMRS, HTSPHS, and Kent Texas; Population 3 (Pluvial Lake Palomas) includes individuals from Pluvial Lake Palomas and Luna Tank, NM.

Grouping	Group	Nucleotide Diversity	Inside/Outside Corridor
Region	West (PLP)	0.012	Inside
Region	Central (Trans Pecos)	0.012	Inside
Region	East	0.012	Outside
Region	Far East	0.027	Outside
Region	North	0.000	Outside
Region Combined	Inside	0.024	Inside
Region Combined	Outside	0.012	Outside
Structure	Pop1	0.014	Both Inside & Outside
Structure	Pop2	0.003	Both Inside & Outside
Structure	Pop3	0.009	Both Inside & Outside

When compared based solely on “Inside” or “Outside” the dust corridor, the nucleotide diversity was noted as 0.024 and 0.012, respectively. A total number of 26 haplotypes (**Table 12**) were found (excluding the putative cryptic species).

Table 12. Haplotypes of *Euchlanis chihuahuaensis* identified using DnaSP from populations that do not include individuals from the new putative cryptic species. Abbreviations are defined in Table 2.

Haplotype	Number	Individuals
Hap_1	5	LNA1 LNA7 P1_3 P2_11 P2_4
Hap_2	5	P1_2 P2_42 P2_43 P2_45 P2_46
Hap_3	1	Drw1
Hap_4	1	P1_1
Hap_5	1	P1_4
Hap_6	1	P1_5
Hap_7	1	P2_10
Hap_8	1	RAT5
Hap_9	1	PET2
Hap_10	1	PGTBB
Hap_11	1	ALB30
Hap_12	1	OSM
Hap_13	8	404A BRH11 BRH14 BRH15 BRH16 BRH5 BRH6 GOK
Hap_14	6	CAT11 RAT2 CAT1 CAT26 CAT5 CAT78
Hap_15	4	CNM MOO1 PET1 PET3
Hap_16	3	LNY2 LNY6 Ret3
Hap_17	1	LNY4
Hap_18	4	P1_17 PET_10 PET_17 PET_40
Hap_19	1	P1_22
Hap_20	1	PET_52
Hap_21	3	PET42 PET44 PET48
Hap_22	1	Alb2
Hap_23	1	KNT1
Hap_24	1	KNT2
Hap_25	1	PET12
Hap_26	1	BEB1

Genetic distances (p-distances) ranged from 0.0089 to 0.0351 with the Western region having larger distances as compared to the others (**Figure 9**). Populations further east and north appear to be less genetically distinct from one another than compared to the Western Region where potential source populations are predicted to reside.

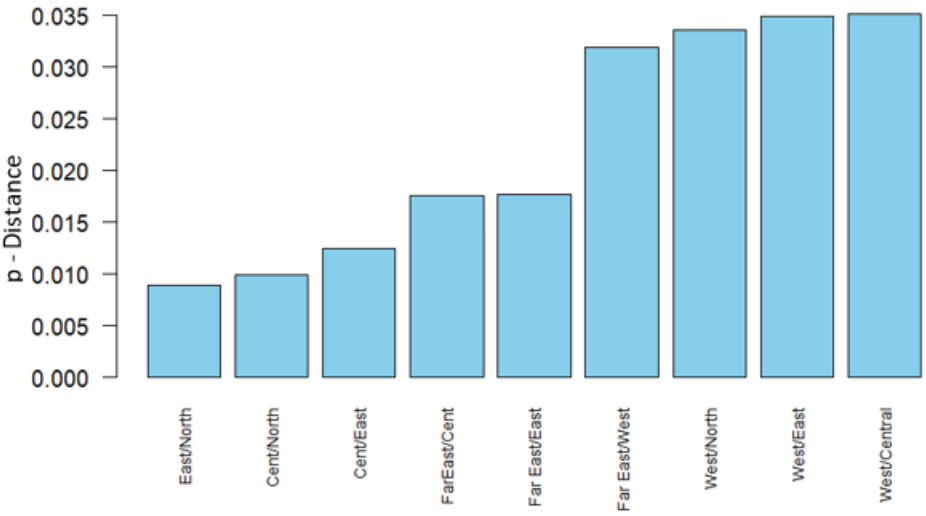

Figure 9. Comparisons of uncorrected "p" genetic distance of partial COI sequences between populations of E.chihuahuaensis partitioned within regions in the Trans Pecos, Southern New Mexico, and Mexico.

Haplotype diversity (**Table 13**) showed that populations in the "West" region and "East" regions had higher levels of haplotype diversity ranging from 0.85 to 0.93, while populations from the "North" had no detectable Hd (0.000). Populations to the "Far East" however showed unique haplotypes for each isolate while the "Central" population group had moderate levels of (Hd) at 0.62.

Table 13. Gene flow and Haplotype Diversity (Hd) analysis using DnaSP V6 (Rozas et al., 2017; 2009). Hd values range from 0.000 indicating no diversity and 1.00 indicating all unique haplotypes.

Population	Number of Sequences	Segregating Sites (S)	Number of Haplotypes (h)	Haplotype Diversity (Hd)	Average Number of Differences (K)	Nucleotide Diversity (Pi)
West	17	34	9	0.853	7.294	0.012
Central	13	33	5	0.628	7.628	0.012
East	18	40	11	0.935	7.699	0.012
North	5	0	1	0.000	0.000	0.000
Far_East	3	25	3	1.000	16.667	0.027

The first haplotype partitioning (**Figure 7**) of the individual isolates, showed substantial mutations between one particular group from Pluvial Lake Palomas – Mibresm River Delta and two other Haplogroups. Three individuals form a putative cryptic species as Haplogroup A. Haplogroups B constitutes individuals from Mexico, Big Bend National Park, IMRS, and Southern New Mexico and Haplogroup C is broadly distributed with haplotypes from the Trans Pecos Region and Southern New Mexico. The Haplotype network also includes the two outgroups of *E. kingi* and *E. dilatata*.

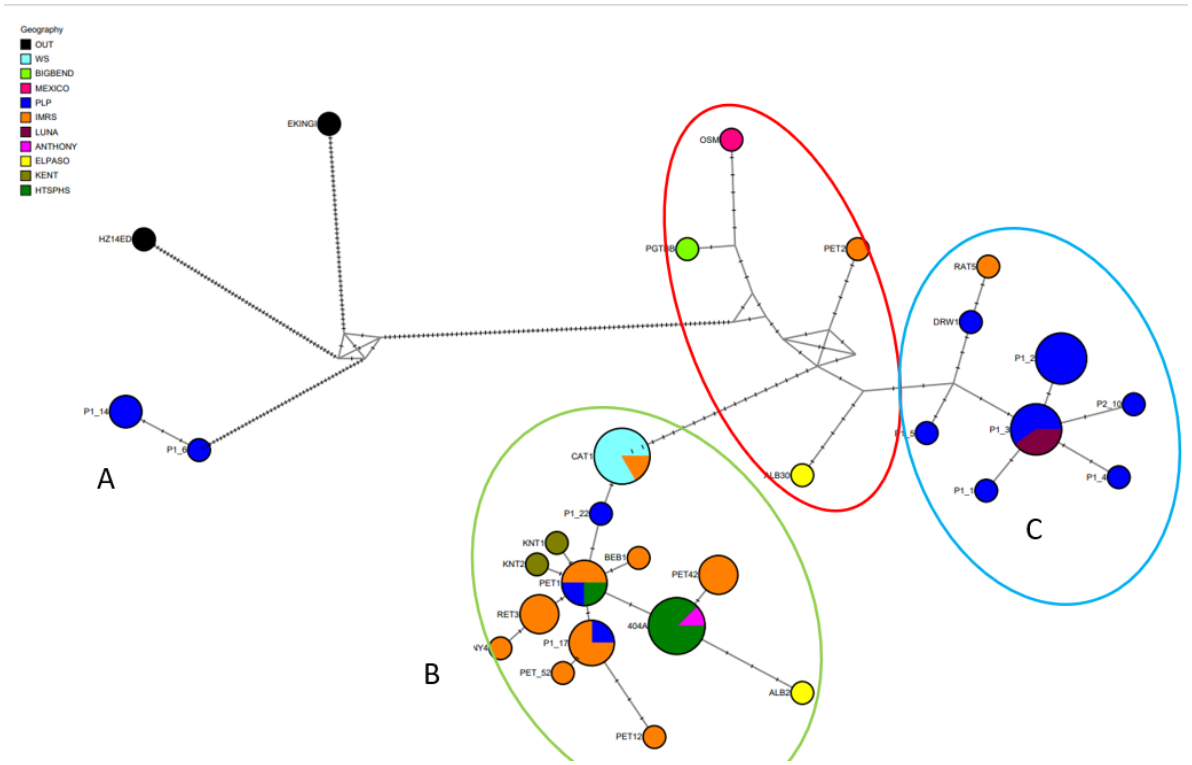

Figure 10. Haplotype network (Median Joining haplotype network from NETWORK v. 2.1.2.5) of *E. chihuahuaensis* based on COI sequences and identified via STRUCTURE, showing the initial partitioning of Group A (with putative cryptic species), and the other two groups (B and C) identified. It also includes the secondary partitioning of Haplogroups 1, 2, and 3 outlined by colored circles: Red (Haplogroup 1), Green (Haplogroup 2), and Blue (Haplogroup 3).

Further analysis without the representatives of the cryptic species resulted in support for three populations (**Figure 7, Bar 2**) and a haplotype map was created with the three haplogroups showing their geographic distribution (**Figure 11)**. Individuals comprising Haplogroup 1 are found in Mexico, IMRS, and Big Bend National Park; however, this only reflects a small sample size of N = 3. Haplogroup 2 has the widest geographic distribution and is found in New Mexico and West Texas. Haplogroup 3 also has a wide distribution; however, it is predominantly found in New Mexico with a couple individuals in Texas.

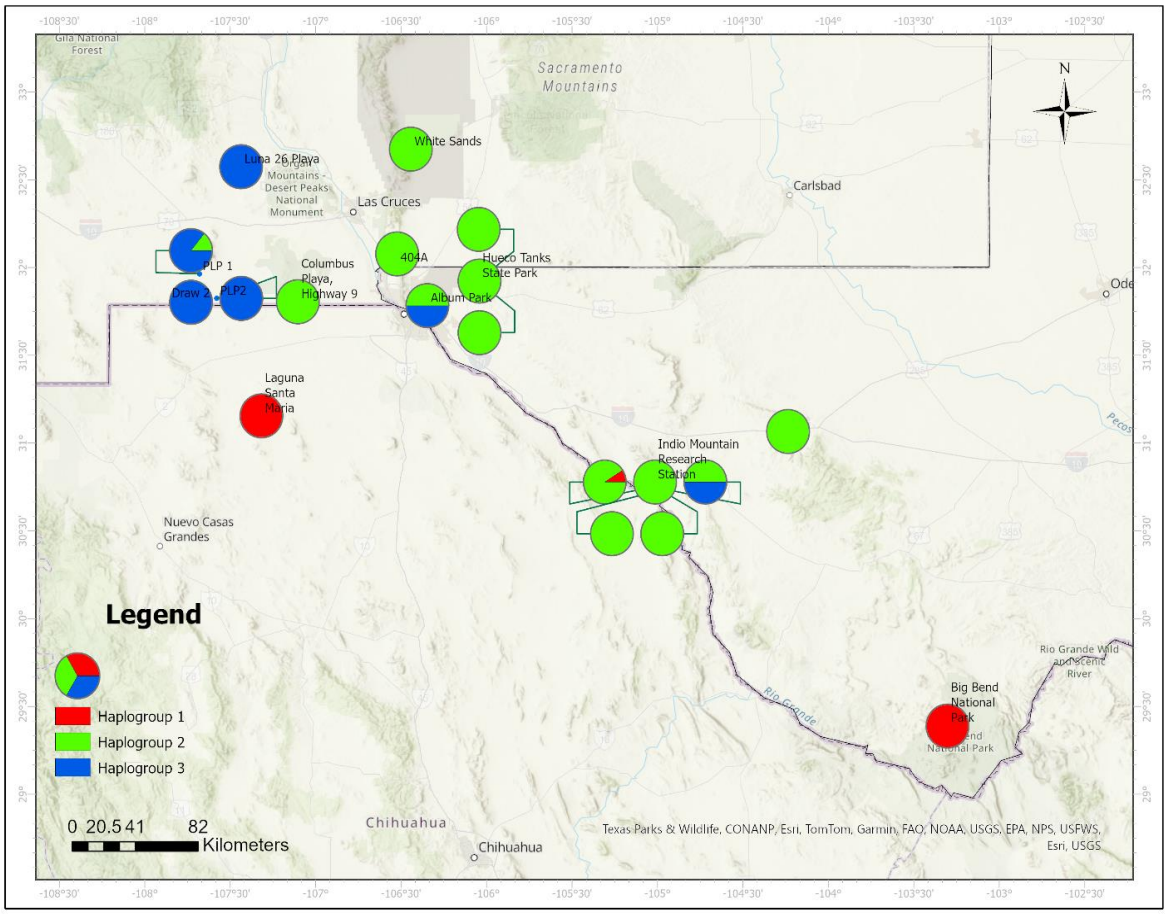

Figure 11. Haplogroup distribution of *Euchlanis chihuahuaensis* in the Trans Pecos Region based on COI sequences. Haplogroup 1 (Mexican Border), 2 (Trans Pecos), and 3 (Pluvial Lake Palomas) are color coded red, green, and blue, respectively. This map does not include isolates from the putative cryptic species.

A haplogroup map consisting of only individuals from Haplogroup 2 was created showing 14 unique haplotypes and their geographic distribution (**Figure 12)**. Haplotype 2 (blue) appears in Southern New Mexico, Hueco Tanks State Park & Historic Site, and at Indio Mountains Research Station. Haplotype 6 is mainly found at White Sands National Park and Indio Mountains Research Station. These two haplotypes have a wide distribution while the other haplotypes have either local distribution (Haplotypes1 and 3) or occur at a single location,

unique haplotypes (ex: Album Park (ALB), Kent Texas (KNT), and Peccary Tank (PET) at IMRS).

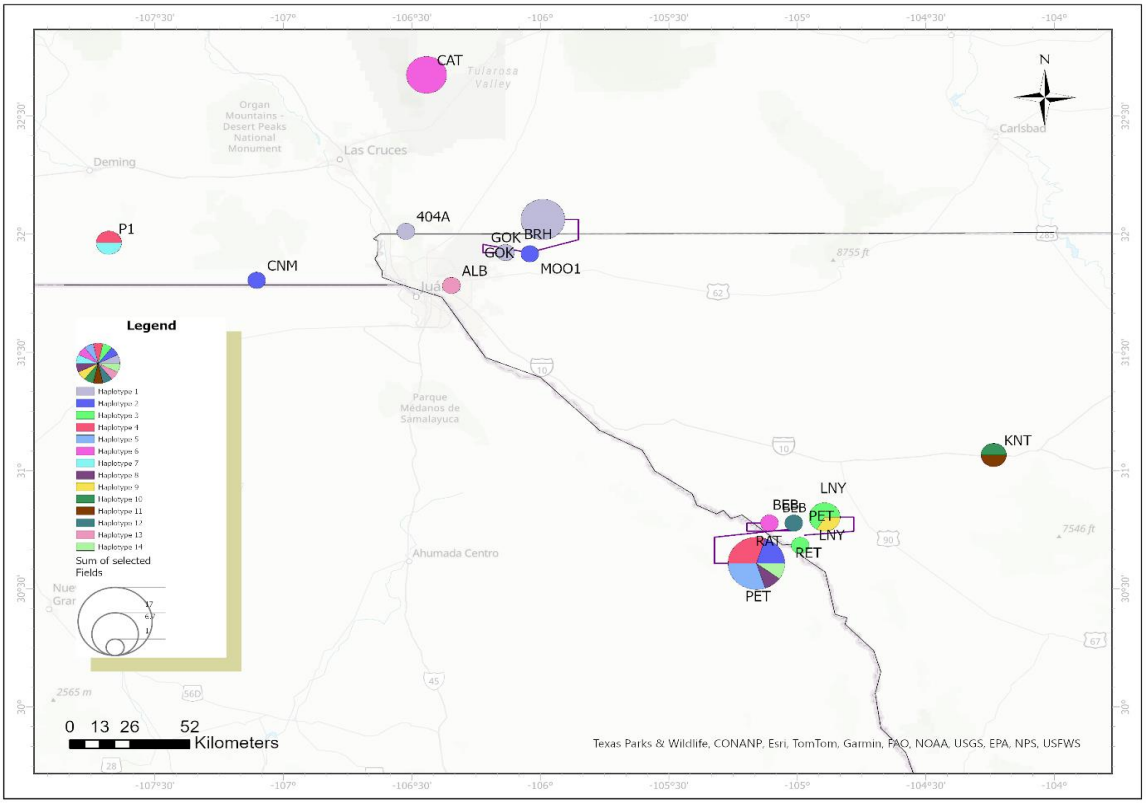

Figure 12. Haplogroup 2 (Trans Pecos) haplotype distribution map in the Trans Pecos, Mexico, and Southern New Mexico regions of *Euchlanis chihuahuensis* isolates from this study. Haplotype frequency is represented by the pie-chart proportion and each haplotype is color coded.

The haplogroup map created for Haplogroup 3 (**Figure 13**) showed nine unique haplotypes in the studied geographic area. Haplotypes 1 and 2 have local distributions between Pluvial Lake # 1 (P1), Pluvial Lake #2 (P2), and Luna 26 tank. The remaining Haplotypes are found at single sites and are unique haplotypes.

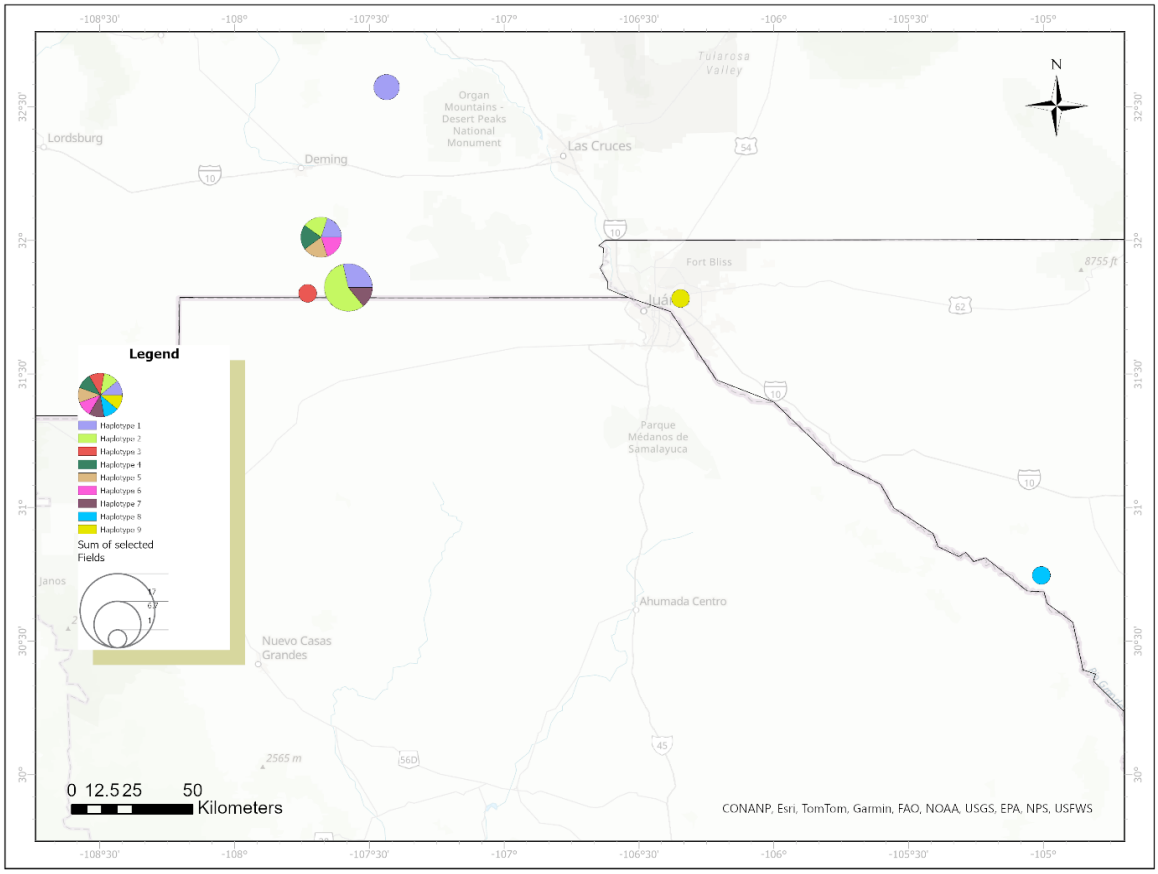

Figure 13. Haplogroup 3 (Pluvial Lake Palomas) haplotype distribution of *Euchlanis chihuahuaensis* individuals in the Trans Pecos, Mexico, and Southern New Mexico regions. Haplotype frequency is represented by the pie-chart proportion and each haplotype is color coded.

A Tajima's D test (**Table 14**) showed a value of -0.005, indicating possible population expansion; however, since results were not statistically significant, it could indicate low sample size.

Table 14. Tajima's D test for neutrality to determine potential population expansion or contraction was calculated in DnaSP V6 (Rozas et al., 2017; 2009) based on COI sequences from the 56 individuals used in this study with a significance set at $p < 0.05$.

Measure	Value
Number of polymorphic (segregating) sites, S	60
Total number of mutations, Eta	63
Average number of nucleotide differences, k	13.692
Nucleotide diversity, Pi	0.022
Theta (per sequence) from Eta	13.715
Theta (per site) from Eta	0.022
Tajima's D	-0.006
Statistical significance	Not significant, P > 0.10

Isolation By Distance

Several Mantel tests for Isolation by Distance (IBD) were conducted using combinations of untransformed and log transformed data, with 300,000 permutations each. The initial Mantel analyses were tested over the entire data set and over each individual haplogroup to showcase any patterns of Isolation by distance (IBD). The Mantel analysis of all combined haplogroups, both untransformed and log transformed, showed a significant relationship between genetic and geographic distances (Mantel r values ranging from 0.26 - 0.38 and all with a significant value of $p < 0.05$) (**Figure 14**). The Mantel test for Haplogroup 2 (**Appendix 15**) produced mantel r statistic values ranging from 0.26 to 0.62 through the various non transformed and log transformed iterations, and all of which showed statistical significance ($p < 0.05$). This Haplogroup (Haplogroup 2) displayed a higher correlation between genetic distance and geographic distance, indicating IBD. Haplogroup 3 also produced statistically significant ($p < 0.05$) Mantel r statistics showing values ranging from 0.13 to 0.33 (**Appendix 16**) which were lower than the other two Mantel tests. This group was the largest dataset, with multiple populations that span hundreds of kilometers; however, many populations consist of very few individuals (1 – 5) which could potentially influence the results.

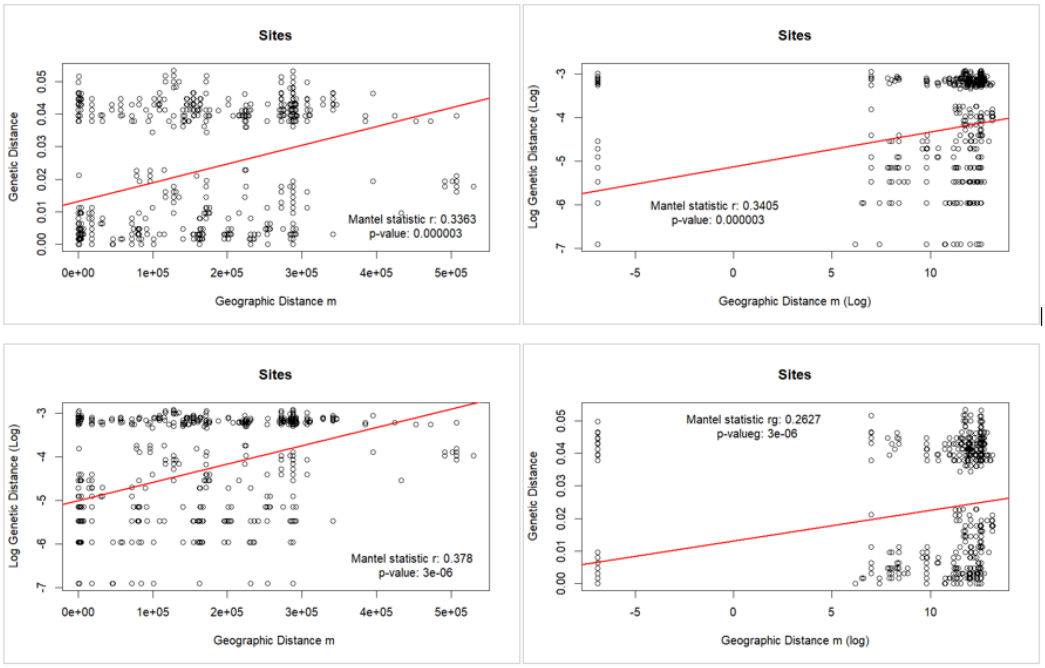

Figure 14. Correlation of geographic distances (m) and pairwise genetic distances (K80) of *E. chihuahuaensis* from all the sites included in this study (without the putative cryptic species).

Populations solely within the aeolian corridor were also tested for IBD using a Mantel. In this case, the test showed significant correlation between genetic and geographic distances, ranging from a Mantel r statistic of 0.379 in the lowest end to 0.572 in highest end, with transformed and untransformed permutations(**Figure 15**).

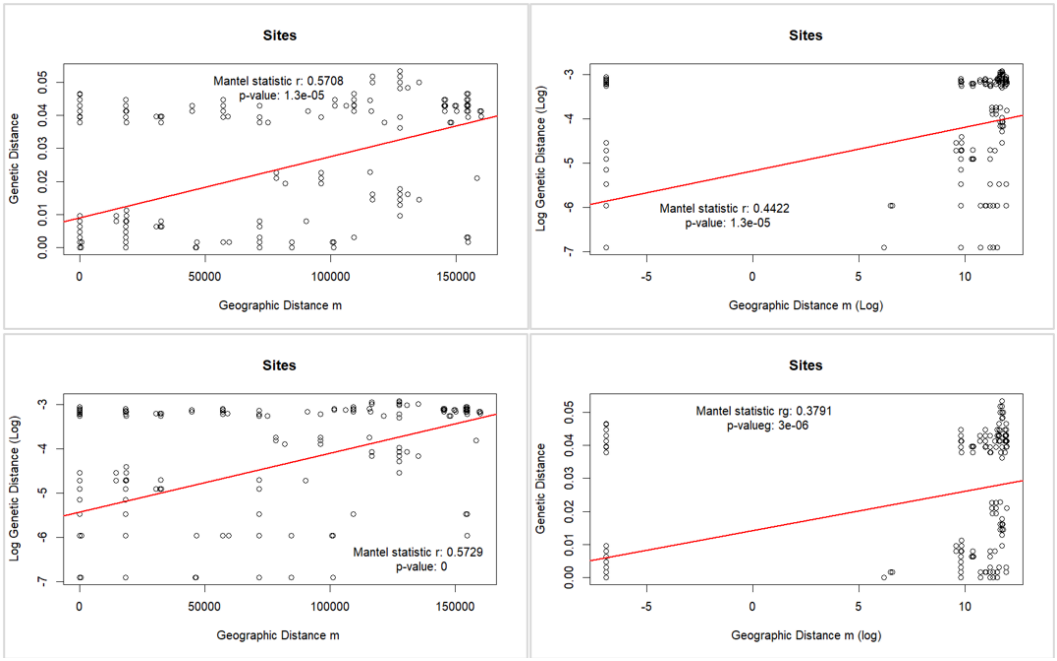

Figure 15. Mantel analysis of Isolation by distance (IBD) of the *Euchlanis chihuahuaensis* populations inside the aeolian corridor. The analysis was conducted with a genetic pairwise distance (K80) matrix composed solely of populations located inside the aeolian corridor and geographic distance. The analysis was conducted with both transformed and untransformed data.

The largest mantel r statistic was that where the genetic distances were log transformed and the geographic distances were not. To test for IBD in populations outside of the aeolian corridor, an additional Mantel test was also performed for those populations. This analysis produced mantel r statistic values which were much lower than those from inside the aeolian corridor. They ranged from 0.09 to 0.24 (**Figure 16**) in the various transformations. The highest Mantel r statistic in these iterations was where both the genetic distances and geographic distances were log transformed.

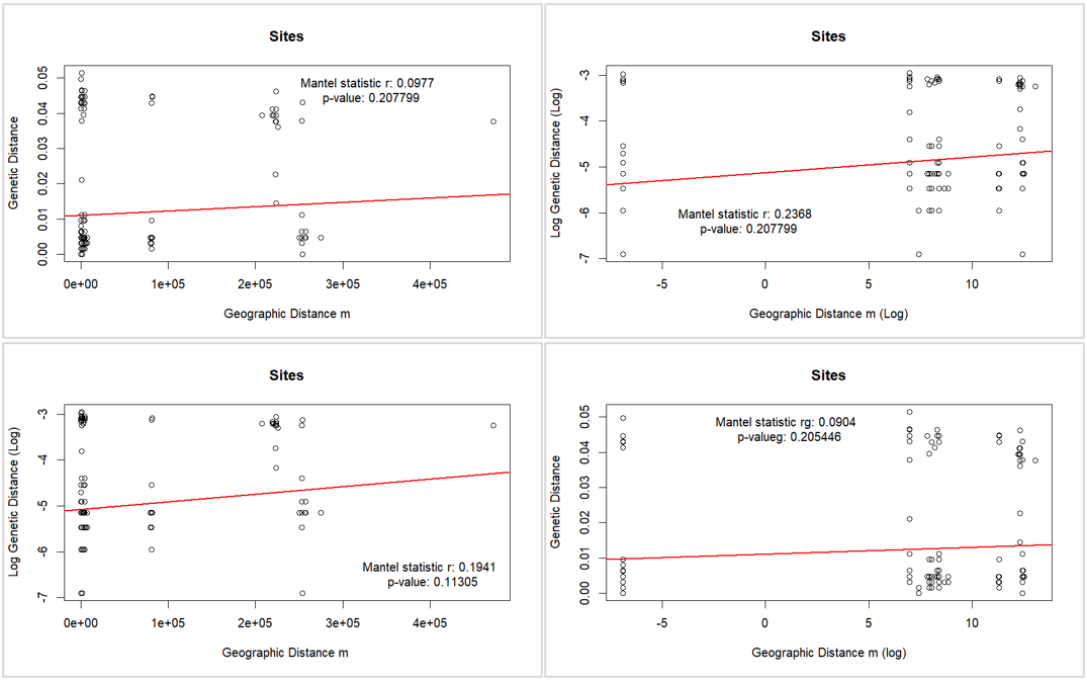

Figure 16. Mantel analysis of Isolation by distance (IBD) of the *Euchlanis chihuahuaensis* populations by location, in relation to the aeolian corridor. The analysis was conducted with a genetic distance matrix (K80) of *E. chihuahuaensis* populations outside the aeolian corridor and a geographic distance matrix. The analysis was conducted with both transformed and untransformed data.

DISCUSSION

Genetic structure of populations has been well documented for many aquatic invertebrates, including rotifers. However, the role of dispersal shaping the structure has only been investigated at the local scale (Vanschoenwinkel, Gielen, Vandewaerde, Seaman, & Brendonck, 2008; Vanschoenwinkel, Gielen, Seaman, & Brendonck, 2008; Cáceres & Soluk, 2002)and has not included representatives of the Rotifera. This research aimed to investigate the genetic structure and potential role of anemochory in facilitating gene flow of the monogonont rotifer *Euchlanis chihuahuaensis*. Clear directional patterns of wind direction and speed throughout the year, over a forty-year period were documented. This regular pattern is important in a system where other dispersal mechanisms are highly limited or nonexistent for aquatic bound organisms. Population structure of *E. chihuahuaensis* populations in the Trans Pecos, Mexico, and Southern New Mexico was evident. Overall, haplotype diversity was relatively high in all the regions, with the exception of the population located at White Sands, which showed no diversity. A few haplotypes showed broad range distributions; however, the majority of the haplotypes were located in single sites. There was a marked difference between population nucleotide diversity from populations located in Southern New Mexico and the other regions. Overall, the populations in the central region of the study site appeared to be similar in characteristics such as haplotype diversity and nucleotide diversity π; however, there are indications of overall lower genetic diversity values from populations outside dust influenced regions (**Table 11**). Nucleotide diversity for the combined outside the aeolian corridor regions was 0.012 compared to the combined overall nucleotide diversity of populations inside the aeolian corridor, which was 0.024. Thus study demonstrates that wind mediated dispersal of rotifer diapausing eggs can help share genetic structure of these arid land populations.

Previous studies examined dispersion of aquatic microinvertebrates across geographic distances and found evidence for local, intermediate, and long-distance dispersal. For example, Pinceel et al. (2015) noted that larger propagule sizes of Branchiopoda resting stages, ranging from 400 to 1600 µm, were able to be lifted off the ground, with surface winds between 5 - 14 km/h (1.4 – 3.9 m/s). Rotifer resting eggs, however, are smaller and range from approximately 50 – 200 µm (Guerrero-Jiménez et al., 2019; Rivas et al., 2018, 2019). A recent wind tunnel study by Arenas-Sánchez et al. (2023) noted that diapausing eggs of another monogonont rotifer species, *Brachionus plicatilis* were able to be lofted at low speeds of 6 km h^{-1} or 1.67 m/s. This study noted that larger, heavier eggs of *B. plicatilis* were more likely to be airlifted than those of *Brachionus rotundiformis*, which is another member of the *B. plicatilis* cryptic species complex. Their study also noted that even at low wind speeds, dispersal was possible. The authors suggest that different mechanisms occur before and during anemochory where dispersal could happen by "bouncing" or staying close to the ground or by getting entrained in the wind and traveling longer distances. Rivas et. al. (2018) noted that higher wind speeds could allow for longer distance dispersal at wind speeds of ~ 40 km^{-1} (11 m/s) which is lower than the average wind gust speed noted in the El Paso region of 22.8 m/s from the National Weather Service from 2013 – 2022 (T. Gill, personal communication, April 02, 2024, **Appendix 12**). Thus, it can.be inferred that wind gust averages throughout the year in the Trans Pecos region would be sufficient to loft and potentially entrain resting eggs and thus facilitate dispersion. Rivas et al. (2018) demonstrated that this is the case and that the majority of particles and matter transported fell within ~ 40 - 600 µm propagule size range. Many of the ephemeral aquatic sites in Northern Chihuahua and Southern New Mexico where these micrometazoan can be found are in areas with average annual wind speeds exceeding 5 m/s, which is higher than the 1.4 – 3.9 m/s wind speeds

noted by Pinceel et al.,(2015) and Arenas-Sánchez et al. (2023). Wind direction and wind speed data from 1980 – 2020 showed that most of the higher winds (> 6 m/s) occurred from November – June and that the predominant direction was from the Southwest direction. Over the span of the forty-year dataset, the predominant directions appeared to oscillate from the Southwest/ West direction during the cooler months of November through May before switching to an originating direction of Southeast, which is associated with the North American Monsoon (Rogash, 2003). Several studies have shown that the dust sources affecting the Paso del Norte Region originate in areas of previously disturbed marginal agricultural land, low-relief alluvial deposits including river floodplains, and the remnants of pluvial lakes such as Paleo Lake Palomas (Baddock et al. 2011, Dominguez Acosta 2009, and Rivera Rivera et al. 2009, 2010). The wind speed and direction in my dataset (1980 – 2020) as well as those from previous studies provides support for regular and predictable dust events, through the "dust corridor" that could facilitate gene flow among populations of zooplankton in isolated ephemeral habitats.

Previous studies focused on gene flow have shown local (Lopes et al., 2016) and regional level (Kimpel et al., 2015) dispersion with unclear levels of long distance (hundreds of kilometers) impacts. Prior studies have shown that rotifer populations are more similar in assemblage and genetic distance at closer (**Table 15**) regional distances (Brown et al., 2020); Kordbacheh et al., 2017; Obertegger et al. 2014); however, there are substantial differences differat larger continental scales (Liang et al., 2022; Kordbacheh et al., 2017; Leasi et al., 2013).

One characteristic that seems to be prevalent in Rotifera is the presence of cryptic species. Species in a cryptic species complex, however, present issues in determining which individuals belong to which species for further analysis. Prior studies have shown that rotifers show high endemism and local levels of similarity (Iakovenko et al., 2015; Kordbacheh et al.,

2017). Furthermore, rotifers in the Chihuahuan Desert have shown high genetic variability even within species complexes, indicating long evolutionary periods of isolation (Kordbacheh et al., 2017, 2019). The initial partitioning in STRUCTURE identified a putative cryptic species as its own population and two other distinct populations in the dataset. Further partitioning, without the putative cryptic species, revealed that the two *Euchlanis chihuahuaensis* populations were subdivided into three separate haplogroups. The haplogroups appeared to have distinct geographic regions with little overlap and contact with the other regions. These regions could potentially be isolated by limited hydrochory and zoochory; however, anemochory in well-defined corridors could bridge the gap between the sites. The dust storms modeled on HYSPLIT indicated potential dust corridors flowing from regions in Northern Mexico towards El Paso Texas, but also occasional Southeastern paths towards IMRS, which in some instances could not rule out aeolian transport from western to eastern sites from October to May and then from eastern to western sites during the monsoon season (June – September). The low number of individuals in this study from outside the corridor region, however, could be limiting our understanding of dispersion along the dust corridor gradient.

The isolated ephemeral habitats sampled in this study are situated in places where dispersal from hydrochory would be less likely. In past studies populations of *Euchlanis dilatata* studied along the Rio Grande, a hydrologically connected system, showed higher levels of genetic differentiation within populations (89.6%) compared to among populations (10.4%) and is indicative of populations in regular contact (Kordbacheh et al., 2017). On the contrary, Kimpel et al. (2015) noted higher local genetic differences among populations (63.2%) of *Synchaeta pectinata* compared to 36.8% within populations that occurred in sites separated by 4 – 50 km. Hydrologically connected populations likely provide more opportunities for panmixia, and the

conservation of alleles as compared to non-hydrologically separated sites where other effects of dispersal could take place such as priority effects, genetic drift, and selection (references). High levels of genetic differentiation between (88.3%) and within populations (11.7%), which was expected with the putative cryptic species included in the analysis. Furthermore, these populations were partitioned into regional populations, and with the removal of the cryptic species, still display high levels of genetic differentiation (58% among;42% within) indicating possible barriers to gene flow that are contributing to the homogenization of the populations. Within population genetic homogeneity is relatively high; however, this still lends some support to my hypothesis that there are genetic differences between populations located inside and those located outside of the dust corridor (**Table 9**). The expectation would be at either spectrum, in that high levels of genetic differentiation among populations could indicate little to no gene flow versus high levels of genetic differences within populations indicating panmixia. This intermediate level of differentiation indicates that there are genetic differences which are measurable, potentially due to geographic barriers or historical events; however, shared ancestry of the populations or gene flow could account for the higher levels of within population differentiation. This sets up a scenario where low levels of gene flow in fragmented populations can influence population structure.

Genetic distances between individuals and populations, along with fixation indices, can elucidate similarities or differences between the individuals or groups (references). Previous studies have shown the varying levels of genetic distance at both regional and continental levels (**Table 15**) and some distinct differences can be noted. For example, Liang et al. (2022) noted higher genetic distances when comparing populations of *P. dolichoptera* and *P. vulgaris* from Southeastern China and North America. They noted genetic distances of 24.8% and 22.3%,

respectively. These values are substantially higher than estimates from populations in regional areas in either continent which are 18.8% and 17.3%, respectively. Other observed populations of monogonont rotifers show much smaller regional distances, ranging from 0 to 8.5% in some populations. One such example of a smaller regional genetic distance would be for P. *vulgaris*, which showed genetic distances between a regional area at 5% within Southeastern China (Liang et al., 2022). Previous studies of the *Euchlanis dilatata* species complex found large genetic distances (22%) in continental populations in North America while estimates within populations ranged from 0 – 2.5 %. This study produced genetic distances similar to those reported by Kordbacheh et al. (2017), Campillo et al. (2011) and Obertegger et al. (2014). Interestingly, the study by Campillo et al. (2011) on genetic structure of *Brachionus plicatilis* was conducted in areas similar to the Paso Del Norte Region (i.e., semi-arid areas near the Southeastern portion of the Iberian Peninsula and near the Monegros Desert).

Ephemeral aquatic habitats in the Chihuahuan Desert have previously been shown to harbor high endemism and diversity (Brown et al., 2020 & Seidel, R. A., Lang, B. K., & Berg, D. J. (2009). One such measure of diversity would be haplotypes, which in the Kordbacheh et at. (2017 study showed that they were distributed across a broad geographic range (over 4000 km). Previous research in similar habitats, such as in the Iberian Peninsula (Campillo et al.2011), noted multiple unique haplotypes in their populations of *B. plicatilis*. This compares similarly to this study in that the Haplogroups that were observed in the Trans Pecos, Mexico, and Southern New Mexico region (**Figure 10**) display discrete, private haplotypes. There are some instances where there is common haplotype between regions, Haplotype 15 for example (**Table 12**), that is found in multiple areas such as in Columbus Playa (CNM), Hueco Tanks State Park & Historic Site (GOK), and Indio Mountains Research Station (PET).

Table 15. Mean genetic distances (uncorrected p-distance of partial COI gene sequences) of Monogononta rotifers from prior studies and compared to those found in the current study. Modified and expanded from Kordbacheh et al. (2018).

Population	Comparison	Mean p-distance	Source
Polyarthra dolichoptera	Southeastern China vs. Eastern N. America	0.248 ± 0.052	Liang et al., 2022
P. vulgaris	Southeastern China vs. Eastern N. America	0.223 ± 0.02	Liang et al., 2022
P. vulgaris	Within Eastern North America	0.049 ± 0.067	Liang et al., 2022
P. dolichoptera	Within Eastern North America	0.188 ± 0.111	Liang et al., 2022
P. dolichoptera	Within Southeastern China	0.173 ± 0.089	Liang et al., 2022
P.dolichoptera	within species	0.044	Obertegger et al., 2014
P.dolichoptera	between species	0.05-0.24	Obertegger et al., 2014
P. vulgaris	Within Southeastern China	0.055 ± 0.088	Liang et al., 2022
Limnas melicerta	Continental - mean genetic distance	0.081 - 0.219	Kordbacheh, L. Wallace, & J. Walsh, 2018
L. ceratophylli	Continental - mean genetic distance	0.151 - 0.2120	Kordbacheh, L. Wallace, & J. Walsh, 2018
Testudinella clypeata	within clades – Sweeden & UK	0.16-4.5	Leasi et al., 2013
Testudinella clypeata	between clades – Sweeden & UK	16.7-27.7	Lasi et al., 2013
Synchaeta spp.	Regional - within clades	0.02–0.027	Obertegger et al., 2012
Synchaeta spp.	Regional - between clades	0.059–0.253	Obertegger et al., 2012
Synchaeta pectinata	Oldenbur-Eastern Friesland vs. South Tyrol	0.085 ± 0.010	Kimpel et al., 2015
S. pectinata	Regionally - Oldenburg-Eastern Friesland	0.057	Kimpel et al., 2015
S. pectinata	Regionally - South Tyrol	0.046	Kimpel et al., 2015
Brachionus plicatilis	Regionally - Iberian Peninsula	0.027	Campillo et al.,2011
Brachionus plicatilis	Regionally – Iberian Peninsula within clades	0.133	Gómez et al., 2002
Brachionus plicatilis	Regionally – Iberian Peninsula between clades	≥ 0.119	Gómez et al., 2002
Euchlanis dilatata	Among Populations - Continental	0 - 0.219	Kordbacheh et al., 2017
Euchlanis dilatata	Within Populations - Continental	0 - 0.025	Kordbacheh et al., 2017
E. chihuahuaensis	Meta population Inside - Dust corridor	0.0237	Current Study
E. chihuahuaensis	Regionally – Trans Pecos	0.02183	Current Study
E. chihuahuaensis	Meta population Outside - Dust corridor	0.0121	Current Study

None of these sites have hydrological connections and are geographically isolated (~ 100-230 km) from one another; however, zoochory could be a potential factor. Most of the haplotypes identified, however, appear to be private haplotypes located at either single sites or local sites. This pattern of haplotypes is similar to that found in the Campillo et al. (2011) study. Here, there were three locations where haplotypes co-occurred: Pluvial Lake Palomas Playa 1(P1), Album Park El Paso, TX (ALB), and Peccary Tank at IMRS (PET). The presence of the same haplotypes in several locations is an indication of long-distance dispersal (reference).

One of the factors that could potentially affect the genetic composition and gene flow of the populations in the Chihuahuan desert is the sheer distance, harshness of the environment, and temporal hydroperiods separating ephemeral aquatic habitats. This separation could have effects on populations by decreasing gene flow the further populations are from one another. The patterns of isolation by distance in this study were significant at different levels of partitioning within the Haplogroups and by regions located inside and outside the aeolian corridor. The Mantel analysis revealed that populations outside the aeolian corridor showed the lowest levels of IBD (0.09, **Figure 16**) and populations inside the aeolian corridor showed significantly higher levels of IBD (0.379 – 0.572). This is counter to the proposed hypothesis that populations inside the corridor were more likely to be similar to one another than those outside the corridor. These high IBD values could be confounded however with other factors such as environmental or ecological factors as described by Jiang et al. (2019). In their study, they noted high among populations genetic diversity, lower within genetic diversity, and IBD in their study of desert pines. Even though *E. chihuahuaensis* is in a different Kingdom, the genetic and environmental patterns are similar to those found by Jiang et al. (2019). Further analysis factoring out ecological factors showed that Isolation by Environment (IBE) was mimicking IBD patterns in

their populations. This can compare to populations of *E. chihuahuaensis* in the Trans Pecos region and inside the aeolian corridor in that the habitat makeup could be more of a factor affecting the genetic structure and makeup of the populations. The populations outside the aeolian corridor however showed substantially lower IBD values (0.09 -0.23) along with lower F_{ST} values compared to populations inside the aeolian corridor (**Figure 8**). The difference in the genetic diversity between the populations in relation to the aeolian corridor could be due to multiple wind corridors, from different? wind directions, entering the Paso Del Norte region and bringing diverse sets of populations into the area. A review of IBD and IBE by Sexton, Hangartner, & Hoffman (2013), they noted that in invertebrates, patterns of IBE were high in populations with higher F_{ST} values and could also co-occur with IBD, with both being factors in the genetic structure of the populations. One of the reasonings would be that even though there could be a large amount of potential for migration and thus gene flow, new migrants arriving to a specific habitat might not be well adapted, environmental filtering, and thus fail to integrate into the local population. This would indicate that ecological factors are potentially more responsible for the patterns of IBD we see than actual geographic distance. Obtaining populations further outside of this central region further into Eastern New Mexico or Eastern Texas and studying the physical and ecological characteristics of the habitats could elucidate any potential IBE or confirm IBD.

Regarding gene flow, many factors such as allopatric barriers, pre-post mating barriers, and geographic distance, can have an effect on the population's genetic composition (Slatkin, 1987). The mitochondrial COI marker has its limitations in determining gene flow directly in that it lacks recombination and is transferred uniparentally (Saville et al.1998). However, gene flow can be potentially inferred via indirect methods such as nucleotide diversity and haplotype

diversity (Slatkin, 1987). In this study, the central or "Trans Pecos" region appeared to have both higher levels of nucleotide diversity (0.012) and Hd (0.63). The West or "Pluvial Lake Palomas" region also showed similar levels of nucleotide diversity (0.011) and higher Hd (0.85). The East group, which was predominantly individuals from IMRS, showed similar levels of nucleotide diversity (0.012) and the highest levels of Hd (0.93). These locations might potentially share in common in that they are all exposed to potential dust storms and are in essence "sinks" of genetic diversity. These higher values, indirectly, could potentially indicate higher levels of gene flow, say compared to a site outside the aeolian corridor such as the White Sands area, which displayed nucleotide diversity and Hd at (0.00). The low number of individuals at this site and others outside the aeolian corridor, however, limit the inferences of that can be made using these diversity measures . The populations displayed unexpected similarities given that the sites are located far apart from one another and not hydrologically connected. The haplotype network showed that many of these isolated populations were in the order of 1-2 mutations different from others, potentially indicating recent evolutionarily divergence.

In this study, the identification of a new putative species was not surprising in that multiple rotifer species have been documented as being part of cryptic species complexes. Such species include, for example the rotifers from the *Polyarthra dolichoptera* complex (Obertegger et al., 2014), the *Brachionus plicatilis* complex (Gómez et al., 2002b., Ortells et al., 2003., Mills et al., 2016), and the *Euchlanis dilatata* complex (Kordbacheh et al., 2017) which would potentially include this new putative species (**Table 15**). A phylogenetic reconstruction (**Appendix 13**) showed *E. chihuahuaensis* as being part of the *Euchlanis dilatata* species complex and part of a monophyletic group with *Euchlanis dilatata, Euchlanis chihuahuaensis,*

and Euchlanis texana. Other aquatic species, such as Cladocera (*Anolella excisa* complex) lend further support to micrometazoans not being cosmopolitan and with high levels of diversity among populations (Neretina et al., 2021). The potential inclusion of a cryptic species can present issues in generalizing genetic diversity patterns intra-specifically (Goodall-Copestake et al., 2012). However, molecular partitioning alone may not be sufficient in delimiting a new species. One of the key features of the biological species concept is reproductive isolation of a species. In the *Euchlanis dilatata* complex, Kordbacheh et al. (2019) described four new species after conducting mating experiments after delineating the putative species. Their results showed that the success rate for mating success between cryptic species ranged from 0 to 1.1%. The low mating success rate between cryptic species gives us an indication of what we might potentially see in *E. chihuahuaensis,* especiallygiven that there are a substantial number of mutations in the COI gene between the putative species and *E. chihuahuaensis.* The three individuals (PLP1_06, PLP_14, PLP_18) belonging to this new putative species displayed substantial genetic mutations from other species in the *E. dilatata* complex, indicating an independently evolving entity co-occurring with *E. chihuahuaensis*. Furthermore, a Bayesian phylogenetic analysis which included the previously identified *Euchlanis dilatata* cryptic species complex, revealed that this putative species is a sister taxon to *E. chihuahuaensis* (see **Appendix B1** and **Appendix B2)** with strong bootstrap support. This putative cryptic species however was not fully confirmed via additional tests to include mating experiments due to no viable populations that survived. Full confirmation would have to be conducted after additional individuals of this species were located and the addition of nuclear DNA sequences as well.

CONCLUSION

In summary, this research highlights the need for continued research in understanding the dynamic meteorological, geographic, and biological interactions that occur regularly that shape populations in Chihuahuan Desert habitats. Some of my results pointed to potential long distance gene flow and migration between populations, which are not hydrologically connected, in the Chihuahuan Desert. Furthermore, the patterns observed in my results could also potentially indicate that processes such as genetic drift and habitat monopolization that could account for some of the variation that was observed. Future directions for this project include sampling additional isolates from the studied populations, obtaining more populations from regions in Mexico, using additional genomic markers, and further outside of potential influence of anemochory along preferred wind transport corridors.

REFERENCES

Arenas-Sanchez, C., Brendonck, L., Garcia-Roger, E.M., Carmona, M.J. & Ortells, R. (2023). Wind dispersal differences between rotifer cryptic species: a proof of principle from a wind tunnel experiment. *Hydrobiologia. 851*, 2895–2907. doi: 10.1007/s10750-023-05349-6.

Baddock, M. C., Gill, T. E., Bullard, J. E., Dominguez Acosta, M., & Rivera Rivera, N. I. (2011). Geomorphology of the Chihuahuan Desert based on potential dust emissions. *Journal of Maps, 7*(1), 249-259. doi:10.4113/jom.2011.1178

Birky, C. W., Adams, J., Gemmel, M., & Perry, J. (2010). Using population genetic theory and DNA sequences for species detection and identification in asexual organisms. *PloS ONE,* 5(5). doi:10.1371/journal.pone.0010609

Bandelt, H.-J., Forster P. & Rohl A. (1999) Median-joining networks for inferring intraspecific phylogenies. *Molecular Biology and Evolution*, 16, 37–48.

Brochet, A. L., Gauthier-Clerc, M., Guillemain, M., Fritz, H., Waterkeyn, A., Baltanás, Á, & Green, A. J. (2009). Field evidence of dispersal of branchiopods, ostracods and bryozoans by Teal (*Anas crecca*) in the Camargue (southern France). *Hydrobiologia, 637*(1), 255-261. doi:10.1007/s10750-009-9975-6

Brown, P. D., Schröder, T., Ríos-Arana, J. V., Rico-Martinez, R., Silva-Briano, M., Wallace, R. L., & Walsh, E. J. (2020). Patterns of rotifer diversity in the Chihuahuan Desert. Diversity, 12(10), 393. doi:10.3390/d12100393

Cáceres, C. E., & Soluk, D. A. (2002). Blowing in the wind: A field test of overland dispersal and colonization by aquatic invertebrates. *Oecologia, 131*(3), 402-408. doi:10.1007/s00442-002-0897-5

Campillo, S., Serra, M., Carmona, M. J., & Gómez, A. (2011). Widespread secondary contact and new glacial refugia in the halophilic rotifer *Brachionus plicatilis* in the Iberian Peninsula. *PLoS ONE, 6*(6). doi:10.1371/journal.pone.0020986

Castiglia, P. J., & Fawcett, P. J. (2006). Large Holocene lakes and climate change in the Chihuahuan Desert. *Geology, 34*(2), 113. doi:10.1130/g22036.1

Coughlan, N. E., Kelly, T. C., Davenport, J., & Jansen, M. A. (2017). Up, up and away: Bird-mediated ectozoochorous dispersal between aquatic environments. *Freshwater Biology, 62*(4), 631-648. doi:10.1111/fwb.12894

Darriba D, Taboada GL, Doallo R, & Posada D. (2012). jModelTest 2: more models, new heuristics and parallel computing. Nature Methods 9(8), 772.

De Jong, M. J., De Jong, J. F., Hoelzel, A. R., & Janke, A. (2020). Sambar: An R package for fast, easy and reproducible population-genetic analyses of biallelic SNP datasets. doi:10.1101/2020.07.23.213793

De Meester, L., Gómez, A., Okamura, B., & Schwenk, K. (2002). The Monopolization Hypothesis and the dispersal–gene flow paradox in aquatic organisms. *Acta Oecologica, 23*(3), 121-135. doi:10.1016/s1146-609x(02)01145-1

Diniz-Filho JA, Soares TN, Lima JS, Dobrovolski R, Landeiro VL, de Campos Telles MP, Rangel TF, Bini LM. Mantel test in population genetics. Genet Mol Biol. 2013 Dec;36(4):475-85. doi: 10.1590/S1415-47572013000400002. Epub 2013 Nov 8. PMID: 24385847; PMCID: PMC3873175.Dinerstein, E., Olson, D., Atchley, J., Loucks, C., Contreras-Balderas, S., Abell, R., Iñigo, E., Enkerlin E., Williams, C. & G. Castilleja. 2000. Ecoregion-Based Conservation in the Chihuahuan Desert: A Biological Assessment. Chapter 3, pp.20.

Dominguez Acosta, M. (2009). The Pluvial Lake Palomas - Samalayuca Dunes System. Dissertation, University of Texas at El Paso. *Open Access Theses & Dissertations., 243*. https://scholarworks.utep.edu/open_etd/243

Earl, Dent A. & vonHoldt, Bridgett M. (2012) STRUCTURE HARVESTER: a website and program for visualizing STRUCTURE output and implementing the Evanno method. Conservation Genetics Resources vol. 4 (2) pp. 359-361 doi: 10.1007/s12686-011-9548-7

Excoffier L. & Lischer, H.E. (2010) Arlequin Suite ver 3.5: a new series of programs to perform population genetics analyses under Linux and Windows. *Molecular Ecology Resources*, 10, 564–567.

Fawcett, P. J., Werne, J. P., Anderson, R. S., Heikoop, J. M., Brown, E. T., Berke, M. A., Smith, S. J., Goff, F., Donohoo-Hurley, L., Cisneros-Dozal, L. M., Schouten, S., Damsté, J. S. S., Huang, Y., Toney, J., Fessenden, J., Woldegabriel, G., Atudorei, V., Geissman, J. W., & Allen, C. D. (2011). Extended megadroughts in the southwestern United States during Pleistocene interglacials *Nature*, *470*, 518-521. doi: 10.1038/nature09839

Folmer, O., Black, M., Hoeh, W., Lutz, R., & Vrijenhoek, R. (1994). DNA primers for amplification of mitochondrial cytochrome c oxidase subunit I from diverse metazoan invertebrates. *Molecular Marine Biology and Biotechnology, 3*(5), 294-299.

Fontaneto, D., Kaya, M., Herniou, E. A., & Barraclough, T. G. (2009). Extreme levels of hidden diversity in microscopic animals (Rotifera) revealed by DNA taxonomy. *Molecular Phylogenetics and Evolution, 53*(1), 182-189. doi:10.1016/j.ympev.2009.04.011

Fujisawa, T., & Barraclough, T. G. (2013). Delimiting species using single-locus data and the Generalized Mixed Yule Coalescent approach: A revised method and evaluation on simulated data sets. *Systematic Biology*, *62*(5), 707-724. doi:10.1093/sysbio/syt033

Guerrero-Jiménez, G., Ramos–Rodríguez, E., Silva-Briano, M., Adabache-Ortiz, A., & Conde-Porcuna, J. M. (2019). Analysis of the morphological structure of diapausing propagules as a potential tool for the identification of rotifer and cladoceran species. *Hydrobiologia*, *847*(1), 243–266. doi:10.1007/s10750-019-04085-0

Gill T.E., Collins J.D., Montelongo M., Novlan D.J., Hardiman, M. and Baddock M. (2016) *A 78-Year Climatology of Aeolian Dust in El Paso, Texas: Relationship to Drought and Large-Scale Teleconnections*. Paper at the 9th International Conference on Aeolian Research (ICAR9). Mildura, Australia. July 2016.

Gomez, A., & Carvalho, G. R. (2000). Sex, parthenogenesis and genetic structure of rotifers: Microsatellite analysis of contemporary and resting egg bank populations. *Molecular Ecology*, *9*(2), 203–214. doi:10.1046/j.1365-294x.2000.00849.x

Gomez, A., Adcock, G. J., Lunt, D. H., & Carvalho, G. R. (2002a). The interplay between colonization history and gene flow in passively dispersing zooplankton: Microsatellite analysis of rotifer resting egg banks. *Journal of Evolutionary Biology, 15*(1), 158-171. doi:10.1046/j.1420-9101.2002.00368.x

Gómez, A., Serra, M., Carvalho, G. R., & Lunt, D. H. (2002b). Speciation in ancient cryptic species complexes: Evidence from the molecular phylogeny of *Brachionus plicatilis* (Rotifera). *Evolution, 56*(7), 1431. doi:10.1554/0014-3820(2002)056[1431:siacsc]2.0.co;2

Goodall-Copestake, W. P., Tarling, G. A., & Murphy, E. J. (2012). On the comparison of population-level estimates of haplotype and nucleotide diversity: A case study using the gene COX1 in Animals. *Heredity, 109*(1), 50–56. doi:10.1038/hdy.2012.12

Guindon S and Gascuel O (2003). A simple, fast and accurate method to estimate large phylogenies by maximum-likelihood. *Systematic Biology 52*: 696-704.

Hijmans R (2022). _geosphere: Spherical Trigonometry_. R package version 1.5-18, <https://CRAN.R-project.org/package=geosphere>.

Iakovenko, N. S., Smykla, J., Convey, P., Kašparová, E., Kozeretska, I. A., Trokhymets, V., Dykyy, I., Plewka, M., Devetter, M., Duris, Z., & Janko, K. (2015). Antarctic bdelloid rotifers: Diversity, endemism and evolution. *Hydrobiologia, 761*(1), 5-43. doi:10.1007/s10750-015-2463-2

Jiang, S., Luo, M.X., Gao, R., H., Zhang, W., Yang, Y.Z., Li, Y., & Liao, P.C. (2019). Isolation-by-environment as a driver of genetic differentiation among populations of the only broad-leaved evergreen shrub *Ammopiptanthus mongolicus* in Asian temperate deserts. *Scientific Reports, 9*(1). doi:10.1038/s41598-019-48472-y

Kimpel, D., Gockel, J., Gerlach, G., & Bininda-Emonds, O. R. (2015). Population structuring in the monogonont rotifer *Synchaeta pectinata*: High genetic divergence on a small geographical scale. *Freshwater Biology, 60(*7), 1364-1378. doi:10.1111/fwb.12574

Koichiro Tamura, Glen Stecher, and Sudhir Kumar (2021) MEGA11: Molecular Evolutionary Genetics Analysis version 11. *Molecular Biology and Evolution* 38:3022-3027

Kordbacheh, A., Garbalena, G., & Walsh, E. J. (2017). Population structure and cryptic species in the cosmopolitan rotifer *Euchlanis dilatata*. *Zoological Journal of the Linnean Society, 181*(4), 757-777. doi:10.1093/zoolinnean/zlx027

Kordbacheh, A., Wallace, R. L., & Walsh, E. J. (2018). Evidence supporting cryptic species within two sessile microinvertebrates, *Limnias melicerta* and *L. ceratophylli* (Rotifera, Gnesiotrocha). *PLOS ONE, 13*(10). doi:10.1371/journal.pone.0205203

Kordbacheh, A., Shapiro, A. N., & Walsh, E. J. (2019). Reproductive isolation, morphological and ecological differentiation among cryptic species of *Euchlanis dilatata*, with the description of four new species. *Hydrobiologia, 844*(1), 221-242. doi:10.1007/s10750-019-3892-0

Lee, J.A., Gill, T.E., Mulligan, K.R., Dominguez Acosta, M., & Perez, A.E. (2009). Land use/land cover and point sources of the 15 December 2003 dust storm in southwestern North America. *Geomorphology, 105*(1-2): 18-27. doi:10.1016/j.geomorph.2007.12.016

Leasi, F., C. Q. Tang, W. H. De Smet, & D. Fontaneto, 2013. Cryptic diversity with wide salinity 166 tolerance in the putative euryhaline *Testudinella clypeata* (Rotifera, Monogononta). *Zoological Journal of the Linnean Society 168*: 17–28.

Liang, D., McManus, G. B., Wang, Q., Sun, X., Liu, Z., Lin, S., & Yang, Y. (2022). Genetic differentiation and phylogeography of rotifer *Polyarthra dolichoptera* and *P. vulgaris* populations between southeastern China and eastern North America: High intercontinental differences. *Ecology and Evolution*, *12*(5). doi:10.1002/ece3.8912

Lopes, P.M., Bozelli, R., Bini, L.M., Santangelo, J.m., & Declerck, S.A. (2016). Contributions of airborne dispersal and dormant propagule recruitment to the Assembly of Rotifer and crustacean zooplankton communities in temporary ponds. *Freshwater Biology, 61(5),* 658 – 669. doi: 10.1111/fwb.12735

Mardulyn, P. (2001). Phylogeography of the Vosges Mountains populations of *Gonioctena pallida* (Coleoptera: Chrysomelidae): A nested clade analysis of mitochondrial DNA haplotypes. *Molecular Ecology, 10*(7), 1751-1763. doi:10.1046/j.0962-1083.2001.01307.x

Miller, M.A., Pfeiffer, W., & Schwartz, T. (2010) Creating the CIPRES Science Gateway for inference of large phylogenetic trees. Proceedings of the Gateway Computing Environments Workshop (GCE), 14 Nov. 2010, New Orleans, LA pp 1 - 8. doi: 10.1109/GCE.2010.5676129

Mills, S., Alcántara-Rodríguez, J. A., Ciros-Pérez, J., Gómez, A., Hagiwara, A., Galindo, K. H., Jersabek, C. D., Malekzadeh-Viayeh, R., Leasi, F., Lee, J.-S., Mark Welch, D. B., Papakostas, S., Riss, S., Segers, H., Serra, M., Shiel, R., Smolak, R., Snell, T. W., Stelzer, C.-P., Tang, C. Q., Wallace, R. L., Fontaneto, D., & Walsh, E. J. (2016). Fifteen species in one: Deciphering the *Brachionus plicatilis* species complex (Rotifera, Monogononta) through DNA taxonomy. Hydrobiologia, 796(1), 39-58. doi:10.1007/s10750-016-2725-7

Nei, M. (1973). Analysis of gene diversity in subdivided populations. *Proceedings of the National Academy of Sciences*, *70*(12), 3321-3323. doi:10.1073/pnas.70.12.3321

Neretina, A.N., Karabanov, D.P., Sacherova, V., & Kotov, A.A. (2021). Unexpected mitochondrial lineage diversity within the genus *Alonella* Sars, 1862 (Crustacea: Cladocera) across the Nothern Hemisphere. *PeerJ, 9.* doi: 10.7717/peerj.10804

Novlan, D.J., Hardiman, M., & Gill, T.E., 2007. A synoptic climatology of blowing dust events in El Paso, Texas from 1932–2005. Preprints, 16th Conference on Applied Climatology, American Meteorological Society, no. J3.12, https://ams.confex.com/ams/pdfpapers/115842.pdf

Obertegger, U., Flaim, G., & Fontaneto, D. (2014). Cryptic diversity within the rotifer *Polyarthra dolichoptera* along an altitudinal gradient. *Freshwater Biology, 59*(11), 2413–2427. doi:10.1111/fwb.12447

Oksanen J., Simpson G., Blanchet F., Kindt R., Legendre P., Minchin P., O'Hara R., Solymos P.,

Stevens M., Szoecs E., Wagner H., Barbour M., Bedward M., Bolker B., Borcard D., Carvalho G.,

Chirico M., De Caceres M., Durand S., Evangelista H., FitzJohn R, Friendly M, Furneaux B, Hannigan G, Hill M, Lahti L, McGlinn D, Ouellette M, Ribeiro Cunha E, Smith T, Stier A, Ter Braak C, Weedon J (2022). vegan: Community Ecology Package_. R package version 2.6-4, <https://CRAN.R-project.org/package=vegan>.

Ortells, R., Gómez, A., & Serra, M. (2003). Coexistence of cryptic Rotifer species: Ecological and genetic characterisation of *Brachionus plicatilis*. *Freshwater Biology, 48*(12), 2194–2202. doi:10.1046/j.1365-2427.2003.01159.x

Paradis E. & Schliep K. (2019). ape 5.0: an environment for modern phylogenetics and evolutionary analyses in R. *Bioinformatics 35*(3), 526-528. doi.org/10.1093/bioinformatics/bty633

Phillipsen, I. C., & Lytle, D. A. (2012). Aquatic insects in a sea of desert: Population genetic structure is shaped by limited dispersal in a naturally fragmented landscape. *Ecography, 36*(6), 731-743. doi:10.1111/j.1600-0587.2012.00002.x

Pinceel, T., L. Brendonck & Vanschoenwinkel, B. 2015. Propagule size and shape may promote local wind dispersal in freshwater zooplankton-a wind tunnel experiment. *Limnology and Oceanography 61*: 122–131

Pritchard, J. K., Stephens, M., & Donnelly, P. (2000). Inference of population structure using multilocus genotype data. *Genetics, 155*(2), 945-959. doi:10.1093/genetics/155.2.945

Prospero, J. M., Ginoux, P., Torres, O., Nicholson, S. E., & Gill, T. E. (2002). Environmental characterization of global sources of atmospheric soil dust identified with the Nimbus 7 Total Ozone Mapping Spectrometer (TOMS) absorbing aerosol product. *Reviews of Geophysics, 40*(1), 1002. doi:10.1029/2000rg000095

Puillandre, N., Lambert, A., Brouillet, S., & Achaz, G (2011). ABGD, Automatic Barcode Gap Discovery for primary species delimitation. *Molecular Ecology, 21*(8), 1864-1877. doi:10.1111/j.1365-294x.2011.05239.x

Reeves, J. (1965). Pluvial Lake Palomas, northwestern Chihuahua, Mexico, and Pleistocene geologic history of south-central New Mexico, in Southwestern New Mexico II, Fitzsimmons, J. Paul; Balk, Christina L., New Mexico Geological Society, Guidebook, 16th Field Conference, pp. 199-203. doi:10.56577/ffc-16.199

Rivas, J. A., Mohl, J. E., Van Pelt, R. S., Leung, M., Wallace, R. L., Gill, T. E., & Walsh, E. J. (2018). Evidence for regional aeolian transport of freshwater micrometazoans in arid regions. *Limnology and Oceanography Letters, 3*(4), 320-330. doi:10.1002/lol2.10072

Rivas, J. A., Schröder, T., Gill, T. E., Wallace, R. L., & Walsh, E. J. (2019). Anemochory of diapausing stages of microinvertebrates in North American drylands. *Freshwater Biology, 64*(7), 1303-1314. doi:10.1111/fwb.13306

Rivera Rivera, N. I., Gill, T. E., Gebhart, K. A., Hand, J. L., Bleiweiss, M. P., & Fitzgerald, R. M. (2009). Wind modeling of Chihuahuan Desert dust outbreaks. *Atmospheric Environment, 43*(2), 347-354. doi:10.1016/j.atmosenv.2008.09.069

Rivera Rivera, N. I., Gill, T. E., Bleiweiss, M. P., & Hand, J. L. (2010). Source characteristics of hazardous Chihuahuan Desert dust outbreaks. *Atmospheric Environment, 44*(20), 2457–2468. doi:10.1016/j.atmosenv.2010.03.019

Rogash, J. (2003). Meteorological Aspects of South-Central and Southwestern New Mexico and Far Western Texas Flash Floods. *National Weather Digest*, 27, 45-52.

Rozas, J. (2009). DNA Sequence Polymorphism Analysis using DnaSP.Pp. 337-350.*In* Posada, D. (ed.) *Bioinformatics for DNA Sequence Analysis; Methods in Molecular Biology Series* Vol. 537**.** Humana Press, NJ, USAR.

Rozas, J., Ferrer-Mata, A., Sánchez-DelBarrio, J. C., Guirao-Rico, S., Librado, P., Ramos-Onsins, S. E., & Sánchez-Gracia, A. (2017). DnaSP 6: DNA sequence polymorphism analysis of large data sets. *Molecular Biology and Evolution, 34*(12), 3299-3302. doi:10.1093/molbev/msx248

Sandor, J. A., & Homburg, J. A. (2017). Anthropogenic soil change in ancient and traditional agricultural fields in arid to semiarid regions of the Americas. *Journal of Ethnobiology, 37*(2), 196. doi:10.2993/0278-0771-37.2.196

Sanger F.l, Nicklen S., & Coulson, A.R. DNA sequencing with chain-terminating inhibitors. *Proceedings of the National Academy of Sciences* USA. 1977 Dec;74(12):5463-7. doi: 10.1073/pnas.74.12.5463. PMID: 271968; PMCID: PMC431765.

Saville, B.J., Kohli, Y., & Anderson, J.B. (1998). MtDNA recombination in a natural population. *Proceedings of the National Academy of Sciences, 95*(3), 1331 – 1335. Doi: 10.1073/pnas.95.3.1331

Schröder, T., & Walsh, E.J. (2007). Cryptic speciation in the cosmopolitan *Epiphanes senta* complex (Monogononta, Rotifera) with the description of new species. *Hydrobiologia*, 593,129-140. doi 10.1007/s10750-007-9066-5

Scuderi, L. A., Laudadio, C. K., & Fawcett, P. J. (2010). Monitoring playa lake inundation in the western United States: Modern analogues to late-holocene lake level change. *Quaternary Research, 73*(1), 48-58. doi:10.1016/j.yqres.2009.04.004

Seidel, R. A., Lang, B. K., & Berg, D. J. (2009). Phylogeographic analysis reveals multiple cryptic species of amphipods (Crustacea: Amphipoda) in Chihuahuan Desert springs. *Biological Conservation, 142*(10), 2303-2313.

Sexton, J.P., Hangartner, S.B., & Hoffmann, A.A. (2013). Genetic isolation by environment or distance: Which pattern of gene flow is most common? *Evolution, 68* (1), 1 -15. doi: 10.1111/evo.12258

Slatkin, M. (1987). Gene flow and the geographic structure of natural populations. *Science, 236* (4803), 787 – 792. Doi: 10:1126/science.3576198

Spöri, Y., Stoch, F., Dellicour, S., Birky, C. W., & Flot, J. (2021). Kot: An automatic implementation of the *K/θ* method for species delimitation. *Biorxiv*, doi:10.1101/2021.08.17.454531

Stein, A. F., R. R. Draxler, G. D. Rolph, B. J. B. Stunder, M. D. Cohen, & Ngan, F.. (2015). NOAA's HYSPLIT atmospheric transport and dispersion modeling system. *Bulletin of the American Meteorological Society, 96*, 2059–2077. doi:10.1175/BAMS-

Stemberger, R. S. (1981). A general approach to the culture of planktonic rotifers. *Canadian Journal of Fisheries and Aquatic Sciences, 38*(6), 721-724. doi:10.1139/f81-095

Sun, R., Lin, F., Huang, P., Ye, X., Lai, J., & Zheng, Y. (2019). Phylogeographical structure of *Liquidambar formosana* Hance revealed by chloroplast phylogeography and species distribution models. *Forests, 10*(10), 858. doi:10.3390/f10100858

Tajima, F. (1989). Statistical method for testing the neutral mutation hypothesis by DNA polymorphism. *Genetics, 123*(3), 585-595. doi:10.1093/genetics/123.3.585

Turner, T. F., Cameron, A. C., Osborne, M. J., & Propst, D. L. (2022). Origins and diversity of peripheral populations of Rio Grande Sucker (*Pantosteus Plebeius*) in the Southwestern United States. *The Southwestern Naturalist, 66*(1), 25-34. doi:10.1894/0038-4909-66.1.25

Vanschoenwinkel, B., Gielen, S., Vandewaerde, H., Seaman, M., & Brendonck, L. (2008). Relative importance of different dispersal vectors for small aquatic invertebrates in a rock pool metacommunity. Ecography, 31(5), 567-577.

Vanschoenwinkel, B., Gielen, S., Seaman, M., & Brendonck, L. (2008). Any way the wind blows-frequent wind dispersal drives species sorting in ephemeral aquatic communities. Oikos, 117(1), 125-134.

Wallace, R. L., Snell, T. W., Ricci, C., & Nogrady, T. (2006). *Rotifera:* (2nd ed.). Backhuys Publishers.

Walsh, E. J. (1989). Oviposition behavior of the littoral Rotifer *Euchlanis dilatata*. *Hydrobiologia, 186-187*(1), 157-161. doi:10.1007/bf00048908

Walsh, E.J., Schroder, T., Wallace, R.L., & Rico-Martinez, R. (2009). Cryptic speciation in Lecane bulla (Monogononta: Rotifera) in Chihuahuan Desert Waters. SIL Proceedings, 1922 – 2010, 30(7), 1046 – 1050, doi: 10.1080/03680770.2009.11002298

Walsh, E. J., May, L., & Wallace, R. L. (2016). A metadata approach to documenting sex in phylum Rotifera: Diapausing embryos, males, and hatchlings from sediments. *Hydrobiologia, 796*(1), 265-276. doi:10.1007/s10750-016-2712-z

Wells, P. V. (1966). Late Pleistocene vegetation and degree of pluvial climatic change in the Chihuahuan Desert. *Science, 153*(3739), 970-975. doi:10.1126/science.153.3739.970

Wright, S. (1950). Genetical structure of populations. Nature, 166(4215), 247-249. doi:10.1038/166247a0

Xiang, X. L., Xi, Y. L., Wen, X. L., Zhang, G., Wang, J. X. and Hu, K. (2011). Genetic differentiation and phylogeographical structure of the *Brachionus calyciflorus* complex in eastern China. Mol. *Ecol.*, *20*, 3027–3044

APPENDIX A

Summary of Detailed results of species delimitation tables, wind characteristics, AMOVA, and MANTEL tests.

Appendix 1a. Species delimitation of *Euchlanis chihuahuaensis* isolates based on partial COI gene sequences and GMYC delimitation method.

Parameter	Value
Method	**Single**
Likelihood of null model	457.55
Maximum likelihood of GMYC model	457.73
Likelihood ratio	0.36
Result of LR test	0.84 (n.s.)
Number of ML clusters	5
Confidence interval (clusters)	1-14
Number of ML entities	5
Confidence interval (entities)	1-60
Threshold time	-0.01

Appendix 1b. Species delimitation of *Euchlanis dilatata* cryptic species complex isolates based on partial COI gene sequences and GMYC single threshold delimitation method of 130 individuals.

Parameter	Value
Method	Single
Likelihood of null model	944.64
Maximum likelihood of GMYC model	945.73
Likelihood ratio	2.18
Result of LR test	0.34 (n.s.)
Number of ML clusters	3
Confidence interval (clusters)	1-33
Number of ML entities	4
Confidence interval (entities)	1-129
Threshold time	-0.07

Appendix 2. Species delimitation of *Euchlanis chihuahuaensis* isolates based on partial COI gene sequences and GMYC partitioning using single threshold method.

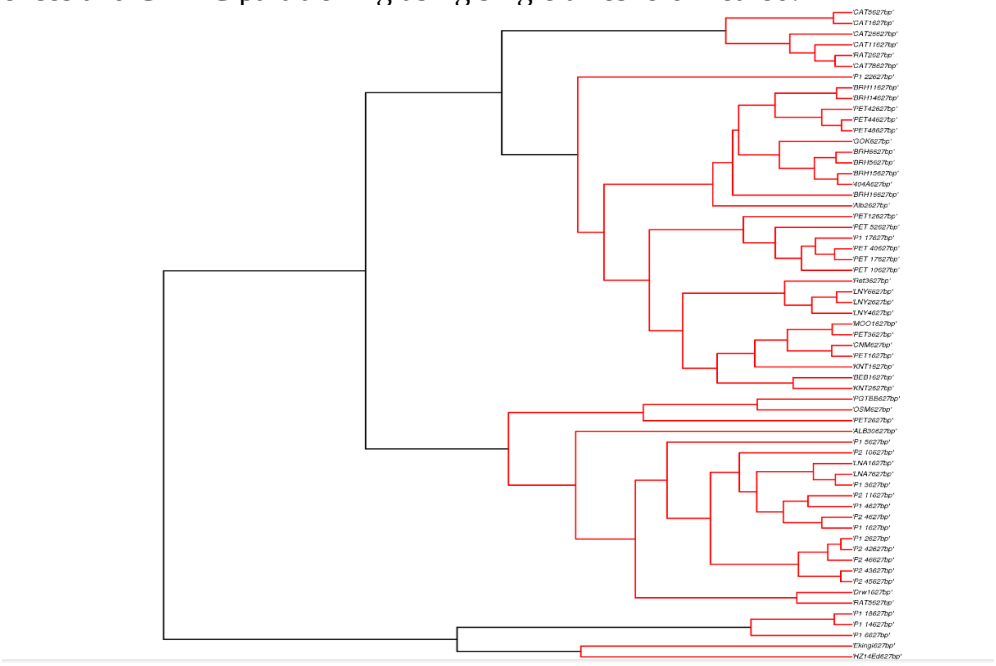

Appendix 3a. Species delimitation of *Euchlanis chihuahuaensis* isolates based on partial COI gene sequences and GMYC multi-threshold method.

Parameter	Value
Method	Multiple
Likelihood of null model	457.5526
Maximum likelihood of GMYC model	458.3819
Likelihood ratio	1.658587
Result of LR test	0.4363575 (n.s.)
Number of ML clusters	9
Confidence interval (clusters)	1-13
Number of ML entities	16
Confidence interval (entities)	1-37
Threshold time	-0.01006869 -0.005070779 -0.002794396 -0.0014567

Appendix 3b. Species delimitation of *Euchlanis dilatata* cryptic species complex isolates based on partial COI gene sequences and GMYC multi-threshold method of 130 individuals.

Parameter	Value
Method	Multiple
Likelihood of null model	944.641
Maximum likelihood of GMYC model	949.8378
Likelihood ratio	10.39361
Result of LR test	0.005534222**
Number of ML clusters	27
Confidence interval (clusters)	23-32
Number of ML entities	43
Confidence interval (entities)	36-67
Threshold time	-0.01730804 br -0.008380733 br -0.003034872

Appendix 3c. Species delimitation of *Euchlanis dilatata* cryptic species complex isolates based on partial COI gene sequences and GMYC multi-threshold method of 130 individuals. Sequences include individuals identified on **Table 2** and from individuals identified in Kordbacheh et al., 2017.

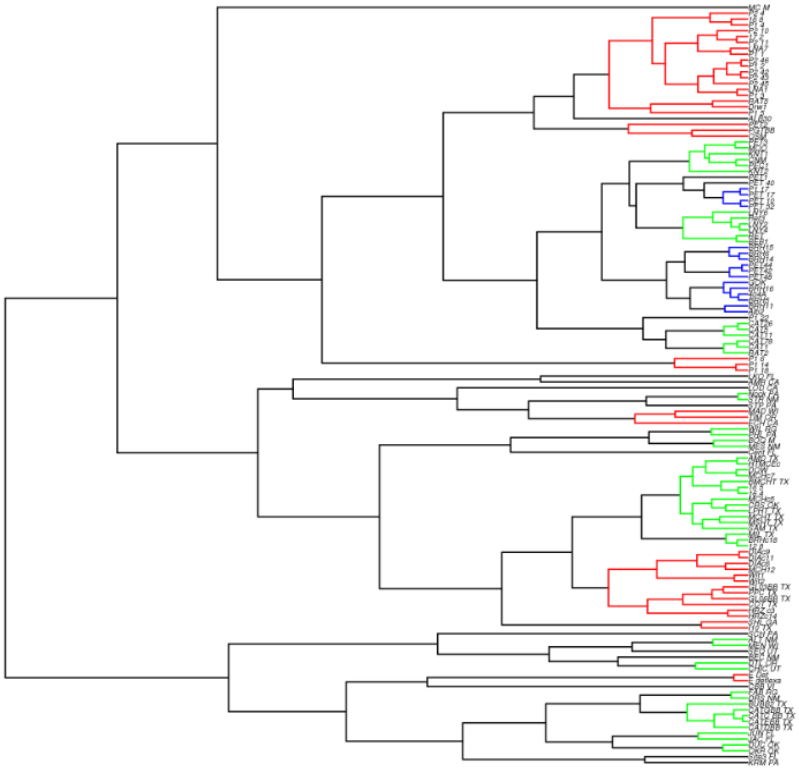

Appendix 4. Species delimitation of *Euchlanis chihuahuaensis* isolates based on partial COI gene sequences and GMYC multi-threshold partitioning method. Sequences include individuals identified on **Table 2** and from individuals identified in Kordbacheh et al., 2017.

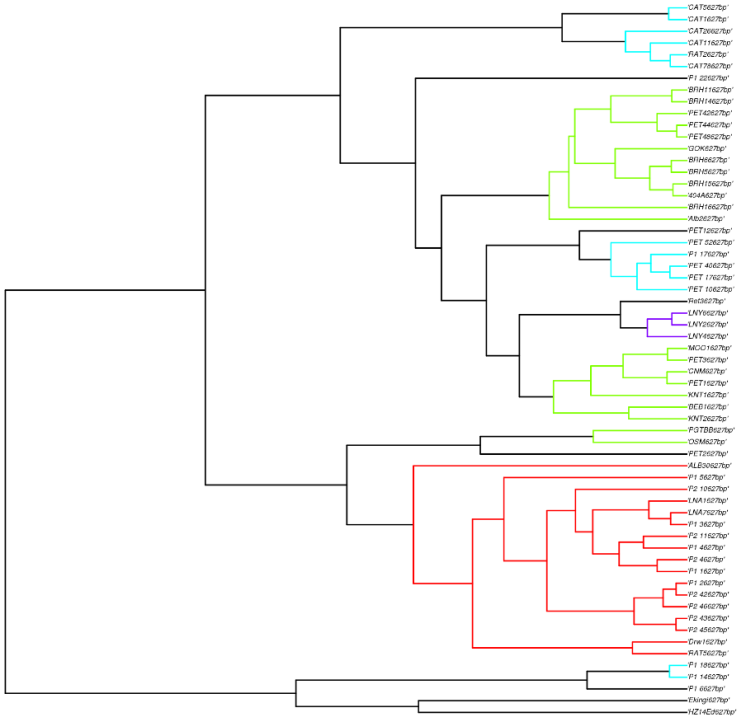

Appendix 5a. Species delimitation of *Euchlanis chihuahuaensis* isolates based on partial COI gene sequences and the *K/θ* method. Sequences include individuals identified on **Table 2** and from individuals identified in Kordbacheh et al., 2017.

Group	Population
1	P1_14, P1_18, P1_6
2	P1_3, P2_4, P2_11, LNA7, LNA1, P2_10, P1_1
3	P1_5
4	P1_2, P2_42, P2_43, P2_45, P2_46, P1_4, Drw1, RAT5
5	PET2
6	ALB30
7	OSM
8	PGTBB
9	CAT1, CAT5, CAT11, CAT26, CAT78, RAT2
10	Alb2
11	PET_52, P1_17, PET_10, PET_17, PET_40
12	PET12
13	LNY4, Ret3, LNY2, LNY6
14	PET1, PET3, CNM, MOO1, 404A, GOK, BRH14, BRH6, BRH5, BRH15, BRH16, BRH11, PET42, PET44, PET48
15	KNT1, KNT2
16	P1_22, BEB1
17	Ekingi - outgroup
18	HZ14Ed - outgroup

Appendix 5b. Species delimitation of the *Euchlanis dilatata* species complex based on partial COI sequences and the *K/θ* method. The new putative cryptic species found at the PLP – Pluvial Lake Palomas (Mimbres River Valley) area is highlighted in yellow and the *Euchlanis chihuahuaensis* isolates used in this study in teal. Sequences include individuals identified on **Table 2** and from individuals identified in Kordbacheh et al., 2017.

Group	Names
1	E_deflexa, E_Def
2	JAC_FL
3	JUN_FL
4	CATDBB_TX, CATC_BB_TX, CATEBB_TX, CATGBB_TX, BUBB2_TX
5	FAB_RG, DRS_NM
6	OKR_OK, DUC_OK
7	KRM_PA
8	Site3_FL
9	MEN_WI
10	ALT_NM
11	DTL_OR
12	CHIC_UT
13	BEC_NM
14	SEQ_UT
15	SCH_PA
16	PHL_PA
17	WIL_RG, MES_NM
18	BOQ_M
19	Cent_FL
20	CBB_VI
21	COT_TX
22	GL03BB_TX, GL06BB_TX
23	HRZc14, HRZ_c3, 12_8, HTMCEc, SAM_TX, MIL_TX, BMCHT_TX, LPHT_TX, AMD_TX, DOW, MCHc7, MCHc5, BRHc18, 16_4, 16_5, MCHT_TX, MSHT_TX, CRS_OK, Wit1, Wit2, DIAc6, MCH12, DIAc11, DIAc9
24	PPC_TX
25	SHL_GA, I10_TX
26	AMR_CA
27	STP_PA
28	STR_NM, Nock_PA
29	LOD_CA
30	TIM_OR
31	ECH_CA
32	MAD_WI
33	LKO_FL
34	MC_M
35	P1_14, P1_18, P1_6
36	P1_2, P2_42, P2_43, P2_45, P2_46, P2_10, P1_1
37	P1_5
38	17_2, LNA1, LNA7, P1_3, P2_11, P2_4, P1_4, 16_8, RAT5, Drw1
39	PET2
40	ALB30
41	OSM
42	PGTBB
43	Alb2
44	LNY2, LNY6, Ret3, LNY4
45	KNT2, P1_17, PET_10, PET_17, PET_40, PET_52
46	KNT1, CNM, MOO, PET1, PET3, PEC1
47	BEB1, RET, PET42, PET44, PET48, 404A, BRH11, BRH14, BRH15, BRH16, BRH5, BRH6, GOK
48	CAT11, RAT2, CAT26, CAT5, CAT78, CAT1, P1_22

Appendix 6. *K/θ* partitioning based on partial sequences of the COI gene for *Euchlanis chihuahuaensis* isolates. Sequences include individuals identified on **Table 2** and from individuals identified in Kordbacheh et al., 2017.

Appendix 7a. ABGD (Automatic Barcode Gap Discovery) partitioning *Euchlanis chihuahuaensis* isolates based on partial sequences of the COI gene. Sequences include individuals identified on **Table 2** and from individuals identified in Kordbacheh et al., 2017.

Parameter	**Value**	
Prior maximal distance	3.59e-02	
Barcode gap distance	0.102	
Distance metric	JC69 Jukes-Cantor MinSlope=1.500000	
Group	**#**	**ID**
1	1	Ekingi
2	1	HZ14Ed – Horizon Tank, IMRS
3	56	CAT1 PGTBB OSM P1_1 P1_2 P1_3 P1_4 P1_5 P1_17 P1_22 P2_4 P2_10 P2_11 P2_42 P2_43 P2_45 P2_46 PET1 PET2 PET3 PET_10 PET12 PET_17 PET_40 PET42 PET44 PET48 PET_52 CAT5 CAT11 CAT26 CAT78 Ret3 RAT2 RAT5 LNY2 LNY4 LNY6 BEB1 Drw1 CNM LNA7 LNA1 404A Alb2 ALB30 KNT1 KNT2 GOK MOO1 BRH14 BRH6 BRH5 BRH15 BRH16 BRH11
4	3	P1_6 P1_14 P1_18

Appendix 7b: Automatic Barcode Gap Discovery (ABGD) analysis of all sequences. *E. chihuahuaensis* isolates are highlighted in light blue. Sequences include individuals identified on **Table 2** and from individuals identified in Kordbacheh et al., 2017.

Group[1] n: 2 ;id: E_deflexa E_Def
Group[2] n: 59 ;id: 404A BRH11 BRH14 BRH15 BRH16 BRH5 BRH6 GOK CNM MOO PET1 PET3 PEC1 PET42 PET44 PET48 KNT2 BEB1 RET CAT11 RAT2 CAT26 CAT5 CAT78 CAT1 P1_22 KNT1 LNY2 LNY6 Ret3 LNY4 P1_17 PET_10 PET_17 PET_40 PET_52 Alb2 17_2 LNA1 LNA7 P1_3 P2_11 P2_4 16_8 P1_2 P2_42 P2_43 P2_45 P2_46 P1_1 P2_10 P1_4 Drw1 RAT5 P1_5 ALB30 PET2 PGTBB OSM
Group[3] n: 28 ;id: 12_8 HTMCEc SAM_TX MIL_TX BMCHT_TX LPHT_TX AMD_TX DOW MCHc7 MCHc5 BRHc18 16_4 16_5 CRS_OK MSHT_TX HRZ_c3 HRZc14 Wit1 Wit2 MCH12 DIAc6 DIAc11 DIAc9 MCHT_TX GL03BB_TX GL06BB_TX COT_TX PPC_TX
Group[4] n: 2 ;id: I10_TX SHL_GA
Group[5] n: 1 ;id: AMR_CA
Group[6] n: 3 ;id: STR_NM Nock_PA STP_PA
Group[7] n: 1 ;id: LOD_CA
Group[8] n: 3 ;id: ECH_CA TIM_OR MAD_WI
Group[9] n: 1 ;id: LKO_FL
Group[10] n: 3 ;id: P1_6 P1_14 P1_18
Group[11] n: 4 ;id: WIL_RG MES_NM PHL_PA BOQ_M
Group[12] n: 1 ;id: Cent_FL
Group[13] n: 1 ;id: CBB_VI
Group[14] n: 2 ;id: CHIC_UT DTL_OR
Group[15] n: 2 ;id: ALT_NM MEN_WI
Group[16] n: 1 ;id: SEQ_UT
Group[17] n: 1 ;id: BEC_NM
Group[18] n: 1 ;id: SCH_PA
Group[19] n: 2 ;id: DUC_OK OKR_OK
Group[20] n: 7 ;id: BUBB2_TX CATC_BB_TX CATEBB_TX CATGBB_TX CATDBB_TX FAB_RG DRS_NM
Group[21] n: 2 ;id: JUN_FL JAC_FL
Group[22] n: 1 ;id: MC_M
Group[23] n: 2 ;id: Site3_FL KRM_PA

Appendix 8a. Poisson Tree Process (PTP) species delimitation results based on partial sequences of the COI gene for *Euchlanis chihuahuaensis* isolates.

Parameter	Value
Acceptance rate	0.54445
Merge	50047
Split	49953
Estimated number of species	19-44
Mean	32.92

Appendix 8b. Poisson Tree Process (PTP) species delimitation results based on partial sequences of the COI gene for *Euchlanis* spp. complex of 130 isolates.

Parameter	Value
Acceptance rate	0.44418
Merge	49822
Split	50178
Estimated number of species	44 - 79
Mean	61.71

Appendix 9. Populations of *Euchlanis chihuahuaensis* identified by STRUCTURE in **Figure 6** (Bar 1) and with Structure Harvester (v0.6.94 July 2014). The initial partitioning included the putative cryptic species (Group A)

Structure Grouping	Sample Sites
Group A	P1_14, P1_18, P1_6
Group B	LNA1, LNA7, P1_2, P1_3, P2_11, P2_4, P2_42, P2_43, P2_45, P2_46, Drw1, P1_1, P1_4, P1_5, P2_10, RAT5, PET2, PGTBB, ALB30, OSM
Group C	404A, BRH11, BRH14, BRH15, BRH16, BRH5, BRH6, CAT11, CNM, GOK, LNY2, LNY4, LNY6, MOO1, P1_17, P1_22, PET_10, PET_17, PET_40, PET_52, PET1, PET3, PET42, PET44, PET48, RAT2, Ret3, Alb2, CAT1, CAT26, CAT5, CAT78, KNT1, KNT2, PET12, BEB1

Appendix 10: Structure Harvester results of K 1-9 for populations of *Euchlanis chihuahuaensis* in the northern Chihuahuan Desert.

# K	Reps	Mean LnP(K)	Stdev LnP(K)	Ln'(K)	|Ln''(K)|	Delta K
##########						
1	2	-1221.3500	0.2121	NA	NA	
2	2	-419.9500	2.1920	801.400000	767.750000	350.245956
3	2	-386.3000	0.5657	33.650000	59.150000	104.563415
4	2	-411.8000	16.1220	-25.500000	14.700000	0.911796
5	2	-422.6000	29.8399	-10.800000	44.640000	1.495983
6	5	-388.7600	31.2353	33.840000	82.130000	2.629398
7	2	-437.0500	11.3844	-48.290000	79.440000	6.977958
8	2	-405.9000	5.9397	31.150000	92.200000	15.522677
9	2	-466.9500	36.1332	-61.050000	NA	NA

Appendix 11. Phylogenetic relationships among isolates of *Euchlanis chihuahuaensis* based on partial COI sequences and reconstructed using Maximum Likelihood (MEGA v 11.0.10) with bootstrap values at the nodes. The outgroups *E. kingi* and *E. dilatata* (HZ14Ed) were used for this reconstruction. This also included the putative cryptic species represented by individuals P1_6, P1_14, and P1_18. Posterior probabilities were noted at 100% for both clades.

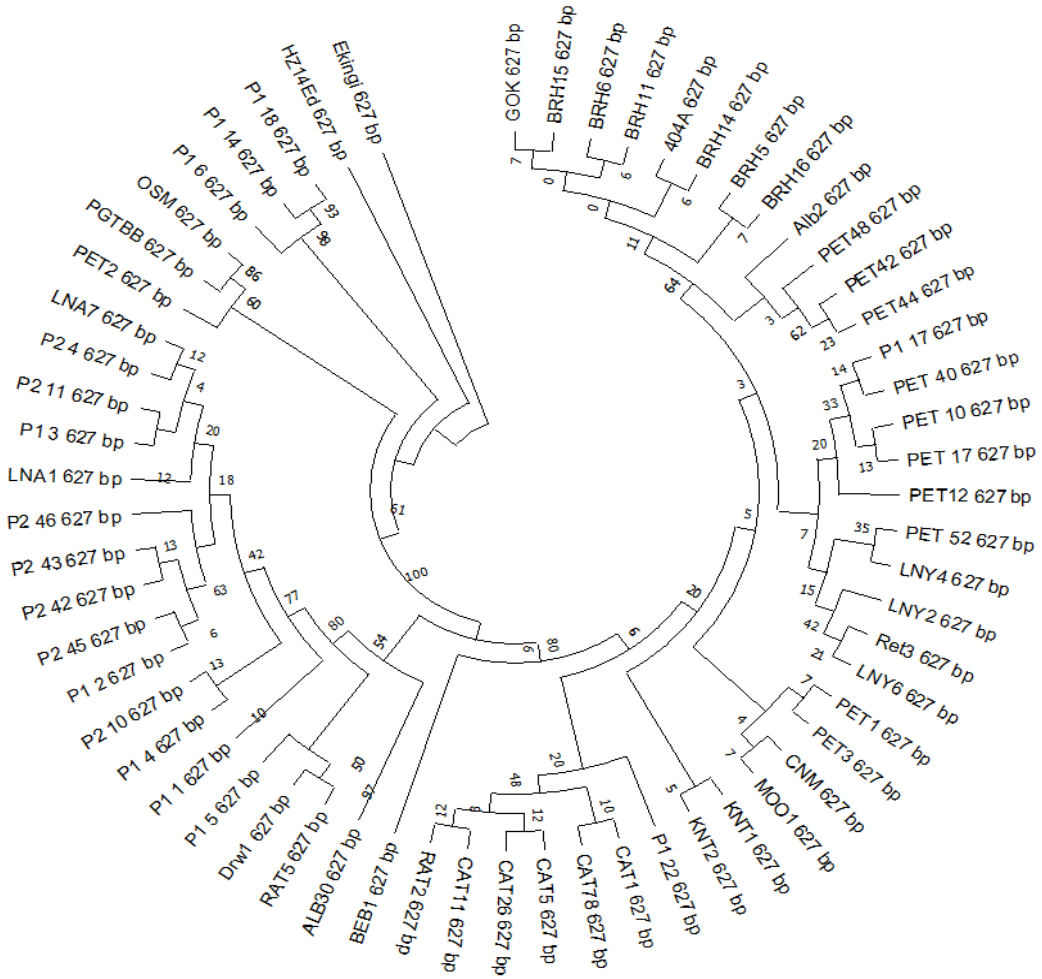

Appendix 12. Monthly average wind speed and peak wind gust speeds from 2013 – 2022 (Thomas E. Gill, personal communication)

Month	Avg Hrs Dust	Avg Windspeed MPH	Avg Peak Gust MPH
January	0.7	7.4	55
February	6.1	8.6	52
March	10.2	9.8	58
April	12.2	11.2	56
May	6.4	10.3	51
June	4.8	9.1	54
July	2.5	7.8	55
August	1.2	7.3	46
September	1.0	7.0	41
October	0.4	6.9	44
November	0.9	7.3	50
December	2.3	7.4	51
Average		8.3	51.1

Appendix 13. AMOVA of populations located solely within the wind corridor. These populations are divided geographically to include West (PLP), Central (Paso Del Norte), Luna (Hatch, NM), and HTSPHS. HTSPHS = Hueco Tanks State Park and Historic Site.

Source of Variation	**d.f.**	**Sum of Squares**	**Variance Components**	**Percentage of Variation**
Among populations	3	77053.075	6.33386 Va	67.29
Within populations	18806	57898.225	3.07871 Vb	32.71
Total	18809	134951.300	9.41257	100.00
Fixation Index (FST)	0.67292			

$P < 0.05$

Appendix 14. AMOVA of *Euchlanis chihuahuaensis* populations solely outside the aeolian corridor, split geographically for the analysis. The regions include East (IMRS), Far East (Kent Texas & BIBE), and North (WISA). IMRS = Indio Mountains Research Station, BIBE = Big Bend National Park, WISA = White Sands National Park

Source of Variation	d.f.	Sum of Squares	Variance Components	Percentage of Variation
Among populations	2	8201.910	1.06871 Va	25.28
Within populations	16299	51483.667	3.15870 Vb	74.72
Total	16301	59685.577	4.22741	100.00
Fixation Index (FST)	0.2528 0			

P < 0.05

Appendix 15. Mantel analysis of Isolation by Distance (IBD) of Eu*chlanis chihuahuaensis* populations Haplogroup. The analysis was conducted with a genetic pairwise distance (K80) matrix of Group B (**Appendix 9)** and geographic distance matrix. The analysis was conducted with both transformed and untransformed data.

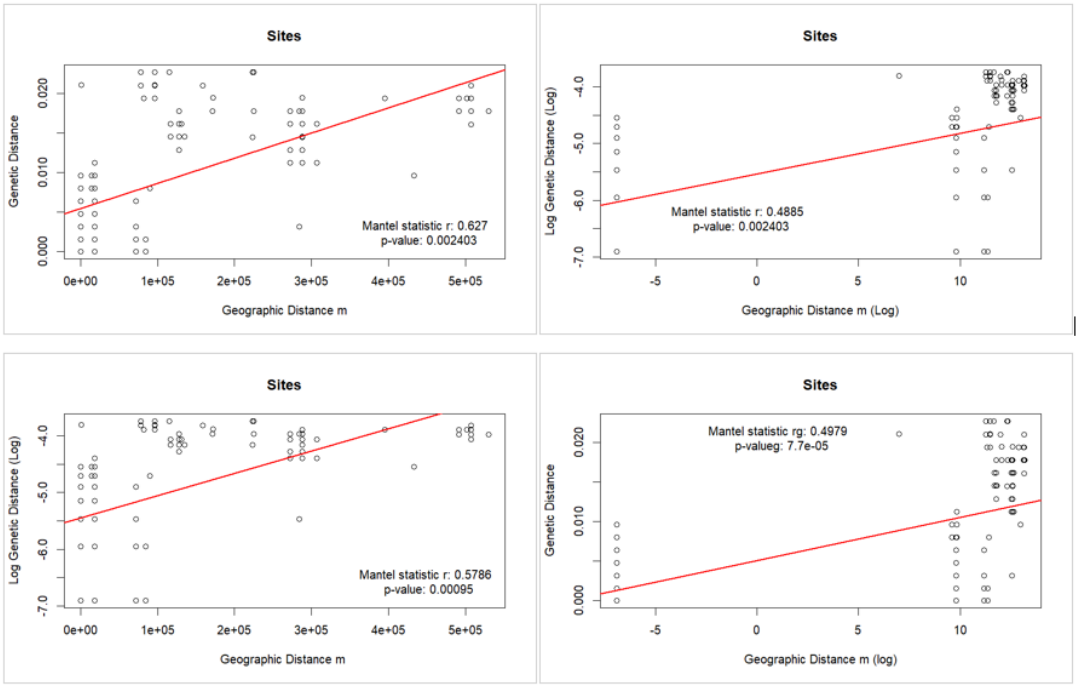

Appendix 16. Mantel analysis of Isolation by Distance (IBD) of *Euchlanis chihuahuaensis* by haplogroup. The analysis was conducted with a genetic pairwise distance (K80) matrix of Group C (**Appendix 9)** and geographic distance matrix. The analysis was conducted with both transformed and untransformed data.

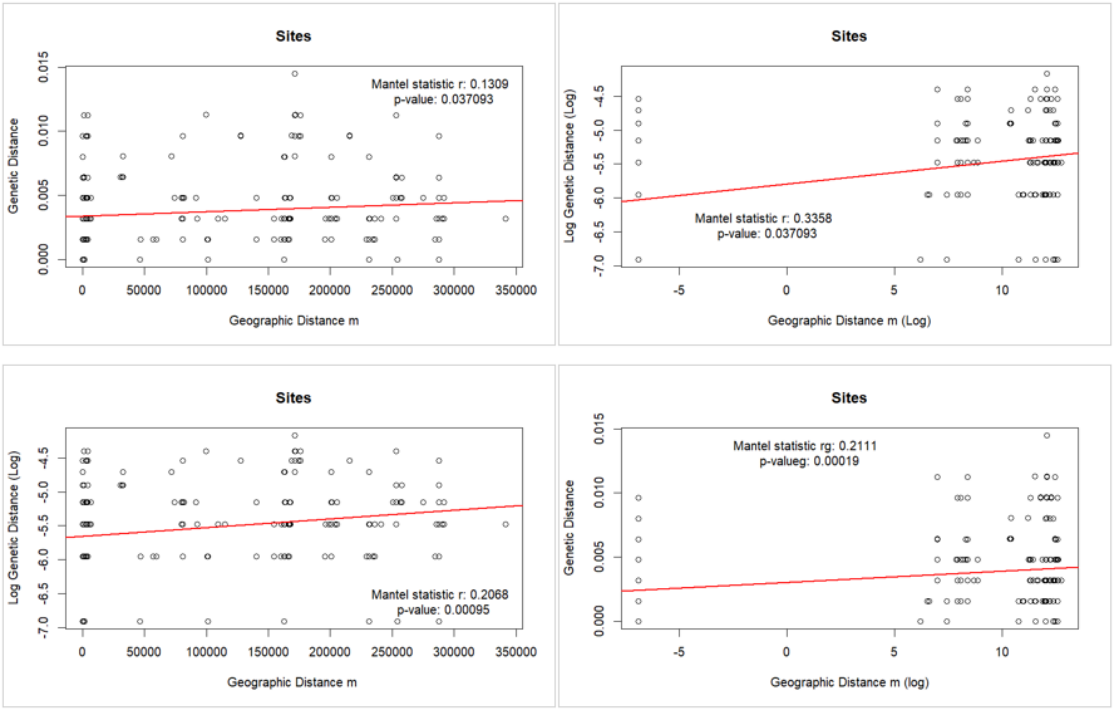

APPENDIX B

Phylogenetic Analyses

Appendix B1: Bayesian analysis of the three PLP1 isolates of the new putative species in blue and the previously identified *Euchlanis chihuahuaensis* individuals in teal.

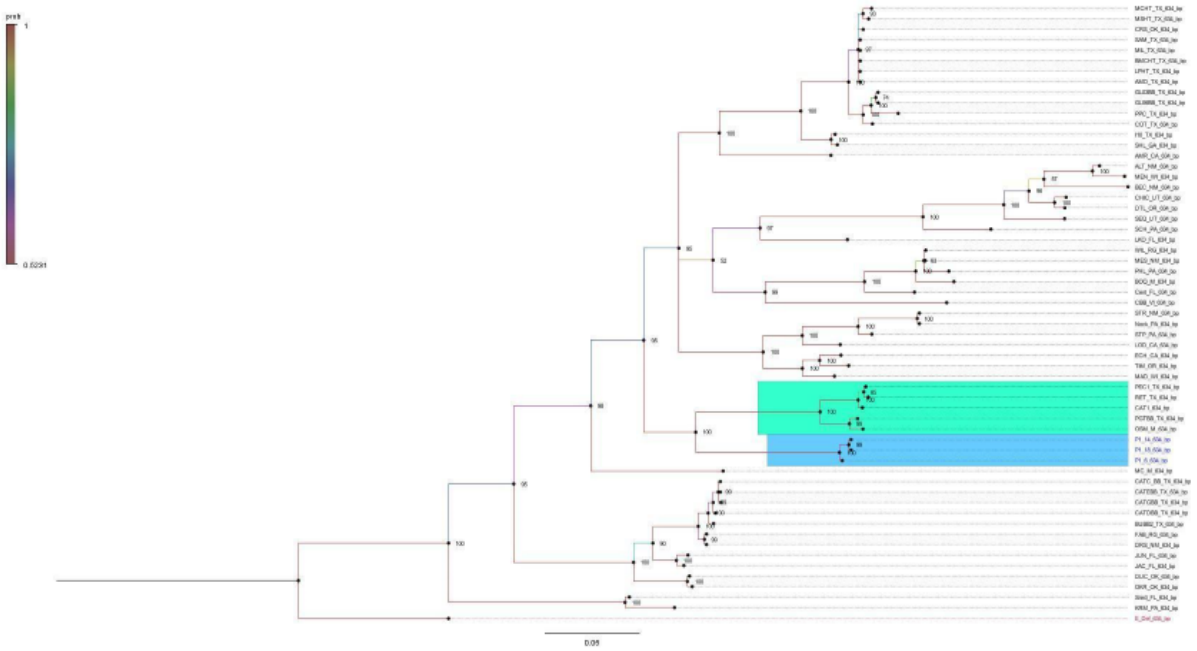

Appendix B2: Bayesian reconstruction of *Euchlanis chihuahuaensis* isolates (identified in light blue) based on partial COI sequences. The putative cryptic species is also noted in darker blue and both at 100.

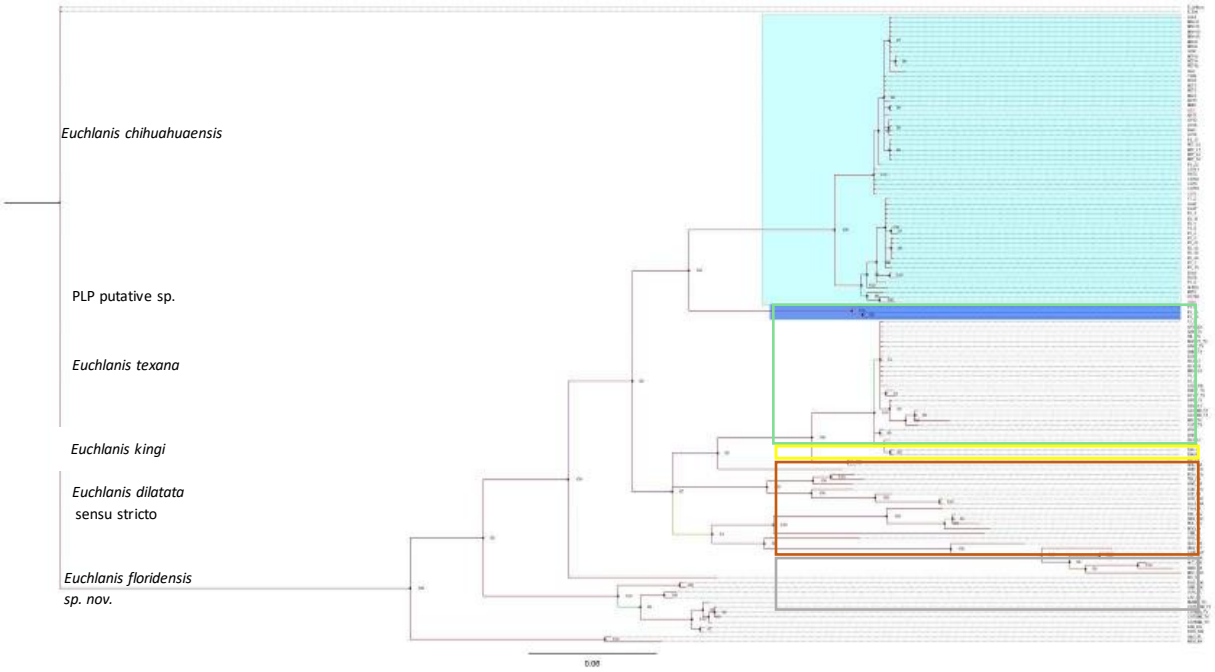

APPENDIX C

COI DNA Sequences used in this study

>Ekingi 627 bp – *Euchlanis kingi* – Crystal Lake, NH - **Outgroup**

ATGAGATTTTTAATTCGTTTAGAGCTAGGTGTTATTGGTCCTTATATTGGTGATGAGC
ACCTCTATAATGTCATGGTCACTGCTCATGCTTTTGTCATGATTTTCTTCATGGTTAT
GCCTATTTCTATGGGTGGCTTCGGTAACTGACTTATTCCTCTTATGTTAGGTGTTGCT
GATATGGCTTTTCCCCGTATGAACAATCTTTCTTTCTGACTATTAATTCCTTCCTTTAC
TTTTTTACTACTTTCTTCTATTCTTGATGCTGGTGTAGGTACCGGCTGAACTGTTTATC
CTCCTTTGTCTGACTCTAAATACCATTCAGGAATCTCAGTTGATTTAGCTATTTTTAG
TCTTCATCTAGCTGGTATTTCTTCTATCTTAGGTAGAATCAATTTTTTTAACTACTATTA
TTTGTTCTCGTACCGCTAAAGCTATTTCTCTTGATCGTATGCCTCTTATGCTTTGAGCT
TTTGCTGTTACTTCTATCCTGCTTGTTACTAGACTTCCTGTCCTAGCCGGTGCTATCAC
AATGTTGCTTACTGATCGTAATTTTAACACTTCATTCTTTGACCCAGCAGGTGGAGGT
AATCCAGTTCTTTATCAACATTTATTTTGATTTTTTGGTCAC

>HZ14Ed 627 bp – Horizon Tank, Indio Mountains Research Stations, Texas, *Euchlanis dilatata* - **Outgroup**

ATAAGATTCCTAATTCGTCTAGAGCTTGGTGTTATCGGCCCTTATATTGGGGACGAG
CACTTATACAACGTTATGGTAACAGCTCATGCTTTTGTTATAATTTTCTTCATGGTTA
TGCCTATTTCTATGGGTGGCTTTGGTAACTGGCTTATTCCTTTAATGCTAGGTGTTGC
TGATATGGCCTTTCCTCGAATGAATAACCTTTCTTTTTGGCTTCTTATTCCTTCATTTA
CATTTTTATTATTATCATCTATCTTAGATGCTGGTGTTGGTACTGGTTGAACTGTTTAT
CCCCCTCTTTCAGATTCTAAGTATCATTCTGGTATTTCTGTTGACTTAGCTATTTTTAG
TCTACATTTAGCAGGTATTTCCTCTATTCTTGGTAGAATTAATTTTTTAACTACTATTA
TCTGTTCTCGTACAGCTAAGGCTATCTCTCTTGACCGAATGCCTCTTATGTTGTGGGC
TTTCGCCGTCACATCTATTCTTCTTGTGACTAGTCTACCTGTTTTAGCTGGTGCTATTA
CTATGCTTCTTACTGATCGTAATTTTAACACTTCTTTTTTTGATCCAGCAGGAGGTGG
TAATCCCGTTCTTTATCAGCATTTGTTCTGATTTTTTGGTCAC

E. chihuahuaensis sequences

>CAT1 627 bp – Cattle Tank White Sands National Park, New Mexico (Genbank Accession #KU665883)

ATAAGATTCCTTATTCGTTTAGAGTTAGGGGTTATTGGTCCTTATATTGGGGATGAAC
ATTTATATAACGTCATGGTTACTGCCCACGCCTTTGTTATGATTTTTTTTATGGTTATG
CCTATTTCTATGGGTGGCTTTGGTAACTGACTTATTCCACTAATGTTGGGTGTTGCTG
ATATGGCTTTCCCACGTATAAATAATCTTTCTTTCTGGCTTCTTATTCCATCTTTCACT
TTTTTATTACTTTCTTCAATTCTTGATGCTGGTGTTGGTACGGGTTGAACTGTTTACCC
TCCCCTATCTGACTCTAAGTATCATTCTGGTATTTCTGTTGATCTAGCTATTTTTAGAC
TTCATTTAGCCGGAATTTCTTCAATTCTTGGTAGAATCAACTTTCTTACTACTATTATT
TGTTCTCGCACAGCAAAAGCTATTTCTCTAGATCGTATGCCTTTAATGTTATGGGCGT
TTGCTGTTACTTCTATTCTTCTTGTTACTAGATTACCCGTTTTAGCTGGTGCCATCACT

ATGCTTTTAACTGATCGAAACTTTAATACCTCTTTTTTTGACCCTGCAGGCGGTGGTA
ACCCAGTACTCTACCAACATTTATTTTGATTTTTTGGTCAC

>PGTBB 627 bp – Paint Gap Tank Big Bend National Park, Texas – (Genbank Accession # KU665841)

ATAAGATTCCTTATTCGTTTAGAGCTTGGGGTTATTGGTCCTTATATTGGGGATGAAC
ATCTATATAATGTTATGGTTACTGCTCATGCCTTTGTTATGATTTTTTTTATGGTTATA
CCTATTTCTATGGGTGGCTTTGGTAACTGACTTATTCCACTAATGTTGGGTGTTGCTG
ATATGGCTTTCCCCCGCATAAATAATCTTTCTTTCTGGCTTCTTATTCCATCTTTCACT
TTTTTATTACTTTCTTCAATTCTTGATGCTGGTGTTGGTACGGGGTGAACGGTTTACC
CTCCCCTATCTGACTCCAAGTATCATTCTGGTATTTCTGTTGATCTAGCTATTTTTAG
ACTTCATTTAGCCGGAATTTCTTCAATTCTTGGTAGAATCAATTTTCTTACTACTATT
ATTTGTTCTCGCACAGCAAAAGCTATTTCTCTAGATCGTATGCCTTTAATATTATGGG
CGTTTGCTGTGACTTCTATTCTTCTTGTTACTAGATTACCCGTATTAGCTGGTGCTATT
ACTATGCTTTTAACTGATCGAAACTTTAATACCTCTTTTTTTGATCCCGCAGGAGGTG
GTAATCCAGTACTCTACCAACATTTATTTTGATTTTTTGGTCAC

>OSM 627 bp – Ojo de Santa Maria, Mexico (Genbank Accession # KU665871)

ATAAGATTCCTTATTCGTTTAGAGTTAGGGGTTATTGGTCCTTATATTGGGGATGAAC
ATCTATATAATGTTATGGTTACTGCTCATGCCTTTGTTATGATTTTTTTTATGGTTATA
CCTATTTCTATGGGTGGCTTTGGTAATTGACTTATTCCACTAATGTTGGGTGTTGCTG
ATATGGCTTTCCCCCGCATAAATAATCTTTCTTTCTGGCTTCTTATTCCATCTTTCACT
TTTTTATTACTTTCTTCAATTCTTGATGCTGGTGTTGGTACGGGGTGAACGGTTTACC
CTCCCCTATCTGACTCCAAGTATCATTCTGGTATTTCTGTTGATCTAGCTATTTTTAG
ACTTCATTTAGCCGGAATTTCTTCAATTCTTGGTAGAATCAATTTTCTTACTACTATT
ATTTGTTCTCGCACAGCAAAAGCTATTTCTCTAGATCGTATGCCTTTAATATTATGGG
CGTTTGCTGTGACTTCTATTCTTCTTGTTACTAGGTTACCCGTATTAGCTGGTGCTATT
ACTATGCTTTTAACTGATCGAAACTTTAATACCTCTTTTTTTGATCCCGCAGGAGGGG
GTAATCCAGTACTCTACCAGCATTTATTTTGATTTTTTGGTCAC

>P1_1 627 bp – Pluvial Lake Palomas Site 1, Mimbres River Delta, New Mexico

ATAAGGTTCCTTATTCGTTTAGAGTTAGGGGTTATTGGTCCTTATATTGGGGATGAAC
ATCTATATAACGTTATGGTTACTGCTCATGCCTTTGTTATGATTTTTTTTATGGTTATA
CCTATTTCTATGGGTGGCTTTGGTAACTGACTTATTCCACTAATGTTGGGTGTTGCTG
ATATAGCTTTCCCGCGCATAAATAATCTTTCTTTCTGGCTTCTTATTCCATCTTTCACT
TTTTTATTACTTTCTTCAATTCTTGATGCTGGTGTTGGTACGGGTTGAACGGTTTACC
CTCCCCTAGCCGGAATTTCTTCAATTCTTGGTAGAATCAATTTTCTTACCACTATTAT
TTGTTCTCGCACAGCAAAAGCTATTTCTCTAGATCGTATGCCTTTAATGTTATGGGCG
TTTGCTGTGACTTCTATTCTTCTTGTTACTAGATTACCAGTATTAGCTGGTGCTATTAC
TATGCTTTTAACTGATCGAAACTTTAATACCTCTTTTTTTGATCCCGCAGGAGGTGGT
AATCCAGTACTCTACCAACATTTATTTTGATTTTTTGGTCAC

>P1_2 627 bp – Pluvial Lake Palomas Site 1, Mimbres River Delta, New Mexico

ATAAGGTTCCTTATTCGTTTAGAGTTAGGAGTTATTGGTCCTTATATTGGGGATGAAC
ATCTATATAACGTTATGGTTACTGCTCATGCCTTTGTTATGATTTTTTTTATGGTTATA
CCTATTTCTATGGGTGGCTTTGGTAACTGACTTATTCCACTAATGTTGGGTGTTGCTG
ATATAGCTTTCCCGCGCATAAATAATCTTTCCTTCTGGCTTCTTATTCCATCTTTCACT
TTTTTATTACTTTCTTCAATTCTTGATGCTGGTGTTGGTACGGGTTGAACGGTTTACC
CTCCCCTATCTGACTCCAAGTATCATTCTGGTATTTCTGTTGATCTAGCTATTTTTAG
ACTTCATTTAGCCGGAATTTCTTCAATTCTTGGTAGAATCAATTTTCTTACCACTATT
ATTTGTTCTCGCACAGCAAAAGCTATTTCTCTAGATCGTATGCCTTTAATGTTATGGG
CGTTTGCTGTGACTTCTATTCTTCTTGTTACTAGATTACCAGTATTAGCTGGTGCTATT
ACTATGCTTTTAACTGATCGAAACTTTAATACCTCTTTTTTTGATCCCGCAGGAGGTG
GTAATCCAGTACTCTACCAACATTTATTTTGATTTTTTGGTCAC

>P1_3 627 bp - Pluvial Lake Palomas Site 1, Mimbres River Delta, New Mexico

ATAAGGTTCCTTATTCGTTTAGAGTTAGGAGTTATTGGTCCTTATATTGGGGATGAAC
ATCTATATAACGTTATGGTTACTGCTCATGCCTTTGTTATGATTTTTTTTATGGTTATA
CCTATTTCTATGGGTGGCTTTGGTAACTGACTTATTCCACTAATGTTGGGTGTTGCTG
ATATAGCTTTCCCGCGCATAAATAATCTTTCTTTCTGGCTTCTTATTCCATCTTTCACT
TTTTTATTACTTTCTTCAATTCTTGATGCTGGTGTTGGTACGGGTTGAACGGTTTACC
CTCCCCTATCTGACTCCAAGTATCATTCTGGTATTTCTGTTGATCTAGCTATTTTTAG
ACTTCATTTAGCCGGAATTTCTTCAATTCTTGGTAGAATCAATTTTCTTACCACTATT
ATTTGTTCTCGCACAGCAAAAGCTATTTCTCTAGATCGTATGCCTTTAATGTTATGGG
CGTTTGCTGTGACTTCTATTCTTCTTGTTACTAGATTACCAGTATTAGCTGGTGCTATT
ACTATGCTTTTAACTGATCGAAACTTTAATACCTCTTTTTTTGATCCCGCAGGAGGTG
GTAATCCAGTACTCTACCAACATTTATTTTGATTTTTTGGTCAC

>P1_4 627 bp – Pluvial Lake Palomas Site 1, Mimbres River Delta, New Mexico

ATAAGGTTCCTTATTCGTTTAGAGTTAGGAGTTATTGGTCCTTATATTGGGGATGAAC
ATCTATATAACGTTATGGTTACTGCTCATGCCTTTGTTATGATTTTTTTTATGGTTATA
CCTATTTCTATGGGTGGCTTTGGTAACTGACTTATTCCACTAATGTTGGGTGTTGCTG
ATATAGCTTTCCCGCGCATAAATAATCTTTCTTTCTGGCTTCTTATTCCATCTTTCACT
TTTTTATTACTTTCTTCAATTCTTGATGCTGGTGTTGGTACGGGTTGAACGGTTTATCC
TCCCCTATCTGACTCCAAGTATCATTCTGGTATTTCTGTTGATCTAGCTATTTTTAGA
CTTCATTTAGCCGGAATTTCTTCAATTCTTGGTAGAATCAATTTTCTTACCACTATTA
TTTGTTCTCGCACAGCAAAAGCTATTTCTCTAGATCGTATGCCTTTAATGTTATGGGC
GTTTGCTGTGACTTCTATTCTTCTTGTTACTAGATTACCAGTATTAGCTGGTGCTATT
ACTATGCTTTTAACTGATCGAAACTTTAATACCTCTTTTTTTGATCCCGCAGGAGGTG
GTAATCCAGTACTCTACCAGCATTTATTTTGATTTTTTGGTCAC

>P1_5 627 bp – Pluvial Lake Palomas Site 1, Mimbres River Delta, New Mexico

ATAAGATTCCTTATTCGTTTAGAGTTAGGAGTTATTGGTCCTTATATTGGGGATGAAC
ATCTATACAACGTTATGGTTACTGCTCATGCCTTTGTTATGATTTTTTTTATGGTTATA
CCTATTTCTATGGGTGGCTTTGGTAACTGACTTATTCCACTAATGTTGGGTGTTGCTG
ATATAGCTTTCCCGCGCATAAATAATCTTTCTTTCTGGCTTCTTATTCCATCTTTCACT

TTTTTATTACTTTCTTCAATTCTTGATGCTGGTGTTGGTACGGGTTGAACGGTTTACC
CTCCCCTATCTGACTCCAAGTATCATTCTGGTATTTCTGTTGATCTAGCTATTTTTAG
ACTTCATTTAGCCGGAATTTCTTCAATTCTTGGTAGAATCAATTTTCTTACCACTATT
ATTTGTTCTCGCACAGCAAAAGCTATTTCTCTAGACCGTATGCCTTTAATGTTATGGG
CGTTTGCTGTGACTTCTATTCTTCTTGTTACTAGATTACCCGTATTAGCTGGTGCTATT
ACTATGCTTTTAACTGATCGAAACTTTAATACCTCTTTTTTTGATCCCGCAGGAGGTG
GTAATCCAGTACTCTACCAACATTTATTTTGATTTTTTGGTCAC

>P1_6 627 bp – Pluvial Lake Palomas Site 1, Mimbres River Delta, New Mexico

ATAAGATTTCTTATTCGTTTAGAGTTGGGGGTTATTGGTCCCTACATTGGAGATGAG
CATCTCTATAATGTCATGGTCACTGCTCACGCTTTCGTTATGATTTTTTTCATGGTTAT
GCCTATTTCTATGGGTGGTTTCGGTAACTGACTTATTCCTCTTATGTTAGGTGTTGCT
GATATGGCTTTTCCTCGAATGAATAATCTTTCCTTCTGATTACTAATCCCTTCTTTTAC
CTTTTTACTCCTTTCTTCAATTTTAGATGCTGGGGTTGGGACTGGATGAACGGTTTAT
CCTCCTCTTTCTGATTCTAAGTATCATTCTGGTATTTCGGTGGACCTAGCTATCTTTA
GCCTTCATTTAGCTGGTATTTCCTCAATCCTTGGTAGAATCAATTTTTTAACTACTAT
TATTTGTTCTCGCACAGCAAAAGCTATTTCTCTAGATCGAATGCCTCTTATGCTTTGA
GCGTTCGCTGTAACGTCAATTCTTCTTGTTACAAGGCTTCCTGTTTTAGCTGGCGCTA
TTACTATGCTTCTAACTGATCGTAATTTTAATACTTCTTTCTTTGATCCAGCAGGTGG
TGGTAACCCTGTACTCTACCAACACTTATTCTGATTTTTTGGTCAC

>P1_14 627 bp – Pluvial Lake Palomas Site 1, Mimbres River Delta, New Mexico

ATAAGATTTCTTATTCGTTTAGAGTTGGGGGTTATTGGTCCCTACATTGGAGATGAG
CATCTCTATAATGTCATGGTCACTGCTCACGCTTTCGTTATGATTTTTTTCATGGTTAT
GCCTATTTCTATGGGTGGTTTCGGTAACTGACTTATTCCTCTTATGTTAGGTGTTGCT
GATATGGCTTTTCCTCGAATGAATAATCTTTCCTTCTGATTACTAATCCCTTCTTTTAC
CTTTTTACTCCTTTCTTCAATTTTAGATGCTGGGGTTGGGACTGGATGAACGGTTTAT
CCTCCCCTTTCTGATTCTAAGTATCATTCTGGTATTTCGGTGGACCTGGCTATCTTTA
GCCTTCATTTAGCTGGTATTTCCTCAATCCTTGGTAGAATCAATTTTTTAACTACTAT
TATTTGTTCTCGCACAGCAAAAGCTATTTCTCTAGATCGAATGCCTCTTATGCTCTGA
GCGTTCGCTGTAACGTCAATTCTTCTTGTTACAAGGCTTCCTGTTTTAGCTGGCGCTA
TTACTATGCTTCTAACTGATCGTAATTTTAATACTTCTTTCTTTGATCCAGCAGGTGG
TGGTAACCCTGTACTCTACCAACACTTATTCTGATTTTTTGGTCAC

>P1_17 627 bp – Pluvial Lake Palomas Site 1– Mimbres River Delta, New Mexico

ATAAGATTCCTTATTCGTTTAGAGTTAGGGGTTATTGGTCCTTATATTGGGGATGAAC
ATTTATATAACGTCATGGTTACTGCCCACGCCTTTGTTATGATTTTTTTTATGGTTATG
CCTATTTCTATGGGTGGCTTTGGTAATTGACTTATTCCACTAATGTTGGGTGTTGCTG
ATATGGCTTTCCCACGTATAAATAATCTTTCTTTCTGGCTTCTTATTCCATCTTTCACT
TTTTTATTACTTTCTTCAATTCTTGATGCTGGTGTTGGTACGGGTTGAACTGTTTACCC
TCCCCTATCTGACTCTAAGTATCATTCTGGTATTTCTGTTGATCTAGCTATTTTTAGAC
TTCATTTAGCAGGAATTTCTTCAATTCTTGGTAGAATCAACTTTCTTACTACTATTAT
TTGTTCTCGCACAGCAAAAGCTATTTCTCTAGATCGTATGCCTTTAATATTATGGGCG

TTTGCTGTTACTTCTATTCTTCTTGTTACTAGATTACCCGTTTTAGCTGGTGCCATCAC
TATGCTTTTAACTGATCGAAACTTTAATACCTCTTTTTTTGACCCTGCAGGCGGTGGT
AACCCAGTACTCTACCAACATTTATTTTGATTTTTTGGTCAC

>P1_18 627 bp – Pluvial Lake Palomas Site 1– Mimbres River Delta, New Mexico

ATAAGATTTCTTATTCGTTTAGAGTTGGGGGTTATTGGTCCCTACATTGGAGATGAG
CATCTCTATAATGTCATGGTCACTGCTCACGCTTTCGTTATGATTTTTTTCATGGTTAT
GCCTATTTCTATGGGTGGTTTCGGTAACTGACTTATTCCTCTTATGTTAGGTGTTGCT
GATATGGCTTTTCCTCGAATGAATAATCTTTCCTTCTGATTACTAATCCCTTCTTTTAC
CTTTTTACTCCTTTCTTCAATTTTAGATGCTGGGGTTGGGACTGGATGAACGGTTTAT
CCTCCCCTTTCTGATTCTAAGTATCATTCTGGTATTTCGGTGGACCTGGCTATCTTTA
GCCTTCATTTAGCTGGTATTTCCTCAATCCTTGGTAGAATCAATTTTTTAACTACTAT
TATTTGTTCTCGCACAGCAAAAGCTATTTCTCTAGATCGAATGCCTCTTATGCTCTGA
GCGTTCGCTGTAACGTCAATTCTTCTTGTTACAAGGCTTCCTGTTTTAGCTGGCGCTA
TTACTATGCTTCTAACTGATCGTAATTTTAATACTTCTTTCTTTGATCCAGCAGGTGG
TGGTAACCCTGTACTCTACCAACACTTATTCTGATTTTTTGGTCAC

>P1_22 627 bp – Pluvial Lake Palomas Site 1– Mimbres River Delta, New Mexico

ATAAGATTCCTTATTCGTTTAGAGTTAGGGGTTATTGGTCCTTATATTGGGGATGAAC
ATTTATATAACGTCATGGTTACTGCCCACGCCTTTGTTATGATTTTTTTTATGGTTATG
CCTATTTCTATGGGTGGCTTTGGTAATTGACTTATTCCACTAATGTTGGGTGTTGCTG
ATATGGCTTTCCCACGTATAAATAATCTTTCTTTCTGGCTTCTTATTCCATCTTTCACT
TTTTTATTACTTTCTTCAATTCTTGATGCTGGTGTTGGTACGGGTTGAACTGTTTACCC
TCCCCTATCTGACTCTAAGTATCATTCTGGTATTTCTGTTGATCTAGCTATTTTTAGAC
TTCATTTAGCCGGAATTTCTTCAATTCTTGGTAGAATCAACTTTCTTACTACTATTATT
TGTTCTCGCACAGCAAAAGCTATTTCTCTAGATCGTATGCCTTTAATGTTATGGGCGT
TTGCTGTTACTTCTATTCTTCTTGTTACTAGATTACCCGTTTTAGCTGGTGCCATCACT
ATGCTTTTAACTGATCGAAACTTTAATACCTCTTTTTTTGACCCTGCAGGCGGTGGTA
ACCCAGTACTCTACCAACATTTATTTTGATTTTTTGGTCAC

>P2_4 627 bp – Pluvial Lake Palomas Site 2– Mimbres River Delta, New Mexico

ATAAGGTTCCTTATTCGTTTAGAGTTAGGAGTTATTGGTCCTTATATTGGGGATGAAC
ATCTATATAACGTTATGGTTACTGCTCATGCCTTTGTTATGATTTTTTTTATGGTTATA
CCTATTTCTATGGGTGGCTTTGGTAACTGACTTATTCCACTAATGTTGGGTGTTGCTG
ATATAGCTTTCCCGCGCATAAATAATCTTTCTTTCTGGCTTCTTATTCCATCTTTCACT
TTTTTATTACTTTCTTCAATTCTTGATGCTGGTGTTGGTACGGGTTGAACGGTTTACC
CTCCCCTATCTGACTCCAAGTATCATTCTGGTATTTCTGTTGATCTAGCTATTTTTAG
ACTTCATTTAGCCGGAATTTCTTCAATTCTTGGTAGAATCAATTTTCTTACCACTATT
ATTTGTTCTCGCACAGCAAAAGCTATTTCTCTAGATCGTATGCCTTTAATGTTATGGG
CGTTTGCTGTGACTTCTATTCTTCTTGTTACTAGATTACCAGTATTAGCTGGTGCTATT
ACTATGCTTTTAACTGATCGAAACTTTAATACCTCTTTTTTTGATCCCGCAGGAGGTG
GTAATCCAGTACTCTACCAACATTTATTTTGATTTTTTGGTCAC

>P2_10 627 bp – Pluvial Lake Palomas Site 2– Mimbres River Delta, New Mexico

ATAAGGTTCCTTATTCGTTTAGAGTTAGGAGTTATTGGTCCTTATATTGGGGATGAAC
ATCTATATAACGTTATGGTTACTGCTCATGCCTTTGTTATGATTTTTTTTATGGTTATA
CCTATTTCTATGGGTGGCTTTGGTAACTGACTTATTCCACTAATGTTGGGTGTTGCTG
ATATAGCTTTCCCGCGCATAAATAATCTTTCTTTCTGGCTTCTTATTCCATCTTTCACT
TTTTTATTACTTTCTTCAATTCTTGATGCTGGTGTTGGTACGGGTTGAACGGTTTACC
CTCCCCTATCTGACTCCAAGTATCATTCTGGTATTTCTGTTGATCTAGCTATTTTTAG
ACTTCATTTAGCCGGAATTTCTTCAATTCTTGGTAGAATCAATTTTCTTACCACTATT
ATTTGTTCTCGCACAGCAAAAGCTATTTCTCTAGATCGTATGCCTCTAATGTTATGGG
CGTTTGCTGTGACTTCTATTCTTCTTGTTACTAGATTACCAGTATTAGCTGGTGCTATT
ACTATGCTTTTAACTGATCGAAACTTTAATACCTCTTTTTTTGATCCCGCAGGAGGTG
GTAATCCAGTACTCTACCAACATTTATTTTGATTTTTTGGTCAC

>P2_11 627 bp – Pluvial Lake Palomas Site 2– Mimbres River Delta, New Mexico

ATAAGGTTCCTTATTCGTTTAGAGTTAGGAGTTATTGGTCCTTATATTGGGGATGAAC
ATCTATATAACGTTATGGTTACTGCTCATGCCTTTGTTATGATTTTTTTTATGGTTATA
CCTATTTCTATGGGTGGCTTTGGTAACTGACTTATTCCACTAATGTTGGGTGTTGCTG
ATATAGCTTTCCCGCGCATAAATAATCTTTCTTTCTGGCTTCTTATTCCATCTTTCACT
TTTTTATTACTTTCTTCAATTCTTGATGCTGGTGTTGGTACGGGTTGAACGGTTTACC
CTCCCCTATCTGACTCCAAGTATCATTCTGGTATTTCTGTTGATCTAGCTATTTTTAG
ACTTCATTTAGCCGGAATTTCTTCAATTCTTGGTAGAATCAATTTTCTTACCACTATT
ATTTGTTCTCGCACAGCAAAAGCTATTTCTCTAGATCGTATGCCTTTAATGTTATGGG
CGTTTGCTGTGACTTCTATTCTTCTTGTTACTAGATTACCAGTATTAGCTGGTGCTATT
ACTATGCTTTTAACTGATCGAAACTTTAATACCTCTTTTTTTGATCCCGCAGGAGGTG
GTAATCCAGTACTCTACCAACATTTATTTTGATTTTTTGGTCAC

>P2_42 627 bp – Pluvial Lake Palomas Site 2– Mimbres River Delta, New Mexico

ATAAGGTTCCTTATTCGTTTAGAGTTAGGAGTTATTGGTCCTTATATTGGGGATGAAC
ATCTATATAACGTTATGGTTACTGCTCATGCCTTTGTTATGATTTTTTTTATGGTTATA
CCTATTTCTATGGGTGGCTTTGGTAACTGACTTATTCCACTAATGTTGGGTGTTGCTG
ATATAGCTTTCCCGCGCATAAATAATCTTTCCTTCTGGCTTCTTATTCCATCTTTCACT
TTTTTATTACTTTCTTCAATTCTTGATGCTGGTGTTGGTACGGGTTGAACGGTTTACC
CTCCCCTATCTGACTCCAAGTATCATTCTGGTATTTCTGTTGATCTAGCTATTTTTAG
ACTTCATTTAGCCGGAATTTCTTCAATTCTTGGTAGAATCAATTTTCTTACCACTATT
ATTTGTTCTCGCACAGCAAAAGCTATTTCTCTAGATCGTATGCCTTTAATGTTATGGG
CGTTTGCTGTGACTTCTATTCTTCTTGTTACTAGATTACCAGTATTAGCTGGTGCTATT
ACTATGCTTTTAACTGATCGAAACTTTAATACCTCTTTTTTTGATCCCGCAGGAGGTG
GTAATCCAGTACTCTACCAACATTTATTTTGATTTTTTGGTCAC

>P2_43 627 bp – Pluvial Lake Palomas Site 2– Mimbres River Delta, New Mexico

ATAAGGTTCCTTATTCGTTTAGAGTTAGGAGTTATTGGTCCTTATATTGGGGATGAAC
ATCTATATAACGTTATGGTTACTGCTCATGCCTTTGTTATGATTTTTTTTATGGTTATA

CCTATTTCTATGGGTGGCTTTGGTAACTGACTTATTCCACTAATGTTGGGTGTTGCTG
ATATAGCTTTCCCGCGCATAAATAATCTTTCCTTCTGGCTTCTTATTCCATCTTTCACT
TTTTTATTACTTTCTTCAATTCTTGATGCTGGTGTTGGTACGGGTTGAACGGTTTACC
CTCCCCTATCTGACTCCAAGTATCATTCTGGTATTTCTGTTGATCTAGCTATTTTTAG
ACTTCATTTAGCCGGAATTTCTTCAATTCTTGGTAGAATCAATTTTCTTACCACTATT
ATTTGTTCTCGCACAGCAAAAGCTATTTCTCTAGATCGTATGCCTTTAATGTTATGGG
CGTTTGCTGTGACTTCTATTCTTCTTGTTACTAGATTACCAGTATTAGCTGGTGCTATT
ACTATGCTTTTAACTGATCGAAACTTTAATACCTCTTTTTTTGATCCCGCAGGAGGTG
GTAATCCAGTACTCTACCAACATTTATTTTGATTTTTTGGTCAC

>P2_45 627 bp – Pluvial Lake Palomas Site 2– Mimbres River Delta, New Mexico

ATAAGGTTCCTTATTCGTTTAGAGTTAGGAGTTATTGGTCCTTATATTGGGGATGAAC
ATCTATATAACGTTATGGTTACTGCTCATGCCTTTGTTATGATTTTTTTTATGGTTATA
CCTATTTCTATGGGTGGCTTTGGTAACTGACTTATTCCACTAATGTTGGGTGTTGCTG
ATATAGCTTTCCCGCGCATAAATAATCTTTCCTTCTGGCTTCTTATTCCATCTTTCACT
TTTTTATTACTTTCTTCAATTCTTGATGCTGGTGTTGGTACGGGTTGAACGGTTTACC
CTCCCCTATCTGACTCCAAGTATCATTCTGGTATTTCTGTTGATCTAGCTATTTTTAG
ACTTCATTTAGCCGGAATTTCTTCAATTCTTGGTAGAATCAATTTTCTTACCACTATT
ATTTGTTCTCGCACAGCAAAAGCTATTTCTCTAGATCGTATGCCTTTAATGTTATGGG
CGTTTGCTGTGACTTCTATTCTTCTTGTTACTAGATTACCAGTATTAGCTGGTGCTATT
ACTATGCTTTTAACTGATCGAAACTTTAATACCTCTTTTTTTGATCCCGCAGGAGGTG
GTAATCCAGTACTCTACCAACATTTATTTTGATTTTTTGGTCAC

>P2_46 627 bp – Pluvial Lake Palomas Site 2– Mimbres River Delta, New Mexico

ATAAGGTTCCTTATTCGTTTAGAGTTAGGAGTTATTGGTCCTTATATTGGGGATGAAC
ATCTATATAACGTTATGGTTACTGCTCATGCCTTTGTTATGATTTTTTTTATGGTTATA
CCTATTTCTATGGGTGGCTTTGGTAACTGACTTATTCCACTAATGTTGGGTGTTGCTG
ATATAGCTTTCCCGCGCATAAATAATCTTTCCTTCTGGCTTCTTATTCCATCTTTCACT
TTTTTATTACTTTCTTCAATTCTTGATGCTGGTGTTGGTACGGGTTGAACGGTTTACC
CTCCCCTATCTGACTCCAAGTATCATTCTGGTATTTCTGTTGATCTAGCTATTTTTAG
ACTTCATTTAGCCGGAATTTCTTCAATTCTTGGTAGAATCAATTTTCTTACCACTATT
ATTTGTTCTCGCACAGCAAAAGCTATTTCTCTAGATCGTATGCCTTTAATGTTATGGG
CGTTTGCTGTGACTTCTATTCTTCTTGTTACTAGATTACCAGTATTAGCTGGTGCTATT
ACTATGCTTTTAACTGATCGAAACTTTAATACCTCTTTTTTTGATCCCGCAGGAGGTG
GTAATCCAGTACTCTACCAACATTTATTTTGATTTTTTGGTCAC

>PET1 627 bp – Peccary Tank, Indio Mountains Research Station, Texas (GenBank Accession # KU564362)

ATAAGATTCCTTATTCGTTTAGAGTTAGGGGTTATTGGTCCTTATATTGGGGATGAAC
ATTTATATAACGTCATGGTTACTGCCCACGCCTTTGTTATGATTTTTTTTATGGTTATG
CCTATTTCTATGGGTGGCTTTGGTAATTGACTTATTCCACTAATGTTGGGTGTTGCTG
ATATGGCTTTCCCACGTATAAATAATCTTTCTTTCTGGCTTCTTATTCCATCTTTCACT
TTTTTATTACTTTCTTCAATTCTTGATGCTGGTGTTGGTACGGGTTGAACTGTTTACCC

TCCCCTATCTGACTCTAAGTATCATTCTGGTATTTCTGTTGATCTAGCTATTTTTAGAC
TTCATTTAGCCGGAATTTCTTCAATTCTTGGTAGAATCAACTTTCTTACTACTATTATT
TGTTCTCGCACAGCAAAAGCTATTTCTCTAGATCGTATGCCTTTAATATTATGGGCGT
TTGCTGTTACTTCTATTCTTCTTGTTACTAGATTACCCGTTTTAGCTGGTGCCATCACT
ATGCTTTTAACTGATCGAAACTTTAATACCTCTTTTTTTGACCCTGCAGGCGGTGGTA
ACCCAGTACTCTACCAACATTTATTTTGATTTTTTGGTCAC

>PET2 627 bp – Peccary Tank, Indio Mountains Research Station, Texas

ATAAGATTCCTTATTCGTTTAGAGTTAGGGGTTATTGGTCCTTATATTGGGGATGAAC
ATCTATATAACGTTATGGTTACTGCTCATGCCTTTGTTATGATTTTTTTTATGGTTATA
CCTATTTCTATGGGTGGCTTTGGTAACTGACTTATTCCACTAATGTTGGGTGTTGCTG
ATATGGCTTTCCCGCGCATAAATAATCTTTCTTTCTGGCTTCTTATTCCATCTTTCACT
TTTTTATTACTTTCTTCAATTCTTGATGCTGGTGTTGGTACGGGGTGAACGGTTTACC
CTCCCCTATCTGACTCCAAGTATCATTCTGGTATTTCTGTTGATCTAGCTATTTTTAG
ACTTCATTTAGCCGGAATTTCTTCAATTCTTGGTAGAATCAATTTTCTTACTACTATT
ATTTGTTCTCGCACAGCAAAAGCTATTTCTCTAGATCGTATGCCTTTAATGTTATGGG
CGTTTGCTGTGACCTCTATCCTTCTTGTTACTAGATTACCCGTATTAGCTGGCGCTAT
TACTATGCTTTTAACTGATCGAAACTTTAATACCTCCTTTTTTGATCCCGCAGGAGGT
GGTAATCCAGTACTCTACCAACATTTATTTTGATTTTTTGGTCAC

>PET3 627 bp – Peccary Tank, Indio Mountains Research Station, Texas

ATAAGATTCCTTATTCGTTTAGAGTTAGGGGTTATTGGTCCTTATATTGGGGATGAAC
ATTTATATAACGTCATGGTTACTGCCCACGCCTTTGTTATGATTTTTTTTATGGTTATG
CCTATTTCTATGGGTGGCTTTGGTAATTGACTTATTCCACTAATGTTGGGTGTTGCTG
ATATGGCTTTCCCACGTATAAATAATCTTTCTTTCTGGCTTCTTATTCCATCTTTCACT
TTTTTATTACTTTCTTCAATTCTTGATGCTGGTGTTGGTACGGGTTGAACTGTTTACCC
TCCCCTATCTGACTCTAAGTATCATTCTGGTATTTCTGTTGATCTAGCTATTTTTAGAC
TTCATTTAGCCGGAATTTCTTCAATTCTTGGTAGAATCAACTTTCTTACTACTATTATT
TGTTCTCGCACAGCAAAAGCTATTTCTCTAGATCGTATGCCTTTAATATTATGGGCGT
TTGCTGTTACTTCTATTCTTCTTGTTACTAGATTACCCGTTTTAGCTGGTGCCATCACT
ATGCTTTTAACTGATCGAAACTTTAATACCTCTTTTTTTGACCCTGCAGGCGGTGGTA
ACCCAGTACTCTACCAACATTTATTTTGATTTTTTGGTCAC

>PET_10 627 bp – Peccary Tank, Indio Mountains Research Station, Texas

ATAAGATTCCTTATTCGTTTAGAGTTAGGGGTTATTGGTCCTTATATTGGGGATGAAC
ATTTATATAACGTCATGGTTACTGCCCACGCCTTTGTTATGATTTTTTTTATGGTTATG
CCTATTTCTATGGGTGGCTTTGGTAATTGACTTATTCCACTAATGTTGGGTGTTGCTG
ATATGGCTTTCCCACGTATAAATAATCTTTCTTTCTGGCTTCTTATTCCATCTTTCACT
TTTTTATTACTTTCTTCAATTCTTGATGCTGGTGTTGGTACGGGTTGAACTGTTTACCC
TCCCCTATCTGACTCTAAGTATCATTCTGGTATTTCTGTTGATCTAGCTATTTTTAGAC
TTCATTTAGCAGGAATTTCTTCAATTCTTGGTAGAATCAACTTTCTTACTACTATTAT
TTGTTCTCGCACAGCAAAAGCTATTTCTCTAGATCGTATGCCTTTAATATTATGGGCG
TTTGCTGTTACTTCTATTCTTCTTGTTACTAGATTACCCGTTTTAGCTGGTGCCATCAC

TATGCTTTTAACTGATCGAAACTTTAATACCTCTTTTTTTGACCCTGCAGGCGGTGGT
AACCCAGTACTCTACCAACATTTATTTTGATTTTTTGGTCAC

>PET12 627 bp – Peccary Tank, Indio Mountains Research Station, Texas

ATAAAATTCCTTATTCGTTTAGAGTTAGGGGTTATTGGTCCTTATATTGGGGATGAAC
ATTTATATAACGTCATGGTTACTGCCCACGCCTTTGTTATGATTTTTTTTATGGTTATG
CCTATTTCTATGGGTGGCTTTGGTAATTGACTTATTCCACTAATGTTGGGTGTTGCTG
ATATGGCTTTCCCACGTATAAATAATCTTTCTTTCTGGCTTCTTATTCCATCTTTCACT
TTTTTATTACTTTCTTCAATTCTTGATGCTGGTGTTGGTACGGGTTGAACTGTTTACCC
TCCCCTATCTGACTCTAAGTATCATTCTGGTATTTCTGTTGATCTAGCTATTTTTAGAC
TTCATTTAGCAGGAATTTCTTCAATTCTTGGTAGAATCAACTTTCTTACTACTATTAT
TTGTTCTCGCACAGCAAAAGCTATTTCTCTAGATCGTATGCCTTTAATATTATGGGCG
TTTGCTGTTACTTCTATTCTTCTTGTTACTAGATTACCCGTTTAAGCTGGTGCCATCAC
TATGCTTTTAACTGAACGAAACTTTAATACCTCTTTTTTTGACCCTGCAGGCGGGGGT
AACCCAGTACTCTACCAACATTTATTTTGATTTTTTGGTCAC

>PET_17 627 bp – Peccary Tank, Indio Mountains Research Station, Texas

ATAAGATTCCTTATTCGTTTAGAGTTAGGGGTTATTGGTCCTTATATTGGGGATGAAC
ATTTATATAACGTCATGGTTACTGCCCACGCCTTTGTTATGATTTTTTTTATGGTTATG
CCTATTTCTATGGGTGGCTTTGGTAATTGACTTATTCCACTAATGTTGGGTGTTGCTG
ATATGGCTTTCCCACGTATAAATAATCTTTCTTTCTGGCTTCTTATTCCATCTTTCACT
TTTTTATTACTTTCTTCAATTCTTGATGCTGGTGTTGGTACGGGTTGAACTGTTTACCC
TCCCCTATCTGACTCTAAGTATCATTCTGGTATTTCTGTTGATCTAGCTATTTTTAGAC
TTCATTTAGCAGGAATTTCTTCAATTCTTGGTAGAATCAACTTTCTTACTACTATTAT
TTGTTCTCGCACAGCAAAAGCTATTTCTCTAGATCGTATGCCTTTAATATTATGGGCG
TTTGCTGTTACTTCTATTCTTCTTGTTACTAGATTACCCGTTTTAGCTGGTGCCATCAC
TATGCTTTTAACTGATCGAAACTTTAATACCTCTTTTTTTGACCCTGCAGGCGGTGGT
AACCCAGTACTCTACCAACATTTATTTTGATTTTTTGGTCAC

>PET_40 627 bp – Peccary Tank, Indio Mountains Research Station, Texas

ATAAGATTCCTTATTCGTTTAGAGTTAGGGGTTATTGGTCCTTATATTGGGGATGAAC
ATTTATATAACGTCATGGTTACTGCCCACGCCTTTGTTATGATTTTTTTTATGGTTATG
CCTATTTCTATGGGTGGCTTTGGTAATTGACTTATTCCACTAATGTTGGGTGTTGCTG
ATATGGCTTTCCCACGTATAAATAATCTTTCTTTCTGGCTTCTTATTCCATCTTTCACT
TTTTTATTACTTTCTTCAATTCTTGATGCTGGTGTTGGTACGGGTTGAACTGTTTACCC
TCCCCTATCTGACTCTAAGTATCATTCTGGTATTTCTGTTGATCTAGCTATTTTTAGAC
TTCATTTAGCAGGAATTTCTTCAATTCTTGGTAGAATCAACTTTCTTACTACTATTAT
TTGTTCTCGCACAGCAAAAGCTATTTCTCTAGATCGTATGCCTTTAATATTATGGGCG
TTTGCTGTTACTTCTATTCTTCTTGTTACTAGATTACCCGTTTTAGCTGGTGCCATCAC
TATGCTTTTAACTGATCGAAACTTTAATACCTCTTTTTTTGACCCTGCAGGCGGTGGT
AACCCAGTACTCTACCAACATTTATTTTGATTTTTTGGTCAC

>PET42 627 bp – Peccary Tank, Indio Mountains Research Station, Texas

ATAAGATTCCTTATTCGTTTAGAGTTAGGGGTTATTGGTCCTTATATTGGGGATGAAC
ATTTATATAACGTCATGGTTACTGCCCACGCCTTTGTTATGATTTTTTTTATGGTTATG
CCTATTTCTATGGGTGGCTTTGGTAATTGACTTATTCCACTAATGTTGGGCGTTGCTG
ATATGGCTTTCCCACGTATAAATAATCTTTCTTTCTGGCTTCTTATTCCATCTTTCACT
TTTTTATTACTTTCTTCAATTCTTGATGCTGGTGTTGGTACGGGTTGAACTGTTTACCC
TCCCCTATCTGACTCTAAGTATCATTCTGGTATTTCTGTTGATCTAGCTATTTTTAGAC
TTCATTTAGCCGGAATTTCTTCAATTCTTGGTAGAATCAACTTTCTTACTACTATTATT
TGTTCTCGCACAGCAAAAGCTATTTCTCTAGATCGTATGCCTTTAATATTATGGGCGT
TTGCTGTTACTTCTATTCTTCTTGTTACTAGATTACCCGTTTTAGCTGGTGCCATCACT
ATGCTTTTAACTGATCGAAACTTTAATACCTCTTTTTTTGACCCTGCAGGCGGCGGTA
ACCCAGTACTCTACCAACATTTATTTTGATTTTTTGGTCAC

>PET44 627 bp –Peccary Tank, Indio Mountains Research Station, Texas

ATAAGATTCCTTATTCGTTTAGAGTTAGGGGTTATTGGTCCTTATATTGGGGATGAAC
ATTTATATAACGTCATGGTTACTGCCCACGCCTTTGTTATGATTTTTTTTATGGTTATG
CCTATTTCTATGGGTGGCTTTGGTAATTGACTTATTCCACTAATGTTGGGCGTTGCTG
ATATGGCTTTCCCACGTATAAATAATCTTTCTTTCTGGCTTCTTATTCCATCTTTCACT
TTTTTATTACTTTCTTCAATTCTTGATGCTGGTGTTGGTACGGGTTGAACTGTTTACCC
TCCCCTATCTGACTCTAAGTATCATTCTGGTATTTCTGTTGATCTAGCTATTTTTAGAC
TTCATTTAGCCGGAATTTCTTCAATTCTTGGTAGAATCAACTTTCTTACTACTATTATT
TGTTCTCGCACAGCAAAAGCTATTTCTCTAGATCGTATGCCTTTAATATTATGGGCGT
TTGCTGTTACTTCTATTCTTCTTGTTACTAGATTACCCGTTTTAGCTGGTGCCATCACT
ATGCTTTTAACTGATCGAAACTTTAATACCTCTTTTTTTGACCCTGCAGGCGGCGGTA
ACCCAGTACTCTACCAACATTTATTTTGATTTTTTGGTCAC

>PET48 627 bp – Peccary Tank, Indio Mountains Research Station, Texas

ATAAGATTCCTTATTCGTTTAGAGTTAGGGGTTATTGGTCCTTATATTGGGGATGAAC
ATTTATATAACGTCATGGTTACTGCCCACGCCTTTGTTATGATTTTTTTTATGGTTATG
CCTATTTCTATGGGTGGCTTTGGTAATTGACTTATTCCACTAATGTTGGGCGTTGCTG
ATATGGCTTTCCCACGTATAAATAATCTTTCTTTCTGGCTTCTTATTCCATCTTTCACT
TTTTTATTACTTTCTTCAATTCTTGATGCTGGTGTTGGTACGGGTTGAACTGTTTACCC
TCCCCTATCTGACTCTAAGTATCATTCTGGTATTTCTGTTGATCTAGCTATTTTTAGAC
TTCATTTAGCCGGAATTTCTTCAATTCTTGGTAGAATCAACTTTCTTACTACTATTATT
TGTTCTCGCACAGCAAAAGCTATTTCTCTAGATCGTATGCCTTTAATATTATGGGCGT
TTGCTGTTACTTCTATTCTTCTTGTTACTAGATTACCCGTTTTAGCTGGTGCCATCACT
ATGCTTTTAACTGATCGAAACTTTAATACCTCTTTTTTTGACCCTGCAGGCGGCGGTA
ACCCAGTACTCTACCAACATTTATTTTGATTTTTTGGTCAC

>PET_52 627 bp – Peccary Tank, Indio Mountains Research Station, Texas

ATAAGATTCCTTATTCGTTTAGAGTTAGGGGTTATTGGTCCTTATATTGGGGATGAAC
ATTTATATAACGTCATGGTTACTGCCCACGCCTTTGTTATGATTTTTTTTATGGTTATG
CCTATTTCTATGGGTGGCTTTGGTAATTGACTTATTCCACTAATGTTGGGTGTTGCTG
ATATGGCTTTCCCACGTATAAATAATCTTTCTTTCTGGCTTCTTATTCCATCTTTCACT

TTTTTATTACTTTCTTCAATTCTTGATGCTGGTGTTGGTACGGGTTGAACTGTTTACCC
TCCCCTATCTGACTCTAAGTATCATTCTGGTATTTCTGTTGATCTAGCTATTTTTAGAC
TTCATTTAGCAGGAATTTCTTCAATTCTTGGTAGAATCAACTTTCTTACTACTATTAT
TTGTTCTCGCACAGCAAAAGCTATTTCTCTAGATCGTATGCCTTTAATATTATGGGCG
TTTGCTGTTACTTCTATTCTTCTTGTTACTAGATTACCCGTTTTAGCTGGTGCCATCAC
TATGCTTTTAACTGATCGAAACTTTAATACCTCTTTTTTTGACCCTGCAGGCGGTGGT
AACCCAGTACTCTACCAACATTTATTTTGATTTTTTGGTCCC

>CAT5 627 bp – Cattle Tank, White Sands National Park, New Mexico

ATAAGATTCCTTATTCGTTTAGAGTTAGGGGTTATTGGTCCTTATATTGGGGATGAAC
ATTTATATAACGTCATGGTTACTGCCCACGCCTTTGTTATGATTTTTTTTATGGTTATG
CCTATTTCTATGGGTGGCTTTGGTAACTGACTTATTCCACTAATGTTGGGTGTTGCTG
ATATGGCTTTCCCACGTATAAATAATCTTTCTTTCTGGCTTCTTATTCCATCTTTCACT
TTTTTATTACTTTCTTCAATTCTTGATGCTGGTGTTGGTACGGGTTGAACTGTTTACCC
TCCCCTATCTGACTCTAAGTATCATTCTGGTATTTCTGTTGATCTAGCTATTTTTAGAC
TTCATTTAGCCGGAATTTCTTCAATTCTTGGTAGAATCAACTTTCTTACTACTATTATT
TGTTCTCGCACAGCAAAAGCTATTTCTCTAGATCGTATGCCTTTAATGTTATGGGCGT
TTGCTGTTACTTCTATTCTTCTTGTTACTAGATTACCCGTTTTAGCTGGTGCCATCACT
ATGCTTTTAACTGATCGAAACTTTAATACCTCTTTTTTTGACCCTGCAGGCGGTGGTA
ACCCAGTACTCTACCAACATTTATTTTGATTTTTTGGTCAC

>CAT11 627 bp – Cattle Tank, White Sands National Park, New Mexico

ATAAGATTCCTTATTCGTTTAGAGTTAGGGGTTATTGGTCCTTATATTGGGGATGAAC
ATTTATATAACGTCATGGTTACTGCCCACGCCTTTGTTATGATTTTTTTTATGGTTATG
CCTATTTCTATGGGTGGCTTTGGTAACTGACTTATTCCACTAATGTTGGGTGTTGCTG
ATATGGCTTTCCCACGTATAAATAATCTTTCTTTCTGGCTTCTTATTCCATCTTTCACT
TTTTTATTACTTTCTTCAATTCTTGATGCTGGTGTTGGTACGGGTTGAACTGTTTACCC
TCCCCTATCTGACTCTAAGTATCATTCTGGTATTTCTGTTGATCTAGCTATTTTTAGAC
TTCATTTAGCCGGAATTTCTTCAATTCTTGGTAGAATCAACTTTCTTACTACTATTATT
TGTTCTCGCACAGCAAAAGCTATTTCTCTAGATCGTATGCCTTTAATGTTATGGGCGT
TTGCTGTTACTTCTATTCTTCTTGTTACTAGATTACCCGTTTTAGCTGGTGCCATCACT
ATGCTTTTAACTGATCGAAACTTTAATACCTCTTTTTTTGACCCTGCAGGCGGTGGTA
ACCCAGTACTCTACCAACATTTATTTTGATTTTTTGGTCAC

>CAT26 627 bp – Cattle Tank, White Sands National Park, New Mexico

ATAAGATTCCTTATTCGTTTAGAGTTAGGGGTTATTGGTCCTTATATTGGGGATGAAC
ATTTATATAACGTCATGGTTACTGCCCACGCCTTTGTTATGATTTTTTTTATGGTTATG
CCTATTTCTATGGGTGGCTTTGGTAACTGACTTATTCCACTAATGTTGGGTGTTGCTG
ATATGGCTTTCCCACGTATAAATAATCTTTCTTTCTGGCTTCTTATTCCATCTTTCACT
TTTTTATTACTTTCTTCAATTCTTGATGCTGGTGTTGGTACGGGTTGAACTGTTTACCC
TCCCCTATCTGACTCTAAGTATCATTCTGGTATTTCTGTTGATCTAGCTATTTTTAGAC
TTCATTTAGCCGGAATTTCTTCAATTCTTGGTAGAATCAACTTTCTTACTACTATTATT
TGTTCTCGCACAGCAAAAGCTATTTCTCTAGATCGTATGCCTTTAATGTTATGGGCGT

TTGCTGTTACTTCTATTCTTCTTGTTACTAGATTACCCGTTTTAGCTGGTGCCATCACT
ATGCTTTTAACTGATCGAAACTTTAATACCTCTTTTTTTGACCCTGCAGGCGGTGGTA
ACCCAGTACTCTACCAACATTTATTTTGATTTTTTGGTCAC

>CAT78 627 bp – Cattle Tank, White Sands National Park, New Mexico

ATAAGATTCCTTATTCGTTTAGAGTTAGGGGTTATTGGTCCTTATATTGGGGATGAAC
ATTTATATAACGTCATGGTTACTGCCCACGCCTTTGTTATGATTTTTTTTATGGTTATG
CCTATTTCTATGGGTGGCTTTGGTAACTGACTTATTCCACTAATGTTGGGTGTTGCTG
ATATGGCTTTCCCACGTATAAATAATCTTTCTTTCTGGCTTCTTATTCCATCTTTCACT
TTTTTATTACTTTCTTCAATTCTTGATGCTGGTGTTGGTACGGGTTGAACTGTTTACCC
TCCCCTATCTGACTCTAAGTATCATTCTGGTATTTCTGTTGATCTAGCTATTTTTAGAC
TTCATTTAGCCGGAATTTCTTCAATTCTTGGTAGAATCAACTTTCTTACTACTATTATT
TGTTCTCGCACAGCAAAAGCTATTTCTCTAGATCGTATGCCTTTAATGTTATGGGCGT
TTGCTGTTACTTCTATTCTTCTTGTTACTAGATTACCCGTTTTAGCTGGTGCCATCACT
ATGCTTTTAACTGATCGAAACTTTAATACCTCTTTTTTTGACCCTGCAGGCGGTGGTA
ACCCAGTACTCTACCAACATTTATTTTGATTTTTTGGTCAC

>Ret3 627 bp – Red Tank, Indio Mountains Research Station, Texas

ATAAGATTCCTTATTCGTTTAGAGTTAGGGGTTATTGGTCCTTATATTGGGGATGAAC
ATTTATATAACGTCATGGTTACTGCCCACGCCTTTGTTATGATTTTTTTTATGGTTATG
CCTATTTCTATGGGTGGCTTTGGTAATTGACTTATTCCACTAATGTTGGGTGTTGCTG
ATATGGCTTTCCCACGTATAAATAATCTTTCTTTCTGGCTTCTTATTCCATCTTTCACT
TTTTTATTACTTTCTTCAATTCTTGATGCTGGTGTTGGTACGGGTTGAACTGTTTACCC
TCCCCTATCTGACTCTAAGTATCATTCTGGTATTTCTGTTGATCTAGCTATTTTTAGAC
TTCATTTAGCCGGAATTTCTTCAATTCTTGGTAGAATCAACTTTCTTACTACTATTATT
TGTTCTCGCACAGCAAAAGCTATTTCTCTAGATCGTATGCCTTTAATATTATGGGCGT
TTGCTGTTACTTCTATTCTTCTTGTTACTAGATTACCAGTTTTAGCTGGTGCCATCACT
ATGCTTTTAACTGATCGAAACTTTAATACCTCTTTTTTTGACCCTGCAGGCGGTGGTA
ACCCAGTACTCTACCAACATTTATTTTGATTTTTTGGTCAC

>RAT2 627 bp – Rattlesnake Tank, Indio Mountains Research Station, Texas

ATAAGATTCCTTATTCGTTTAGAGTTAGGGGTTATTGGTCCTTATATTGGGGATGAAC
ATTTATATAACGTCATGGTTACTGCCCACGCCTTTGTTATGATTTTTTTTATGGTTATG
CCTATTTCTATGGGTGGCTTTGGTAACTGACTTATTCCACTAATGTTGGGTGTTGCTG
ATATGGCTTTCCCACGTATAAATAATCTTTCTTTCTGGCTTCTTATTCCATCTTTCACT
TTTTTATTACTTTCTTCAATTCTTGATGCTGGTGTTGGTACGGGTTGAACTGTTTACCC
TCCCCTATCTGACTCTAAGTATCATTCTGGTATTTCTGTTGATCTAGCTATTTTTAGAC
TTCATTTAGCCGGAATTTCTTCAATTCTTGGTAGAATCAACTTTCTTACTACTATTATT
TGTTCTCGCACAGCAAAAGCTATTTCTCTAGATCGTATGCCTTTAATGTTATGGGCGT
TTGCTGTTACTTCTATTCTTCTTGTTACTAGATTACCCGTTTTAGCTGGTGCCATCACT
ATGCTTTTAACTGATCGAAACTTTAATACCTCTTTTTTTGACCCTGCAGGCGGTGGTA
ACCCAGTACTCTACCAACATTTATTTTGATTTTTTGGTCAC

>RAT5 627 bp – Rattlesnake Tank, Indio Mountains Research Station, Texas

ATAAGATTCCTTATTCGTTTAGAGTTAGGAGTTATTGGTCCTTATATTGGGGATGAAC
ATCTATATAACGTTATGGTTACTGCTCATGCCTTTGTTATGATTTTTTTTATGGTTATA
CCTATTTCTATGGGTGGCTTTGGTAATTGACTTATTCCACTAATGTTGGGTGTTGCTG
ATATAGCTTTCCCGCGCATAAATAATCTTTCTTTTTGGCTTCTTATTCCATCTTTCACT
TTTTTATTACTTTCTTCAATTCTTGATGCTGGTGTTGGTACGGGTTGAACGGTTTACC
CTCCCCTATCTGACTCCAAGTATCATTCTGGTATTTCTGTTGATCTAGCTATTTTTAG
ACTTCATTTAGCCGGAATTTCTTCAATTCTTGGTAGAATCAATTTTCTTACCACTATT
ATTTGCTCTCGCACAGCAAAAGCCATTTCTCTAGATCGTATGCCTTTAATGTTATGGG
CGTTTGCTGTGACTTCTATTCTTCTTGTTACTAGATTACCCGTATTAGCTGGTGCTATT
ACTATGCTTTTAACTGATCGAAACTTTAATACCTCTTTTTTTGATCCCGCAGGAGGTG
GTAATCCAGTACTCTACCAACACTTATTTTGATTTTTTGGTCAC

>LNY2 627 bp – Lonely Tank, Indio Mountains Research Station, Texas

ATAAGATTCCTTATTCGTTTAGAGTTAGGGGTTATTGGTCCTTATATTGGGGATGAAC
ATTTATATAACGTCATGGTTACTGCCCACGCCTTTGTTATGATTTTTTTTATGGTTATG
CCTATTTCTATGGGTGGCTTTGGTAATTGACTTATTCCACTAATGTTGGGTGTTGCTG
ATATGGCTTTCCCACGTATAAATAATCTTTCTTTCTGGCTTCTTATTCCATCTTTCACT
TTTTTATTACTTTCTTCAATTCTTGATGCTGGTGTTGGTACGGGTTGAACTGTTTACCC
TCCCCTATCTGACTCTAAGTATCATTCTGGTATTTCTGTTGATCTAGCTATTTTTAGAC
TTCATTTAGCCGGAATTTCTTCAATTCTTGGTAGAATCAACTTTCTTACTACTATTATT
TGTTCTCGCACAGCAAAAGCTATTTCTCTAGATCGTATGCCTTTAATATTATGGGCGT
TTGCTGTTACTTCTATTCTTCTTGTTACTAGATTACCAGTTTTAGCTGGTGCCATCACT
ATGCTTTTAACTGATCGAAACTTTAATACCTCTTTTTTTGACCCTGCAGGCGGTGGTA
ACCCAGTACTCTACCAACATTTATTTTGATTTTTTGGTCAC

>LNY4 627 bp – Lonely Tank, Indio Mountains Research Station, Texas

ATAAGATTCCTTATTCGTTTAGAGTTAGGGGTTATTGGTCCTTATATTGGGGATGAAC
ATTTATATAACGTCATGGTTACTGCCCACGCCTTTGTTATGATTTTTTTTATGGTTATG
CCTATTTCTATGGGTGGCTTTGGTAATTGACTTATTCCACTAATGTTGGGTGTTGCTG
ATATGGCTTTCCCACGTATAAATAATCTTTCTTTCTGGCTTCTTATTCCATCTTTCACT
TTTTTATTACTTTCTTCAATTCTTGATGCTGGTGTTGGTACGGGTTGAACTGTTTACCC
TCCCCTATCTGACTCTAAGTATCATTCTGGTATTTCTGTTGATCTAGCTATTTTTAGAC
TTCATTTAGCCGGAATTTCTTCAATTCTTGGTAGAATCAACTTTCTTACTACTATTATT
TGTTCTCGCACAGCAAAAGCTATTTCTCTAGATCGTATGCCTTTAATATTATGGGCGT
TTGCTGTTACTTCTATTCTTCTTGTTACTAGATTACCAGTTTTAGCTGGTGCCATCACT
ATGCTTTTAACTGATCGAAACTTTAATACCTCTTTTTTTGACCCTGCAGGCGGTGGTA
ACCCAGTACTCTACCAACATTTATTTTGATTTTTTGGTCCC

>LNY6 627 bp – Lonely Tank, Indio Mountains Research Station, Texas

ATAAGATTCCTTATTCGTTTAGAGTTAGGGGTTATTGGTCCTTATATTGGGGATGAAC
ATTTATATAACGTCATGGTTACTGCCCACGCCTTTGTTATGATTTTTTTTATGGTTATG

CCTATTTCTATGGGTGGCTTTGGTAATTGACTTATTCCACTAATGTTGGGTGTTGCTG
ATATGGCTTTCCCACGTATAAATAATCTTTCTTTCTGGCTTCTTATTCCATCTTTCACT
TTTTTATTACTTTCTTCAATTCTTGATGCTGGTGTTGGTACGGGTTGAACTGTTTACCC
TCCCCTATCTGACTCTAAGTATCATTCTGGTATTTCTGTTGATCTAGCTATTTTTAGAC
TTCATTTAGCCGGAATTTCTTCAATTCTTGGTAGAATCAACTTTCTTACTACTATTATT
TGTTCTCGCACAGCAAAAGCTATTTCTCTAGATCGTATGCCTTTAATATTATGGGCGT
TTGCTGTTACTTCTATTCTTCTTGTTACTAGATTACCAGTTTTAGCTGGTGCCATCACT
ATGCTTTTAACTGATCGAAACTTTAATACCTCTTTTTTTGACCCTGCAGGCGGTGGTA
ACCCAGTACTCTACCAACATTTATTTTGATTTTTTGGTCAC

>BEB1 627 bp – Bailey Evans, Site B,Indio Mountains Research Station, Texas

ATAAGATTCCTTATTCGTTTAGAGTTAGGGGTTATTGGTCCTTATATTGGGGATGAAC
ATTTATATAACGTCATGGTTACTGCCCACGCCTTTGTTATGATTTTTTTTATGGTTATA
CCTATTTCTATGGGTGGCTTTGGTAATTGACTTATTCCACTAATGTTGGGTGTTGCTG
ATATGGCTTTCCCACGTATAAATAATCTTTCTTTCTGGCTTCTTATTCCATCTTTCACT
TTTTTATTACTTTCTTCAATTCTTGATGCTGGTGTTGGTACGGGTTGAACTGTTTACCC
TCCCCTATCTGACTCTAAGTATCATTCTGGTATTTCTGTTGATCTAGCTATTTTTAGAC
TTCATTTAGCCGGAATTTCTTCAATTCTTGGTAGAATCAACTTTCTTACTACTATTATT
TGTTCTCGCACAGCAAAAGCTATTTCTCTAGATCGTATGCCTTTAATATTATGGGCGT
TTGCTGTTACTTCTATTCTTCTTGTTACTAGATTACCCGTTTTAGCTGGTGCCATCACT
ATGCTTTTAACTGATCGAAACTTTAATACCTCTTTTTTTGACCCTGCAGGCGGTGGTA
ACCCAGTACTCTACCAACATTTATTTTGATTTTTTGGTCAC

>Drw1 627 bp – Draw 1, Columbus, New Mexico

ATAAGATTCCTTATTCGTTTAGAGTTAGGAGTTATTGGTCCTTATATTGGGGATGAAC
ATCTATATAACGTTATGGTTACTGCTCATGCCTTTGTTATGATTTTTTTTATGGTTATA
CCTATTTCTATGGGTGGCTTTGGTAATTGACTTATTCCACTAATGTTGGGTGTTGCTG
ATATAGCTTTCCCGCGCATAAATAATCTTTCTTTTTGGCTTCTTATTCCATCTTTCACT
TTTTTATTACTTTCTTCAATTCTTGATGCTGGTGTTGGTACGGGTTGAACGGTTTACC
CTCCCCTATCTGACTCCAAGTATCATTCTGGTATTTCTGTTGATCTAGCTATTTTTAG
ACTTCATTTAGCCGGAATTTCTTCAATTCTTGGTAGAATCAATTTTCTTACCACTATT
ATTTGTTCTCGCACAGCAAAAGCTATTTCTCTAGATCGTATGCCTTTAATGTTATGGG
CGTTTGCTGTGACTTCTATTCTTCTTGTTACTAGATTACCCGTATTAGCTGGTGCTATT
ACTATGCTTTTAACTGATCGAAACTTTAATACCTCTTTTTTTGATCCCGCAGGAGGTG
GTAATCCAGTACTCTACCAACACTTATTTTGATTTTTTGGTCAC

>CNM 627 bp – Columbus Playa, Highway 09, New Mexico

ATAAGATTCCTTATTCGTTTAGAGTTAGGGGTTATTGGTCCTTATATTGGGGATGAAC
ATTTATATAACGTCATGGTTACTGCCCACGCCTTTGTTATGATTTTTTTTATGGTTATG
CCTATTTCTATGGGTGGCTTTGGTAATTGACTTATTCCACTAATGTTGGGTGTTGCTG
ATATGGCTTTCCCACGTATAAATAATCTTTCTTTCTGGCTTCTTATTCCATCTTTCACT
TTTTTATTACTTTCTTCAATTCTTGATGCTGGTGTTGGTACGGGTTGAACTGTTTACCC
TCCCCTATCTGACTCTAAGTATCATTCTGGTATTTCTGTTGATCTAGCTATTTTTAGAC

TTCATTTAGCCGGAATTTCTTCAATTCTTGGTAGAATCAACTTTCTTACTACTATTATT
TGTTCTCGCACAGCAAAAGCTATTTCTCTAGATCGTATGCCTTTAATATTATGGGCGT
TTGCTGTTACTTCTATTCTTCTTGTTACTAGATTACCCGTTTTAGCTGGTGCCATCACT
ATGCTTTTAACTGATCGAAACTTTAATACCTCTTTTTTTGACCCTGCAGGCGGTGGTA
ACCCAGTACTCTACCAACATTTATTTTGATTTTTTGGTCAC

>LNA7 627 bp – Luna Tank, Highway 26, New Mexico

ATAAGGTTCCTTATTCGTTTAGAGTTAGGAGTTATTGGTCCTTATATTGGGGATGAAC
ATCTATATAACGTTATGGTTACTGCTCATGCCTTTGTTATGATTTTTTTTATGGTTATA
CCTATTTCTATGGGTGGCTTTGGTAACTGACTTATTCCACTAATGTTGGGTGTTGCTG
ATATAGCTTTCCCGCGCATAAATAATCTTTCTTTCTGGCTTCTTATTCCATCTTTCACT
TTTTTATTACTTTCTTCAATTCTTGATGCTGGTGTTGGTACGGGTTGAACGGTTTACC
CTCCCCTATCTGACTCCAAGTATCATTCTGGTATTTCTGTTGATCTAGCTATTTTTAG
ACTTCATTTAGCCGGAATTTCTTCAATTCTTGGTAGAATCAATTTTCTTACCACTATT
ATTTGTTCTCGCACAGCAAAAGCTATTTCTCTAGATCGTATGCCTTTAATGTTATGGG
CGTTTGCTGTGACTTCTATTCTTCTTGTTACTAGATTACCAGTATTAGCTGGTGCTATT
ACTATGCTTTTAACTGATCGAAACTTTAATACCTCTTTTTTTGATCCCGCAGGAGGTG
GTAATCCAGTACTCTACCAACATTTATTTTGATTTTTTGGTCAC

>LNA1 627 bp - Luna Tank, Highway 26, New Mexico

ATAAGGTTCCTTATTCGTTTAGAGTTAGGAGTTATTGGTCCTTATATTGGGGATGAAC
ATCTATATAACGTTATGGTTACTGCTCATGCCTTTGTTATGATTTTTTTTATGGTTATA
CCTATTTCTATGGGTGGCTTTGGTAACTGACTTATTCCACTAATGTTGGGTGTTGCTG
ATATAGCTTTCCCGCGCATAAATAATCTTTCTTTCTGGCTTCTTATTCCATCTTTCACT
TTTTTATTACTTTCTTCAATTCTTGATGCTGGTGTTGGTACGGGTTGAACGGTTTACC
CTCCCCTATCTGACTCCAAGTATCATTCTGGTATTTCTGTTGATCTAGCTATTTTTAG
ACTTCATTTAGCCGGAATTTCTTCAATTCTTGGTAGAATCAATTTTCTTACCACTATT
ATTTGTTCTCGCACAGCAAAAGCTATTTCTCTAGATCGTATGCCTTTAATGTTATGGG
CGTTTGCTGTGACTTCTATTCTTCTTGTTACTAGATTACCAGTATTAGCTGGTGCTATT
ACTATGCTTTTAACTGATCGAAACTTTAATACCTCTTTTTTTGATCCCGCAGGAGGTG
GTAATCCAGTACTCTACCAACATTTATTTTGATTTTTTGGTCAC

>404A 627 bp – Anthony Gap, Highway 404, New Mexico

ATAAGATTCCTTATTCGTTTAGAGTTAGGGGTTATTGGTCCTTATATTGGGGATGAAC
ATTTATATAACGTCATGGTTACTGCCCACGCCTTTGTTATGATTTTTTTTATGGTTATG
CCTATTTCTATGGGTGGCTTTGGTAATTGACTTATTCCACTAATGTTGGGTGTTGCTG
ATATGGCTTTCCCACGTATAAATAATCTTTCTTTCTGGCTTCTTATTCCATCTTTCACT
TTTTTATTACTTTCTTCAATTCTTGATGCTGGTGTTGGTACGGGTTGAACTGTTTACCC
TCCCCTATCTGACTCTAAGTATCATTCTGGTATTTCTGTTGATCTAGCTATTTTTAGAC
TTCATTTAGCCGGAATTTCTTCAATTCTTGGTAGAATCAACTTTCTTACTACTATTATT
TGTTCTCGCACAGCAAAAGCTATTTCTCTAGATCGTATGCCTTTAATATTATGGGCGT
TTGCTGTTACTTCTATTCTTCTTGTTACTAGATTACCCGTTTTAGCTGGTGCCATCACT

ATGCTTTTAACTGATCGAAACTTTAATACCTCTTTTTTTGACCCTGCAGGCGGCGGTA
ACCCAGTACTCTACCAACATTTATTTTGATTTTTTGGTCAC

>Alb2 627 bp – Album Park, El Paso, Texas

ATAAGATTCCTTATTCGTTTAGAGTTAGGGGTTATTGGTCCTTATATTGGGGATGAAC
ATTTATATAACGTCATAGTTACTGCCCACGCCTTTGTTATGATTTTTTTTATGGTTATG
CCTATTTCTATGGGTGGCTTTGGTAATTGGCTTATTCCACTAATATTGGGTGTTGCTG
ATATGGCTTTCCCACGTATAAATAATCTTTCTTTCTGGCTTCTTATTCCATCTTTCACT
TTTTTATTACTTTCTTCAATTCTTGATGCTGGTGTTGGTACGGGTTGAACTGTTTACCC
TCCCCTATCTGACTCTAAGTATCATTCTGGTATTTCTGTTGATCTAGCTATTTTTAGAC
TTCATTTAGCCGGAATTTCTTCAATTCTTGGTAGAATCAACTTTCTTACTACTATTATT
TGTTCTCGCACAGCAAAAGCTATTTCTCTAGATCGTATACCTTTAATATTATGGGCGT
TTGCTGTTACTTCTATTCTTCTTGTTACTAGATTACCCGTTTTAGCTGGTGCCATCACT
ATGCTTTTAACTGATCGAAACTTTAATACCTCTTTTTTTGACCCTGCAGGCGGCGGTA
ACCCAGTACTCTACCAACATTTATTTTGATTTTTTGGTCAC

>ALB30 627 bp – Album Park, El Paso, Texas

ATAAGATTCCTTATTCGTTTAGAGTTAGGGGTTATTGGTCCTTATATTGGGGACGAA
CATCTATATAACGTTATGGTTACTGCTCATGCCTTTGTTATGATTTTTTTTATGGTTAT
ACCTATTTCTATGGGTGGCTTTGGTAACTGACTTATTCCACTAATGTTGGGTGTCGCT
GATATAGCTTTCCCGCGCATAAATAATCTTTCTTTCTGGCTTCTTATTCCATCTTTCAC
TTTTTTATTACTTTCTTCAATTCTTGATGCTGGTGTTGGTACGGGTTGAACGGTTTACC
CTCCCCTATCTGACTCCAAGTATCATTCTGGTATTTCTGTTGATCTAGCTATTTTTAG
ACTTCATTTAGCCGGAATTTCTTCAATTCTTGGTAGAATCAATTTTCTTACTACTATT
ATTTGTTCTCGCACAGCAAAAGCTATTTCTCTAGATCGTATGCCTTTAATGTTATGGG
CGTTTGCTGTAACTTCTATTCTTCTTGTTACTAGATTGCCCGTATTAGCTGGTGCCATT
ACTATGCTTTTAACTGATCGAAACTTTAATACCTCTTTTTTTGATCCCGCAGGAGGTG
GTAATCCAGTACTCTACCAACATTTATTTTGATTTTTTGGTCAC

>KNT1 627 bp – Kent Bridge Tank, Kent, Texas

ATAAGATTCCTTATTCGTTTAGAGTTAGGGGTTATTGGTCCTTATATTGGGGATGAAC
ATTTATATAACGTCATGGTTACTGCCCACGCCTTTGTTATGATTTTTTTTATGGTTATG
CCTATTTCTATGGGTGGCTTTGGTAATTGACTTATTCCACTAATGTTGGGTGTTGCTG
ATATGGCTTTCCCACGTATAAATAATCTTTCTTTCTGGCTTCTTATTCCATCTTTCACT
TTTTTATTACTTTCTTCAATTCTTGATGCTGGTGTTGGTACTGGTTGAACTGTTTACCC
TCCCCTATCTGACTCTAAGTATCATTCTGGTATTTCTGTTGATCTAGCTATTTTTAGAC
TTCATTTAGCCGGAATTTCTTCAATTCTTGGTAGAATCAACTTTCTTACTACTATTATT
TGTTCTCGCACAGCAAAAGCTATTTCTCTAGATCGTATGCCTTTAATATTATGGGCGT
TTGCTGTTACTTCTATTCTTCTTGTTACTAGATTACCCGTTTTAGCTGGTGCCATCACT
ATGCTTTTAACTGATCGAAACTTTAATACCTCTTTTTTTGACCCTGCAGGCGGTGGTA
ACCCAGTACTCTACCAACATTTATTTTGATTTTTTGGTCAC

>KNT2 627 bp – Kent Bridge Tank, Kent, Texas

ATAAGATTCCTTATTCGTTTAGAGTTAGGGGTTATTGGTCCTTATATTGGGGATGAAC
ATTTATATAACGTCATGGTTACTGCCCACGCCTTTGTTATGATTTTTTTTATGGTTATG
CCTATTTCTATGGGTGGCTTTGGTAATTGACTTATTCCACTAATGTTGGGTGTTGCTG
ATATGGCTTTCCCACGTATAAATAATCTTTCTTTCTGGCTTCTTATTCCATCTTTCACT
TTTTTATTACTTTCTTCAATTCTTGATGCTGGTGTTGGTACGGGTTGAACTGTTTACCC
TCCCCTATCTGACTCTAAGTATCATTCTGGTATTTCTGTTGATCTAGCTATTTTTAGAC
TTCATTTAGCCGGAATTTCTTCAATTCTTGGTAGAATCAACTTTCTTACTACTATTATT
TGTTCTCGCACAGCAAAAGCTATTTCTCTAGATCGTATGCCTTTAATATTATGAGCGT
TTGCTGTTACTTCTATTCTTCTTGTTACTAGATTACCCGTTTTAGCTGGTGCCATCACT
ATGCTTTTAACTGATCGAAACTTTAATACCTCTTTTTTTGACCCTGCAGGCGGTGGTA
ACCCAGTACTCTACCAACATTTATTTTGATTTTTTGGTCAC

>GOK 627 bp – Gray Oak – Hueco Tanks State Park and Historic Site, Texas

ATAAGATTCCTTATTCGTTTAGAGTTAGGGGTTATTGGTCCTTATATTGGGGATGAAC
ATTTATATAACGTCATGGTTACTGCCCACGCCTTTGTTATGATTTTTTTTATGGTTATG
CCTATTTCTATGGGTGGCTTTGGTAATTGACTTATTCCACTAATGTTGGGTGTTGCTG
ATATGGCTTTCCCACGTATAAATAATCTTTCTTTCTGGCTTCTTATTCCATCTTTCACT
TTTTTATTACTTTCTTCAATTCTTGATGCTGGTGTTGGTACGGGTTGAACTGTTTACCC
TCCCCTATCTGACTCTAAGTATCATTCTGGTATTTCTGTTGATCTAGCTATTTTTAGAC
TTCATTTAGCCGGAATTTCTTCAATTCTTGGTAGAATCAACTTTCTTACTACTATTATT
TGTTCTCGCACAGCAAAAGCTATTTCTCTAGATCGTATGCCTTTAATATTATGGGCGT
TTGCTGTTACTTCTATTCTTCTTGTTACTAGATTACCCGTTTTAGCTGGTGCCATCACT
ATGCTTTTAACTGATCGAAACTTTAATACCTCTTTTTTTGACCCTGCAGGCGGCGGTA
ACCCAGTACTCTACCAACATTTATTTTGATTTTTTGGTCAC

>MOO1 627 bp – Moon Pool - Hueco Tanks State Park and Historic Site, Texas

ATAAGATTCCTTATTCGTTTAGAGTTAGGGGTTATTGGTCCTTATATTGGGGATGAAC
ATTTATATAACGTCATGGTTACTGCCCACGCCTTTGTTATGATTTTTTTTATGGTTATG
CCTATTTCTATGGGTGGCTTTGGTAATTGACTTATTCCACTAATGTTGGGTGTTGCTG
ATATGGCTTTCCCACGTATAAATAATCTTTCTTTCTGGCTTCTTATTCCATCTTTCACT
TTTTTATTACTTTCTTCAATTCTTGATGCTGGTGTTGGTACGGGTTGAACTGTTTACCC
TCCCCTATCTGACTCTAAGTATCATTCTGGTATTTCTGTTGATCTAGCTATTTTTAGAC
TTCATTTAGCCGGAATTTCTTCAATTCTTGGTAGAATCAACTTTCTTACTACTATTATT
TGTTCTCGCACAGCAAAAGCTATTTCTCTAGATCGTATGCCTTTAATATTATGGGCGT
TTGCTGTTACTTCTATTCTTCTTGTTACTAGATTACCCGTTTTAGCTGGTGCCATCACT
ATGCTTTTAACTGATCGAAACTTTAATACCTCTTTTTTTGACCCTGCAGGCGGTGGTA
ACCCAGTACTCTACCAACATTTATTTTGATTTTTTGGTCAC

>BRH14 627 bp – Behind Ranch House, Hueco Tanks State Park and Historic Site, Texas

ATAAGATTCCTTATTCGTTTAGAGTTAGGGGTTATTGGTCCTTATATTGGGGATGAAC
ATTTATATAACGTCATGGTTACTGCCCACGCCTTTGTTATGATTTTTTTTATGGTTATG
CCTATTTCTATGGGTGGCTTTGGTAATTGACTTATTCCACTAATGTTGGGTGTTGCTG
ATATGGCTTTCCCACGTATAAATAATCTTTCTTTCTGGCTTCTTATTCCATCTTTCACT

TTTTTATTACTTTCTTCAATTCTTGATGCTGGTGTTGGTACGGGTTGAACTGTTTACCC
TCCCCTATCTGACTCTAAGTATCATTCTGGTATTTCTGTTGATCTAGCTATTTTTAGAC
TTCATTTAGCCGGAATTTCTTCAATTCTTGGTAGAATCAACTTTCTTACTACTATTATT
TGTTCTCGCACAGCAAAAGCTATTTCTCTAGATCGTATGCCTTTAATATTATGGGCGT
TTGCTGTTACTTCTATTCTTCTTGTTACTAGATTACCCGTTTTAGCTGGTGCCATCACT
ATGCTTTTAACTGATCGAAACTTTAATACCTCTTTTTTTGACCCTGCAGGCGGCGGTA
ACCCAGTACTCTACCAACATTTATTTTGATTTTTTGGTCAC

>BRH6 627 bp – Behind Ranch House, Hueco Tanks State Park and Historic Site, Texas

ATAAGATTCCTTATTCGTTTAGAGTTAGGGGTTATTGGTCCTTATATTGGGGATGAAC
ATTTATATAACGTCATGGTTACTGCCCACGCCTTTGTTATGATTTTTTTTATGGTTATG
CCTATTTCTATGGGTGGCTTTGGTAATTGACTTATTCCACTAATGTTGGGTGTTGCTG
ATATGGCTTTCCCACGTATAAATAATCTTTCTTTCTGGCTTCTTATTCCATCTTTCACT
TTTTTATTACTTTCTTCAATTCTTGATGCTGGTGTTGGTACGGGTTGAACTGTTTACCC
TCCCCTATCTGACTCTAAGTATCATTCTGGTATTTCTGTTGATCTAGCTATTTTTAGAC
TTCATTTAGCCGGAATTTCTTCAATTCTTGGTAGAATCAACTTTCTTACTACTATTATT
TGTTCTCGCACAGCAAAAGCTATTTCTCTAGATCGTATGCCTTTAATATTATGGGCGT
TTGCTGTTACTTCTATTCTTCTTGTTACTAGATTACCCGTTTTAGCTGGTGCCATCACT
ATGCTTTTAACTGATCGAAACTTTAATACCTCTTTTTTTGACCCTGCAGGCGGCGGTA
ACCCAGTACTCTACCAACATTTATTTTGATTTTTTGGTCAC

>BRH5 627 bp v Behind Ranch House, Hueco Tanks State Park and Historic Site, Texas

ATAAGATTCCTTATTCGTTTAGAGTTAGGGGTTATTGGTCCTTATATTGGGGATGAAC
ATTTATATAACGTCATGGTTACTGCCCACGCCTTTGTTATGATTTTTTTTATGGTTATG
CCTATTTCTATGGGTGGCTTTGGTAATTGACTTATTCCACTAATGTTGGGTGTTGCTG
ATATGGCTTTCCCACGTATAAATAATCTTTCTTTCTGGCTTCTTATTCCATCTTTCACT
TTTTTATTACTTTCTTCAATTCTTGATGCTGGTGTTGGTACGGGTTGAACTGTTTACCC
TCCCCTATCTGACTCTAAGTATCATTCTGGTATTTCTGTTGATCTAGCTATTTTTAGAC
TTCATTTAGCCGGAATTTCTTCAATTCTTGGTAGAATCAACTTTCTTACTACTATTATT
TGTTCTCGCACAGCAAAAGCTATTTCTCTAGATCGTATGCCTTTAATATTATGGGCGT
TTGCTGTTACTTCTATTCTTCTTGTTACTAGATTACCCGTTTTAGCTGGTGCCATCACT
ATGCTTTTAACTGATCGAAACTTTAATACCTCTTTTTTTGACCCTGCAGGCGGCGGTA
ACCCAGTACTCTACCAACATTTATTTTGATTTTTTGGTCAC

>BRH15 627 bp – Behind Ranch House, Hueco Tanks State Park and Historic Site, Texas

ATAAGATTCCTTATTCGTTTAGAGTTAGGGGTTATTGGTCCTTATATTGGGGATGAAC
ATTTATATAACGTCATGGTTACTGCCCACGCCTTTGTTATGATTTTTTTTATGGTTATG
CCTATTTCTATGGGTGGCTTTGGTAATTGACTTATTCCACTAATGTTGGGTGTTGCTG
ATATGGCTTTCCCACGTATAAATAATCTTTCTTTCTGGCTTCTTATTCCATCTTTCACT
TTTTTATTACTTTCTTCAATTCTTGATGCTGGTGTTGGTACGGGTTGAACTGTTTACCC
TCCCCTATCTGACTCTAAGTATCATTCTGGTATTTCTGTTGATCTAGCTATTTTTAGAC
TTCATTTAGCCGGAATTTCTTCAATTCTTGGTAGAATCAACTTTCTTACTACTATTATT
TGTTCTCGCACAGCAAAAGCTATTTCTCTAGATCGTATGCCTTTAATATTATGGGCGT

TTGCTGTTACTTCTATTCTTCTTGTTACTAGATTACCCGTTTTAGCTGGTGCCATCACT
ATGCTTTTAACTGATCGAAACTTTAATACCTCTTTTTTTGACCCTGCAGGCGGCGGTA
ACCCAGTACTCTACCAACATTTATTTTGATTTTTTGGTCAC

>BRH16 627 bp – Behind Ranch House, Hueco Tanks State Park and Historic Site, Texas

ATAAGATTCCTTATTCGTTTAGAGTTAGGGGTTATTGGTCCTTATATTGGGGATGAAC
ATTTATATAACGTCATGGTTACTGCCCACGCCTTTGTTATGATTTTTTTTATGGTTATG
CCTATTTCTATGGGTGGCTTTGGTAATTGACTTATTCCACTAATGTTGGGTGTTGCTG
ATATGGCTTTCCCACGTATAAATAATCTTTCTTTCTGGCTTCTTATTCCATCTTTCACT
TTTTTATTACTTTCTTCAATTCTTGATGCTGGTGTTGGTACGGGTTGAACTGTTTACCC
TCCCCTATCTGACTCTAAGTATCATTCTGGTATTTCTGTTGATCTAGCTATTTTTAGAC
TTCATTTAGCCGGAATTTCTTCAATTCTTGGTAGAATCAACTTTCTTACTACTATTATT
TGTTCTCGCACAGCAAAAGCTATTTCTCTAGATCGTATGCCTTTAATATTATGGGCGT
TTGCTGTTACTTCTATTCTTCTTGTTACTAGATTACCCGTTTTAGCTGGTGCCATCACT
ATGCTTTTAACTGATCGAAACTTTAATACCTCTTTTTTTGACCCTGCAGGCGGCGGTA
ACCCAGTACTCTACCAACATTTATTTTGATTTTTTGGTCAC

>BRH11 627 bp – Behind Ranch House, Hueco Tanks State Park and Historic Site, Texas

ATAAGATTCCTTATTCGTTTAGAGTTAGGGGTTATTGGTCCTTATATTGGGGATGAAC
ATTTATATAACGTCATGGTTACTGCCCACGCCTTTGTTATGATTTTTTTTATGGTTATG
CCTATTTCTATGGGTGGCTTTGGTAATTGACTTATTCCACTAATGTTGGGTGTTGCTG
ATATGGCTTTCCCACGTATAAATAATCTTTCTTTCTGGCTTCTTATTCCATCTTTCACT
TTTTTATTACTTTCTTCAATTCTTGATGCTGGTGTTGGTACGGGTTGAACTGTTTACCC
TCCCCTATCTGACTCTAAGTATCATTCTGGTATTTCTGTTGATCTAGCTATTTTTAGAC
TTCATTTAGCCGGAATTTCTTCAATTCTTGGTAGAATCAACTTTCTTACTACTATTATT
TGTTCTCGCACAGCAAAAGCTATTTCTCTAGATCGTATGCCTTTAATATTATGGGCGT
TTGCTGTTACTTCTATTCTTCTTGTTACTAGATTACCCGTTTTAGCTGGTGCCATCACT
ATGCTTTTAACTGATCGAAACTTTAATACCTCTTTTTTTGACCCTGCAGGCGGCGGTA
ACCCAGTACTCTACCAACATTTATTTTGATTTTTTGGTCAC

CURRICULUM VITA

Tristan Chavez-Poeschel was born in Panama City, Panama and grew up throughout the United States and Germany. He has a special fondness for the Midwest and has now made El Paso, Texas his home. He has always had an interest in the natural world and is constantly seeking out new places and experiences. Tristan started out with little understanding as to the role of higher education, and as a result spent his early years in the US Army and working in the health field. He attained his first degree in Criminal Justice, which allowed him to have a full career in the insurance industry. Tristan decided to return to finish a graduate degree and completed a second Bachelor's degree in biology prior to starting his Master's program in Environmental Science at UTEP. He presented at the XVI International Rotifer Symposium poster session in Zagreb, Croatia in 2022 and at the International Conference on Aeolian Research (ICAR) in Las Cruces, New Mexico, in 2023. He believes in the transformative power of higher education and looks to help others. Tristan is pursuing a doctorate in Biology at Northern Illinois University with a focus on population genetics and hopes to be able to not only help others but also to help in conservation and find a path forward in our changing world and climate.

Contact Information: tristancpoe@gmail.com